

# A Sublinear-Time Quantum Algorithm for High-Dimensional Reaction Rates

Tyler Kharazi,<sup>1,\*</sup> Ahmad M. Alkadri,<sup>2</sup> Kranthi K. Mandadapu,<sup>2,3</sup> and K. Birgitta Whaley<sup>1,3,4,†</sup>

<sup>1</sup>*Department of Chemistry, University of California, Berkeley*

<sup>2</sup>*Department of Chemical and Biomolecular Engineering, University of California, Berkeley*

<sup>3</sup>*Chemical Sciences Division, Lawrence Berkeley National Laboratory, Berkeley, California*

<sup>4</sup>*Berkeley Quantum Information and Computation Center, University of California, Berkeley*

(Dated: January 23, 2026)

The Fokker-Planck equation models rare events across sciences, but its high-dimensional nature challenges classical computers. Quantum algorithms for such non-unitary dynamics often suffer from exponential decay in success probability. We introduce a quantum algorithm that overcomes this for computing reaction rates. Using a sum-of-squares representation, we develop a Gaussian linear combination of Hamiltonian simulations (Gaussian-LCHS) to represent the non-unitary propagator with  $O\left(\sqrt{t\|H\|}\log(1/\epsilon)\right)$  queries to its block encoding. Crucially, we pair this with a novel technique to directly estimate matrix elements without exponential decay. For  $\eta$  pairwise interacting particles discretized with  $N$  plane waves per degree of freedom, we estimate reactive flux to error  $\epsilon$  using  $\tilde{O}\left((\eta^{5/2}\sqrt{t\beta}\alpha_V + \eta^{3/2}\sqrt{t/\beta}N)/\epsilon\right)$  quantum gates, where  $\alpha_V = \max_r |V'(r)/r|$ . For non-convex potentials, the sharpest classical worst-case analytical bounds to simulate the related overdamped Langevin equation scale as  $O(te^{\Omega(\eta)}/\epsilon^4)$ . This implies an exponential separation in particle number  $\eta$ , a quartic speedup in  $\epsilon$ , and quadratic speedup in  $t$ . While specialized classical heuristics may outperform these bounds in practice, this demonstrates a rigorous route toward quantum advantage for high-dimensional dissipative dynamics.

---

\* kharaztd@berkeley.edu

† whaley@berkeley.edu

## CONTENTS

I. Introduction	3
A. Overview and Contributions of this work	6
II. Prior work	8
A. Quantum Algorithms	8
B. Classical Algorithms	8
III. Overview of methodology	10
A. Background on Kolmogorov equations	10
B. Matrix square root and Gaussian-LCHS	11
C. Non-unitary overlap circuit	13
D. Discussion on reactant state preparation	14
IV. Analysis and construction of core subroutines	15
A. Block encoding sum-of-squares Fokker-Planck operator	16
B. Block encoding propagator with Gaussian-LCHS	16
C. Overlap estimation algorithm	19
V. Discussion	20
Acknowledgments	22
References	22
A. Bound on Lipschitz constant (Proof of Theorem 1)	27
B. Technical Background on Kolmogorov Equations	30
C. Equilibrium state preparation in locally convex region	32
1. Quantum reactant (product) state preparation	34
D. Background on quantum algorithms	38
1. Block encoding	38
2. Quantum Signal Processing	39
3. The original LCHS method	40
E. Error Bounds on Gaussian-LCHS	41
1. Truncation error bounds	41
2. Quadrature Error Bounds	42
3. Bound on LCHS subnormalization factor	43
4. Simulation error bounds	44
F. Multiplexed QSP (Proof of Lemma 6)	46
G. Non-unitary overlap circuit	48
H. Block encoding dilated matrix square root	50
I. Consistency of plane wave discretization	51
J. Detailed construction of block encoding	53
1. Block Encoding Potential Gradient	53
2. Block encoding gradient operator	56
3. Proof of Theorem 5	56

## I. INTRODUCTION

Many questions in the sciences and engineering involve answering the question “how quickly does a system cross a barrier?”—for example: how fast a protein folds into its functional shape [1, 2], how rapidly a crystal nucleus forms during materials processing [3], how often a chemical reaction proceeds in a crowded solvent [4], how quickly a glassy system relaxes [5], how long it takes for charged particles to escape magnetic confinement in a plasma [6], or how frequently a market variable hits a regulatory or contractual threshold [7, 8]. Transition path theory (TPT) provides a powerful framework to answer these questions for classical dynamical systems [9–11]. TPT is formulated in the language of the forward and backward Kolmogorov equations (FKE and BKE, respectively). The FKE, also known as the Fokker-Planck equation, describes the deterministic evolution of the probability distribution for a stochastic process with a given initial distribution. The solution of the BKE on the other hand provides the so-called committor function, which encodes the probability of a trajectory emanating from some point in the configuration space, given that it terminates at some fixed region in configuration space. The committor function additionally provides an optimal external force to generate reactive trajectories [12, 13]. The (F)BKE framework provides a compact, operator-level description of reaction rates, reaction pathways, and transition state ensembles [9, 14, 15].

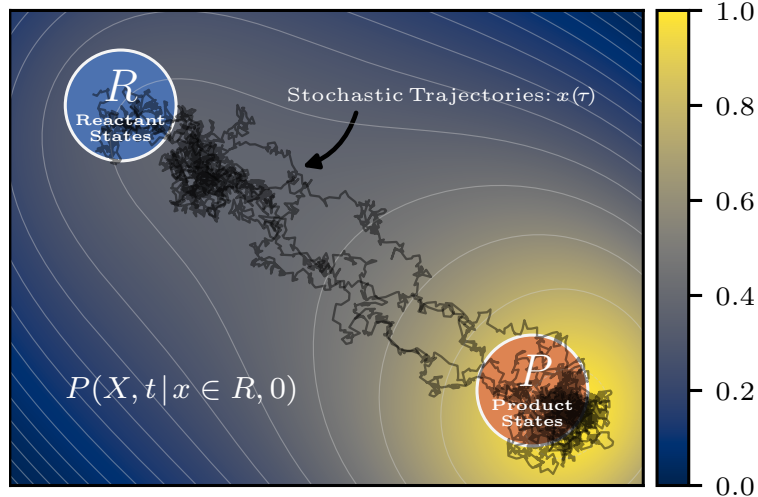


FIG. 1: Stochastic trajectories from an overdamped Langevin equation starting from region  $R$  terminate in the configuration space with probabilities given by the Fokker-Planck equation. The stochastic trajectories terminate at some point  $\mathbf{X}(t)$  in the configuration space with probability  $P(\mathbf{X}, t | \mathbf{x} \in R, 0)$  obtained by solving the Fokker-Planck equation with an initial condition corresponding to the equilibrium distribution over  $R$ .

The steady-state committor function is obtained by solving the Dirichlet boundary value problem associated with the BKE,

$$(-\nabla V \cdot \nabla + \beta^{-1} \Delta) q(\mathbf{x}) = 0, \text{ s.t. } q(\mathbf{x}) = 0 \text{ for } \mathbf{x} \in R, \text{ and } q(\mathbf{x}) = 1 \text{ for } \mathbf{x} \in P, \quad (1)$$

where  $V(\mathbf{x})$  is a potential (containing in general both inter-particle and external potentials),  $-\nabla V(\mathbf{x})$  is the associated force, and  $R$  and  $P$  are (typically) disjoint subsets of the full configuration space that label the reactant and product states. Given the committor  $q(\mathbf{x})$  as above, the steady-state reaction rate can then be obtained from the expectation value

$$k_{RP} = \beta^{-1} \int d\mathbf{x} \mu(\mathbf{x}) \|\nabla q(\mathbf{x})\|^2, \quad (2)$$

with  $\mu(\mathbf{x}) = e^{-\beta V(\mathbf{x})}/\mathcal{Z}$  the equilibrium Boltzmann distribution associated with the potential  $V$  and inverse temperature  $\beta$  [12].

An alternative approach to estimating reaction rates is to simulate the system’s relaxation under the FKE dynamics for a time proportional to the mixing time  $t_{\text{mix}} \sim 1/\Delta_{\text{gap}}$ , corresponding to the inverse of smallest non-zero eigenvalue of the generator. The dynamical generator for the FKE is the formal adjoint of the BKE and can be expressed as the differential operator

$$\mathcal{F}[\rho] = \nabla \cdot (\rho \nabla V + \beta^{-1} \nabla \rho), \quad (3)$$

with the associated first-order-in-time PDE

$$\begin{aligned}\partial_t \rho(t) &= \mathcal{F}[\rho](t), \\ \rho(0) &= \rho_0.\end{aligned}\tag{4}$$

In this setting, the (time-dependent) reaction rate can be expressed in terms of a thermally weighted sum over classical transition matrix elements between initial and final configurations in the regions  $R$  and  $P$  respectively,

$$k_{RP}(T) := \frac{1}{T\bar{p}_R} \int d\mathbf{x} \int d\mathbf{x}' 1_P(\mathbf{x}') P(\mathbf{x}', T | \mathbf{x}, 0) \mu(\mathbf{x}) 1_R(\mathbf{x}) \equiv \frac{1}{T\bar{p}_R} \langle 1_P, e^{T\mathcal{F}} 1_R \rangle_\mu, \tag{5}$$

with

$$1_R(\mathbf{x}) = \begin{cases} 1 & \mathbf{x} \in R \\ 0 & \text{else} \end{cases}, \tag{6}$$

and

$$\bar{p}_R = \int d\mathbf{x} 1_R(\mathbf{x}) \mu(\mathbf{x}). \tag{7}$$

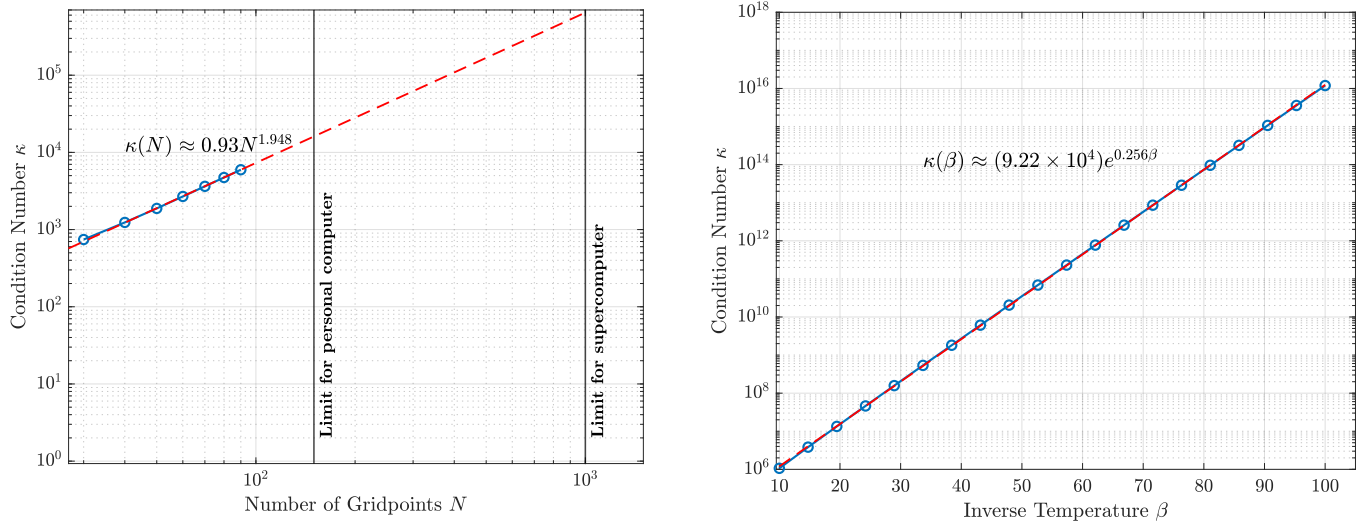
Here  $P(\mathbf{x}', T | \mathbf{x}, 0)$  is the probability of being in state  $x'$  at time  $T$  given the state  $x$  at time 0 and is obtained by the propagator for the FPE,

$$P(\mathbf{x}', T | \mathbf{x}, 0) = \langle \mathbf{x}', e^{T\mathcal{F}} \mathbf{x} \rangle_\mu. \tag{8}$$

The time-dependent reaction rate can be interpreted as the probability of a trajectory starting in thermal state  $R$  to terminate in state  $P$  at time  $T$ , and the equilibrium reaction rate is obtained in the limit as  $T \rightarrow \infty$ . We shall use the notation  $\langle \cdot, \cdot \rangle_\mu$  to refer to the  $\mu$ -weighted classical inner product and reserve the bra-ket notation for quantum states. With this, we see that the factor  $\langle 1_P, e^{T\mathcal{F}} 1_R \rangle_\mu$  is the overlap between the final state  $1_P(x)$  and the time-propagated state  $1_R(x)$  (under the thermal measure  $\mu$ ). We shall refer to such quantities as propagator overlaps.

Computation of both the BKE and FKE face two significant challenges. (i) The curse of dimensionality [16, 17]. A system of  $\eta$  many particles in  $d$  spatial dimensions using grid-based or spectral discretization of Eq. (1) leads to a state space that scales exponentially as  $O(N^{\eta d})$  where  $N$  is the number of grid points or basis functions per degree of freedom. (ii) The rare event sampling problem. For trajectory-based estimators, such as molecular dynamics, where long-time integration, poor mixing at low temperature  $T$  (i.e., large  $\beta$ ) [18, Chapter 22][19], and exponentially rare barrier crossings lead to high variance and large sample complexity, despite variance-reduction heuristics [13, 20–22]. Recent classical work (e.g., tensor-network and hierarchical tensor solvers, semigroup and learned surrogates) offers important progress yet still encounters exponential or steep polynomial scaling in either state space dimension  $d$ , number of particles  $\eta$ , or time horizon  $T$  [12, 13, 23, 24].

Quantum computers offer a potential path forward by operating in a Hilbert space whose dimension grows exponentially with the number of qubits, naturally accommodating high-dimensional state spaces. However, quantum algorithms for linear, non-unitary dynamics like the F(B)KE face their own fundamental challenges. First, consider the approach of solving the steady-state BKE (1) via a quantum linear systems algorithm (QLSA). The time complexity of both quantum and classical linear solvers scales with the condition number  $\kappa$  of the generator. For the Kolmogorov equations, the presence of a non-trivial zero mode (the equilibrium Boltzmann distribution) implies that the spectral gap, and hence  $\kappa$ , can be exponentially small for metastable systems [25]. While classical iterative methods can invert symmetric positive definite linear systems with  $O(\sqrt{\kappa} \log(\frac{1}{\epsilon}))$  overhead (see e.g. Ref. [26]), QLSA's require  $\Omega(\kappa)$  queries to the input oracle to perform the same task [27], negating any potential quantum advantage in this regime. We briefly note that the work of Ref. [28] develops a QLSA to invert the class of semi-definite matrices that we consider in this work with  $O(\sqrt{\kappa})$  complexity. However, this algorithm would scale exponentially with the particle number  $\eta$  for our BKE example (see Proposition 16 of Ref. [28] for more details). Since the condition number is also an essential *input* parameter to linear-solve-based quantum algorithms, obtaining these estimates is an important step prior to the execution of the quantum algorithm. However, obtaining tight analytical upper bounds on  $\kappa$  for particular problem instances is difficult in general, and numerical estimates for large systems are intractable due to the high dimensionality. Nevertheless, useful insight is still gained by making such estimates for smaller sizes. In Fig. 2 we show the results of numerical estimation of the condition numbers for the BKE in a set of small problem instances with three particles interacting via a symmetric double-well potential in a single spatial dimension, together with extrapolation to larger sizes (larger numbers of grid points  $N$  in Fig. 2(a), and larger numbers of particles in Fig. 2(b)).



(a) Condition number  $\kappa$  versus grid resolution  $N$  for particle number  $\eta = 3$ ; a log-log least-squares fit (red dashed line) yields  $\kappa(N) \approx 0.93N^{1.948}$ , indicating an approximately quadratic dependence on the grid resolution.

(b) Condition number  $\kappa$  versus inverse temperature  $\beta$  for a single particle in a double well potential over the interval  $[-4, 4]$  with  $N = 2000$  grid points, evaluated over the range of  $\beta \in [10, 100]$ . An exponential fit to the numerical data yields  $\kappa \approx (9.22 \times 10^4)e^{0.256\beta}$  which nearly matches the theoretically predicted scaling of  $\kappa(N, \beta) \sim (N/L)^2 e^{\beta/4}$ .

FIG. 2: Scaling of the condition number  $\kappa$  of the finite-difference discretized BKE generator for the one-dimensional double-well ( $V(x) = x^4 - x^2$ ) test problem as a function of the number of gridpoints per particle  $N$  and inverse temperature  $\beta$ . Condition numbers are estimated using MATLAB’s `condest` function [29]. With a barrier height of  $\frac{1}{4}$  separating the local minima in the wells, our numerical estimates are consistent with the asymptotic scaling  $\kappa(N, \beta) \sim C N^2 e^{\beta/4}$ . However, it is computationally intractable to determine the scaling with particle number  $\eta$ . Vertical lines in panel (a) indicate rough limits for feasible direct sparse solves on a personal workstation and on current exascale-class systems (e.g., the Frontier supercomputer at Oak Ridge National Laboratory [30]). These limits are based on simple extrapolations of available memory, according to the  $\sim N^\eta$  growth of the full configuration-space dimension. Even though exascale nodes such as those on Frontier provide on the order of a terabyte of combined CPU and high-bandwidth GPU memory, the exponential growth in state-space size quickly outstrips practical storage requirements for fully discretized many-body operators. Consequently, the “curse of dimensionality” associated with grid-based discretization of the BKE operator is typically avoided in classical computing by employing alternative high-dimensional techniques—such as tensor-network or sampling-based methods—as discussed in Sec. I.

Performing time evolution until the mixing time also scales asymptotically as  $O(\kappa)$ , due to the relationship between the spectral gap, the mixing time  $t_{\text{mix}}$ , and the condition number. This can be shown as follows. If the underlying (discrete) stochastic process is generated by some negative semi-definite matrix  $\mathcal{F}$  with  $\lambda_{\max} = \|\mathcal{F}\|_2$ , implementing the operation  $e^{t_{\text{mix}}\mathcal{F}}$  requires  $\Omega(\lambda_{\max} t_{\text{mix}}) = \Omega\left(\lambda_{\max} \frac{1}{\Delta_{\text{gap}}}\right) = \Omega(\kappa)$  queries to an oracle for the matrix elements of  $\mathcal{F}$  [31]. For metastable systems, or those with a non-convex potential, the smallest non-zero eigenvalue of the generator  $\mathcal{F}$  can be exponentially small (see e.g., Ref. [25]), leading to exponentially large condition numbers and mixing times. In many circumstances, however, it is not necessary to sample from the steady state, but instead to sample from the low-lying eigenstates of the generator, e.g. in the applications explored in Refs. [32–36].

This is especially relevant when the system exhibits metastability, since in this situation a significant number of low-lying excited states may be separated by a large *effective* gap from the rest of the spectrum (see e.g., Chapter 8.4 of Ref. [37]). A diagrammatic description of this idea is provided in Fig. 3. In scenarios where one wishes to sample from the equilibrium and metastable states, this effective gap can be much larger than the true ground state gap, leading to much shorter mixing times and a significant advantage over linear solvers.

This can also be straightforwardly demonstrated by the following argument. Consider some normalized initial state  $|\psi\rangle = \sum_{j \geq 0} c_j |\phi_j\rangle$ , with  $|\phi_j\rangle$  eigenstates of the generator  $\mathcal{F}$  of Eq. (3), and the coefficient associated with the steady state (with eigenvalue zero)  $c_0 \neq 0$ . Suppose  $|\phi_1\rangle$  has eigenvalue  $0 < \epsilon_1 = \Delta_{\text{gap}}$  and  $|\phi_2\rangle$  has eigenvalue  $\epsilon_2$ , with

$\epsilon_1 < \epsilon_2$ . Then

$$\begin{aligned} e^{-tL} |\psi\rangle &= c_0 |\phi_0\rangle + c_1 e^{-t\epsilon_1} |\phi_1\rangle + c_2 e^{-t\epsilon_2} |\phi_2\rangle + O(e^{-t\epsilon_2}) \\ &= c_0 |\phi_0\rangle + e^{-t\epsilon_1} (c_1 |\phi_1\rangle + c_2 e^{-t(\epsilon_2-\epsilon_1)} |\phi_2\rangle) + O(e^{-t\epsilon_2}) \end{aligned}$$

and to ensure that the support on  $|\phi_2\rangle$  is arbitrarily small, it suffices to choose  $\frac{1}{\epsilon_2-\epsilon_1} < t < \frac{1}{\epsilon_1}$ . Therefore, when  $\epsilon_2 - \epsilon_1 \gg \epsilon_1$ , and it is sufficient to sample only from the ground state *and* low energy configurations, we can expect a corresponding reduction in the effective simulation time  $t$ .

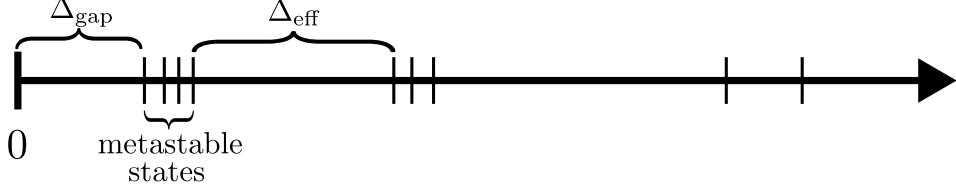


FIG. 3: A diagrammatic description of the spectral characterization of metastability. There may be many low-lying eigenstates corresponding to local minima of the potential energy surface. The effective gap  $\Delta_{\text{eff}}$  corresponds to the gap between the largest of these metastable states and the next largest eigenvalue of the generator.

A more fundamental challenge remains for time evolution based quantum algorithms for non-unitary dynamics, which we term the stability-dissipation conflict. For a linear system  $\partial_t \mathbf{u}(t) = A\mathbf{u}(t)$ , the solution is  $\mathbf{u}(t) = e^{tA}\mathbf{u}(0)$ . On the one hand, if  $A$  has eigenvalues with positive real part and  $\mathbf{u}(0)$  is supported on the corresponding eigenvectors, then the solution norm increases exponentially with  $t$  and the system is unstable. On the other hand, if  $A$  contains negative real spectrum, the solution norm can decay exponentially with  $t$ , leading to exponentially small success probabilities in preparing  $|\mathbf{u}(t)\rangle$ . While block encoding methods can approximate  $e^{tA}$  with  $O(t \text{ polylog}(1/\epsilon))$  queries to the block encoding of  $A$  the overall complexity including the post-selection overhead becomes  $\tilde{O}\left(\frac{\|\mathbf{u}(0)\|}{\|\mathbf{u}(t)\|} t \text{ polylog}(1/\epsilon)\right)$ . Thus when  $\text{Re}(A) < 0$ ,  $\|\mathbf{u}(t)\| \in O(e^{-t})$  leading to an exponential time complexity for the quantum algorithm. This conflict between stability and dissipation is at the core of the difficulty in designing quantum algorithms for preparing the solution state of dissipative non-unitary PDEs.

### A. Overview and Contributions of this work

Before summarizing our technical contributions, we emphasize the central computational object studied in this work. Many quantities of interest in stochastic dynamics, such as reaction rates, transport coefficients, and response functions, can be expressed as matrix elements and/or correlation functions of the Fokker-Planck propagator. Such examples include transport coefficients [38, 39], Van Hove correlation functions (from which dynamic structure factors can be computed) [40, 41], and response functions [42]. In operator form, these are often represented as overlaps (or linear combinations thereof) that are represented as

$$\langle A, e^{t\mathcal{F}} B \rangle, \quad (9)$$

where  $\mathcal{F}$  is the Fokker-Planck generator and  $A$  and  $B$  are observables. Rather than attempting to prepare the full time-evolved or stationary probability density, our approach targets the direct estimation of such propagator overlaps, which encode the desired physical information and admit a more favorable quantum complexity. Specifically, we focus on the time-dependent reactive flux,

$$\nu_{RP}(t) = \langle P | e^{\mathcal{H}_\beta t} | R \rangle, \quad (10)$$

which are expressed in terms of quantum states  $|R\rangle$  and  $|P\rangle$  encoding the reactant and product regions, and the generator  $\mathcal{H}_\beta$ , which is a self-adjoint representation of the FKE generator obtained via similarity transformation. This approach circumvents the two primary quantum hurdles mentioned above: it avoids the condition number problem of linear solvers because it relies on time evolution, not steady state calculation, and it also avoids the potentially exponential state preparation cost because we directly estimate matrix elements (overlaps) of the propagator without needing to prepare the state  $e^{t\mathcal{H}_\beta} |R\rangle$ .

Building on the correlation function formulation, we introduce in this work a quantum algorithm to efficiently estimate matrix elements of the Fokker-Planck operator. To achieve this, we make three core contributions. First,

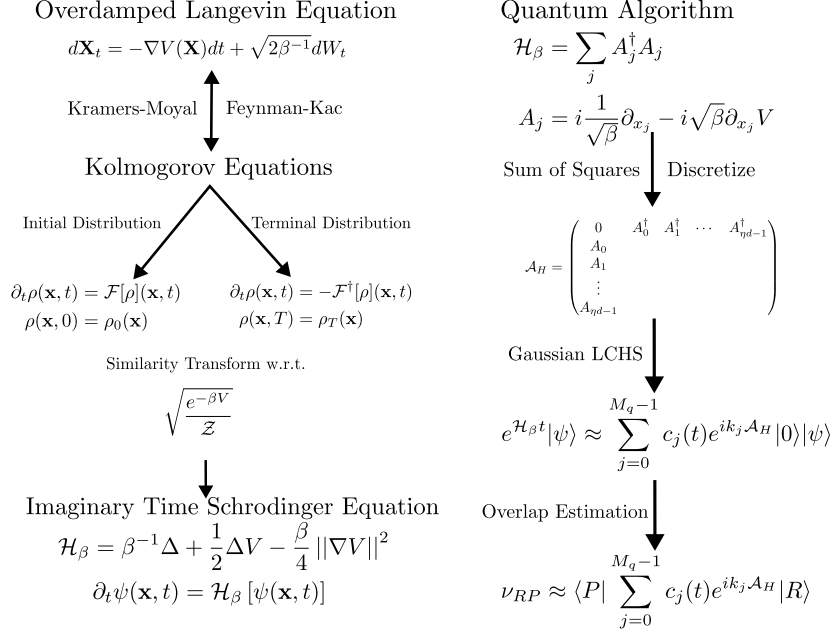


FIG. 4: A graphical description of how the Hamiltonian model is obtained, and how the algorithm is constructed. In the column on the left, a stochastic Langevin equation can be related to backward and forward Kolmogorov equations via the Feynman-Kac formula and Kramers-Moyal expansion respectively. By performing a similarity transformation of the generator  $\mathcal{F}$  with the square root of the equilibrium density, we obtain an imaginary time Schrodinger equation with Hamiltonian  $\mathcal{H}_\beta$ . This Hamiltonian can then be expressed as a sum-of-squares using the decomposition given by operators  $A_j$  that we define below. Then, dilating into the Hermitian matrix  $\mathcal{A}_H$ , and performing Hamiltonian simulation with  $\mathcal{A}_H$ , we can approximate time evolution under  $\mathcal{H}_\beta$  via the Gaussian-LCHS formula. Finally, we can apply the non-unitary overlap estimation algorithm to estimate the reactive flux,  $\langle P | e^{\mathcal{H}_\beta t} | R \rangle$ .

in Sec. III B we introduce an improved LCHS [43, 44] for time-independent negative semi-definite matrices  $H$  that can be expressed as  $H = -\mathcal{A}^2$ . In Sec. IV B we construct a block encoding of the propagator with query complexity  $\tilde{O}\left(\sqrt{t\|H\|\log(1/\epsilon)}\right)$ , a near-quadratic improvement in the scaled simulation time  $t\|H\|$  over Refs. [43–45], and saturates the fast-forwarded complexity for time evolution of this class of systems predicted in Ref. [46]. We combine this bound with a technique that we term "multiplexed QSP" that implements this block encoding with gate complexity matching the query complexity of the LCHS method.

Second, in Sec. III C we show that this overall sub-linear-in- $t$  dependence persists for the ubiquitous case of estimating overlaps of the non-unitary propagator. This behavior is obtained by a novel generalization of the Hadamard test for non-unitary matrices that avoids a major post-selection bottleneck by estimating the matrix elements  $e^{iHt}$  directly from its LCU representation, without encountering the exponential success probability decay associated with preparing the full solution state. This circuit succeeds with probability  $\Omega(1)$ , independent of the simulation time  $t$ . For estimating overlaps of purely dissipative dynamics, this construction provides a potentially exponential speedup over quantum algorithms that require state preparation and postselection. We believe the non-unitary overlap estimation algorithm introduced here will have many potential applications in quantum algorithms in addition to the particular use case of the FKE in this paper.

Third, we obtain resource estimation costs for many of the subroutines. We apply these general techniques to the Fokker-Planck equation for  $\eta$  pair-wise interacting particles in  $d$  spatial dimensions, discretized with  $N = 2^n$  plane wave modes per degree of freedom. Although we do not discuss the state preparation of  $|R\rangle$  and  $|P\rangle$  in detail, we describe in Sec. III D a method for fast thermal state preparation in locally convex regions, corresponding to local minima of the potential energy surface. We then provide explicit circuits, and estimates of subnormalization factors, for block encoding the necessary operators and show that the reactive flux can be estimated to additive error

$\epsilon$  using  $\tilde{O}\left(\frac{\eta^{5/2}\sqrt{t\beta}\alpha_V + \eta^{3/2}\sqrt{\frac{t}{\beta}}N}{\epsilon}\right)$  quantum gates (Secs. IV and V). Crucially, we prove (Theorem 1) that for radially symmetric pair potentials with bounded second derivative, that the Lipschitz constant of the potential gradient scales as  $\Omega(\eta)$ .

Together with the sharp analytical bounds of Ref. [47] (see Eq. (11)) for non-convex potentials, our results imply that our quantum algorithm achieves an exponential improvement with respect to  $\eta$ , a quartic improvement with respect to  $\epsilon$ , and a quadratic improvement with respect to  $t$ , relative to these classical bounds. We emphasize that our results should not be interpreted as a speedup over all classical simulation methods. Instead, our contribution is to identify a class of physically relevant observables—expressible as correlation functions of the Fokker–Planck propagator—that are provably hard to compute with guaranteed error in the worst case using classical algorithms under standard assumptions, yet can be estimated efficiently by our quantum approach.

The rest of the paper is organized as follows. In Sec. II we review quantum and classical algorithms for classical PDEs that preceded this work. We additionally perform a comparison between our quantum algorithm and the best known analytical bounds on the worst-case complexity for simulating the related overdamped Langevin dynamics. In Sec. III we introduce the necessary background, detail the matrix square root, discuss the mapping from Fokker–Planck to an imaginary time Schrödinger equation, and define the reaction rate in terms of overlaps of the propagator. We then review the main subroutines of the algorithm, and present the quantum circuit for estimating non-unitary overlaps. In Sec. IV we provide an analysis of the complexity of our algorithm, as well as detailed resource estimates to construct the necessary block encodings. We then conclude in Sec. V with a summary and a discussion on open questions and directions for future work.

## II. PRIOR WORK

### A. Quantum Algorithms

There have been several distinct approaches to solving linear non-unitary differential equations on quantum computers. These include algorithms based on solving a quantum linear systems problem to prepare history states [48, 49], time stepping [50], and mapping the non-unitary propagator to a linear combination of unitaries [43, 44, 51]. In particular, our work leverages the LCHS technique developed in Refs. [43, 44], which provides a near-optimal construction for preparing the non-unitary propagator as a block encoding. Quantum PDE solvers occur in a broad range of settings, e.g., the wave equation [52], electrodynamics [53], molecular dynamics [54], the Fokker–Planck equation [55], the simulation of classical coupled oscillators [56], and even some non-linear PDEs [57–60]. There have also been some general studies on the efficiency of quantum differential equation solvers [61, 62], as well as the establishment of complexity theoretic lower bounds [46]. However, except in some very special circumstances where it is possible to map the underlying linear differential equation to a Schrödinger equation, such as was observed in Refs. [53, 56], it has continued to be challenging to identify problem instances where quantum computers can provide guaranteed exponential or even significant polynomial speedups over classical solvers.

In addition to generic algorithmic developments for solving linear PDEs, we briefly review some prior work on the development of specific quantum algorithms for applications closely related to our F(B)KE problems. Ref. [63] considers the problem of estimating hitting times and sampling from Gibbs states using the spectral gap amplification approach, which shares similar properties to the Gaussian-LCHS approach that we use in this work. Ref. [64] develops quantum algorithms for preparing purifications of thermal states with bounds based on fluctuation theorems from statistical mechanics. Ref. [55] develops a quantum algorithm for the Fokker–Planck equation applying the Schrödingerization technique and similarly employ a finite difference discretization. However, as shown in their Theorem 3.2, that algorithm has time complexity  $\Omega(t^2)$  unlike the  $O(\sqrt{t})$  scaling of our reaction rate computation. Most recently, Ref. [65] considered preparation of thermal states of the Fokker–Planck equation, using eigenstate filtering and replica exchange to sample from non-log-concave distributions, together with the sum of squares decomposition from Ref. [66].

### B. Classical Algorithms

In addition to the aforementioned quantum algorithms, there has been significant progress on the side of classical algorithms for the F(B)KE problems. Algorithms that approximate the committor function, which is obtained by solving a Dirichlet boundary value problem for the steady-state of the backward generator (BKE), have been proposed using tensor networks [67], machine learning approaches [12, 68–70], and point-cloud discretization of the Fokker–Planck operator [71]. For the Fokker–Planck equation itself, similar classical algorithms have been proposed

based on hierarchical tensor networks[72] and machine learning [24]. These algorithms perform well under various assumptions, such as i) being efficiently representable as a matrix product operator or tensor train, ii) the solution is effectively restricted to a quasi one-dimensional region referred to as a “reaction tube”, or iii) that the solution is well approximated by only a small number of low-lying eigenfunctions. These methods have been quite effectively applied to the one and two-dimensional Ginzburg-Landau model and double well potentials, but stop short of addressing high-dimensional problem instances involving multiple interacting particles. However, none of these approaches can provide the same level of provable performance guarantees as a quantum algorithm performing direct numerical simulations of the underlying PDE, and are further unlikely to scale to the billions or even trillions of degrees of freedom that are needed to represent the full dynamical generator for many-body systems.

Classical trajectory sampling methods also offer a promising counterpart to direct numerical solution of the high-dimensional PDE. In this setting, one solves the PDE by computing an expectation value over independent realizations of the underlying stochastic process. When one wishes to approximate the distribution over a small number of points in the configuration space, trajectory-based methods circumvent the exponential scaling in state space. Due to the independence of each trajectory, these methods can be implemented in a highly parallelizable manner. Estimating the reaction rate by sampling trajectories has cost  $\mathcal{C} = (\text{number of trajectories}) \times (\text{cost per time step}) \times (\text{number of time steps})$ . The number of trajectories is  $O(1/\epsilon^2)$  by standard Monte-Carlo methods. The cost per time step is naively  $O(\eta^2)$ , but can be improved to  $O(\eta \log(\eta))$  using the fast-multipole method [73] or neighbor lists. The number of time steps is  $T/\Delta t$ , where  $\Delta t$  is the time step size and  $T$  the total simulation time.

For non-convex potentials, the step size  $\Delta t$  can be chosen according to Theorem 2 of Ref. [47], which provides a sharp estimate of the step size to control the bias of  $\Delta t \sim \frac{\epsilon^2 e^{-\gamma R^2}}{2^{10} R^2 \eta}$ , where  $R \geq \|x(0)\|_2$  controls the radius outside of which the potential is strongly convex and  $\gamma$  is the Lipschitz constant for the potential gradient  $\nabla V$  over the domain (see section 2.1 of Ref. [47] and Ref. [74]). Here,  $\epsilon$  controls the error in the Wasserstein 1 norm, which for the confining potentials that we consider in this work is equivalent to weak convergence and convergence of first moments [75]. It is natural to assume  $R \in O(1)$ , but the Lipschitz constant  $\gamma$  may scale with the particle number  $\eta$  as well as the domain size, as is the case for the pairwise potentials we consider in this work. Indeed, we show in Theorem 1 that for the radially symmetric pair potentials made up of functions with bounded second derivative, the Lipschitz constant for the many-body potential gradient is  $\Theta(\eta)$ , meaning that the linear scaling with  $\eta$  is asymptotically tight. Thus, to simulate the overdamped Langevin equation with a non-convex potential up to time  $T$  and sample  $O(1/\epsilon^2)$  trajectories to estimate the reaction rates leads to an overall classical complexity of

$$\mathcal{C} \sim \frac{2^{10} T R^2 \eta^2 \log(\eta) e^{R^2 \gamma}}{\epsilon^4} \in O\left(\frac{T \eta^2 \log(\eta) e^{\Theta(\eta)}}{\epsilon^4}\right). \quad (11)$$

Therefore, our algorithm represents a quadratic speedup in the simulation time  $T$ , a quartic speedup in the accuracy  $\epsilon$ , and an *exponential* speedup in  $\eta$ , relative to the best known classical analytical bounds.

**Theorem 1.** *Let  $V : \mathbb{R} \rightarrow \mathbb{R}$  and assume that  $\nabla V$  is Lipschitz continuous with Lipschitz constant  $\gamma > 0$ . Further assume that  $\nabla V$  is everywhere differentiable. Let  $r_{ij} = \|\mathbf{x}_i - \mathbf{x}_j\|$  for all  $\mathbf{x}_i, \mathbf{x}_j$ . For  $\eta > 2$ , define the pair potential*

$$V_{\text{pair}} = \sum_{i=0}^{\eta-1} \sum_{j < i} V(r_{ij}).$$

*Then, the Lipschitz constant  $\text{Lip}(\nabla V_{\text{pair}}) \in \Omega(\eta\gamma)$ .*

The proof of this theorem is given in Appendix A.

Our complexity comparison assumes equivalent oracles for initial state access: classical methods require sampling from the Boltzmann distribution restricted to  $R$  and  $P$ , while our quantum algorithm analogously requires a coherent encoding of the quantum states  $|R\rangle$  and  $|P\rangle$ . This oracle model comparison isolates the dynamical computation.

We also wish to note that in practice, classical algorithms could outperform the worst-case estimates of Eq. (11). Under stronger assumptions on the convexity of the potential, when targeting the weak error estimates (i.e., producing  $\epsilon$  accurate expectation values), there exist classical methods (e.g., that of Ref. [76]) that can achieve a stepsize scaling as  $O(\sqrt{\epsilon})$ , leading to an overall  $\epsilon^{-2.5}$  scaling rather than the  $\epsilon^{-4}$  scaling predicted in Eq. (11). Although the stringent requirements on the convexity of the potential are required in order for the analytical statements to hold, numerical evidence suggests that these techniques may be more efficient in some circumstances, leading to a potentially reduced classical complexity. Nevertheless, this discrepancy between analytical predictions and the performance in practice of classical algorithms further highlights the difficulty of conducting a proper comparison of quantum and classical solvers for this task.

### III. OVERVIEW OF METHODOLOGY

#### A. Background on Kolmogorov equations

The Fokker-Planck equation (or forward Kolmogorov equation (FKE)) describes the deterministic evolution of a probability distribution over all possible stochastic trajectories associated with an overdamped Langevin equation. Some additional details on the Kolmogorov equations and derivations of some of the facts we present here can be found in Appendix B. Recall the expression for the dynamical generator of the FKE,

$$\mathcal{F}[\rho] = \nabla \cdot (\rho \nabla V + \beta^{-1} \nabla \rho), \quad (12)$$

and the associated first-order-in-time PDE,

$$\begin{aligned} \partial_t \rho(t) &= \mathcal{F}[\rho](t), \\ \rho(0) &= \rho_0, \end{aligned} \quad (13)$$

with  $\beta$  the inverse temperature,  $\rho_0$  an initial condition, and  $V$  a “confining” potential, meaning that  $V(|x|) \rightarrow \infty$  as  $x \rightarrow \infty$ . The assumption that  $V$  is confining is technical, in that it ensures both that  $\mathcal{F}$  is negative semi-definite, and that the equilibrium state is unique and Boltzmann distributed [19]. We note, however, that in non-confining potentials these properties may also be recovered by the enforcement of a homogeneous Neumann boundary condition.

Under the similarity transformation generated by  $\rho_\beta = \sqrt{\frac{e^{-\beta V}}{\mathcal{Z}}}$ , we have

$$\begin{aligned} \text{Ad}_{\rho_\beta}(\mathcal{F}) &:= \rho_\beta^{-1} \mathcal{F}[\rho_\beta] \\ \text{Ad}_{\rho_\beta}(\mathcal{F}) &= \beta^{-1} \Delta - \frac{\beta}{4} \|\nabla V\|^2(x) + \frac{1}{2} \Delta V(x) =: \mathcal{H}_\beta, \end{aligned} \quad (14)$$

where  $\mathcal{Z}$  is the partition function and  $\mathcal{H}_\beta$  is an explicitly self-adjoint Schrödinger-type operator. In the self-adjoint representation,  $\mathcal{H}_\beta$  admits a direct decomposition into a sum of squares

$$\begin{aligned} \mathcal{H}_\beta &= - \sum_{j \in [\eta d]} A_j^\dagger A_j \\ A_j &= -i \left( \sqrt{\beta^{-1}} \partial_{x_j} - \frac{\sqrt{\beta}}{2} F_j \right), \end{aligned} \quad (15)$$

where  $F_j = -\partial_{x_j} V$  is interpreted as a multiplication operator.

As described in Appendix B, the reaction rate can be expressed with respect to the generator  $\mathcal{H}_\beta$  as

$$k_{RP}(T) := \frac{1}{T} \sqrt{\frac{\bar{p}_R}{\bar{p}_P}} \langle P | e^{T\mathcal{H}_\beta} | R \rangle, \quad (16)$$

where

$$|R\rangle = \int 1_R(x) \frac{e^{-\beta V(x)/2}}{\sqrt{\mathcal{Z} \bar{p}_R}} |x\rangle, \quad (17)$$

$\bar{p}_R$  is the equilibrium probability of the region  $R$ ,

$$\bar{p}_R = \int dx 1_R(x) \mu(x), \quad (18)$$

and  $\mu(x) = \frac{e^{-\beta V(x)}}{\mathcal{Z}}$  is the equilibrium measure. From Eq. (16) we can identify the reactive flux,

$$\nu_{RP}(T) := \langle P | e^{T\mathcal{H}_\beta} | R \rangle = \langle 1_P, e^{T\mathcal{F}} 1_R \rangle_\mu. \quad (19)$$

This work will focus on developing a quantum algorithm for estimating the reactive flux, interpreted as the propagator overlap Eq. (19). With a small additional overhead to compute estimates to  $\bar{p}_R$  and  $\bar{p}_P$ , and access to the quantum state  $|R\rangle$  and  $|P\rangle$ , this information can then be used to compute the time-dependent reaction rate Eq. (16). Moreover, an estimate of reactive flux can also provide estimates of hitting times, since

$$\tau_{RP} := \inf\{t > 0 : \nu_{RP}(t) > 0\}. \quad (20)$$

This work may also readily be extended to compute the probabilities of transition states. The probability of realizing a transition state  $x$  at some time  $t$  is expressed as

$$\pi_{AB}(x, t) = \langle B | \rho^{-1} e^{(T-t)\mathcal{H}_\beta} \rho | x \rangle \langle x | \rho e^{t\mathcal{H}_\beta} \rho^{-1} | A \rangle. \quad (21)$$

Using  $|A| \equiv \text{vol}(A)$ , with  $\Pi_x = |x\rangle \langle x|$ , this can be simplified to

$$\pi_{AB}(x, t) \propto \frac{1}{\sqrt{|A| |B|}} \sum_{y' \in B, y \in A} \langle y' | e^{(T-t)\mathcal{H}_\beta} e^{-\beta V/2} \Pi_x e^{-\beta V/2} e^{t\mathcal{H}_\beta} | y \rangle. \quad (22)$$

Thus, the computation of the transition density, i.e., the probability of reaching a transition state located at configuration  $x$  at time  $t$  can also be reduced to computation of the overlap of a non-unitary matrix, albeit involving a more complex propagator correlation function.

## B. Matrix square root and Gaussian-LCHS

Broadly speaking, the recently developed LCHS and related methods [43, 44, 51, 77] show how to construct a function closely related to the Fourier transform of  $e^{-xt}$  that has exponentially rapid decay in Fourier space. Intuitively, just as the Feynman path integral provides a description of quantum states as a superposition over classical trajectories, the LCHS method can be regarded as providing a description of classical dynamics by] a linear combination over quantum trajectories. In this work we consider a scenario where we have access to a matrix  $\mathcal{A} = \mathcal{A}^\dagger$  such that  $-\mathcal{A}^2 = H$ , for  $H = H^\dagger \preceq 0$ , up to an embedding into a larger block-diagonal matrix, i.e.,  $\mathcal{A}^2$  may be of the form

$$-\mathcal{A}^2 = \begin{pmatrix} H & 0 \\ 0 & * \end{pmatrix}, \quad (23)$$

with  $*$  any square matrix and the 0 entries corresponding to rectangular matrices with zeros of appropriate dimension. For the Fokker-Planck generator in self-adjoint form, Eqs. (14) - (15), the dilated matrix square root  $\mathcal{A}$  takes the form

$$\mathcal{A} = \begin{pmatrix} 0 & A_0^\dagger & \cdots & A_{d\eta-1}^\dagger \\ A_0 & & & \\ \vdots & & & \\ A_{d\eta-1} & & & \end{pmatrix}, \quad (24)$$

with the  $A_j$  given by Eq. (15). Notice that this is distinct from the idea of a *block encoding*, where the off-diagonal entries are unknown quantities that ensure the overall unitarity of the block encoding. It is the block *diagonal* structure of  $\mathcal{A}^2$  that allows us to efficiently operate on  $H$ , since the top-left block of  $\mathcal{A}^2$  is decoupled from the rest of  $\mathcal{A}^2$ . In the case of time-independent  $H$  and  $\mathcal{A}$ , the LCHS approach naturally translates to this scenario, and efficient access to  $\mathcal{A}$  can provide a significant speedup over the input model for standard LCHS. We call this approach *Gaussian-LCHS*.

We begin with the observation that the Fourier transform of the function  $f_t(x) = e^{-x^2 t}$  is

$$\hat{f}_t(k) = \frac{e^{-k^2/4t}}{\sqrt{2t}}. \quad (25)$$

By assumption,  $H$  and  $\mathcal{A}$  are time-independent, and therefore the eigenvalues  $x$  of  $\mathcal{A}$  have no explicit dependence on  $t$ . Therefore the  $t$  dependence of the propagator  $e^{-\mathcal{A}^2 t}$  can be absorbed into the kernel function  $\hat{f}_t(k)$  and as a result, we have the relation

$$e^{-x^2 t} = \frac{1}{\sqrt{2\pi}} \int_{\mathbb{R}} \hat{f}_t(k) e^{-ikx} dk. \quad (26)$$

As with standard LCHS we truncate the domain of integration to an interval of finite width,

$$\tilde{f}_t(x) = \int_{-L_G}^{L_G} \hat{f}_t(k) e^{-ikx} dk, \quad (27)$$

where  $L_G \in \mathbb{R}^+$  is the truncation wavenumber. We show in Appendix E 1 that  $L_G$  can be chosen  $O\left(\sqrt{t \log(1/\epsilon)}\right)$ .

Exploiting the relationship that  $(\langle 0 | \otimes I)(-\mathcal{A}^2)(|0\rangle \otimes I) = H$ , where the dimension of  $|0\rangle$  is the dimension of  $H$  and the dimension  $I$  is the remainder, we can approximate  $e^{tH} = (\langle 0 | \otimes I)e^{-t\mathcal{A}^2}(|0\rangle \otimes I)$  using queries to a block encoding of  $\mathcal{A}$ , denoted  $U_{\mathcal{A}}$ . Since  $\mathcal{A}$  is Hermitian, the spectral theorem ensures that  $\mathcal{A}$  has real eigenvalues, and the Fourier transform formula Eq. (26) for  $x \in \mathbb{R}$  extends to the matrix-valued case by simply allowing  $x$  to be any eigenvalue of  $\mathcal{A}$ . To obtain a discrete sum, we follow the LCHS approach and apply a quadrature scheme to approximate Eq. (27). Following these steps, we obtain

$$e^{-\mathcal{A}^2 t} \approx \frac{1}{2\sqrt{t\pi}} \int_{-L_G}^{L_G} e^{-k^2/4t} e^{-ik\mathcal{A}} dk \approx \sum_{j=0}^{M_q-1} c_j(t) e^{-ik_j\mathcal{A}}, \quad (28)$$

where  $M_q \in O(L_G)$  is the number of quadrature points, and the coefficients  $c_j(t) = w_j e^{-k(j)^2/4t}$  with  $w_j$  the quadrature weights. This is derived in Appendix E 2. In Appendix E 3 we show that  $\alpha_g \equiv \sum_j |c_j(t)| \in O(1)$ .

When access to  $\mathcal{A}$  is provided via a block encoding and  $\alpha$  is the block encoding subnormalization factor, we can employ the Jacobi-Anger expansion, which provides a rapidly convergent polynomial approximation to  $\exp(\pm ikx)$  where the required polynomial degree scales as  $O(k\alpha + \log(1/\epsilon))$  [45]. Using quantum signal processing (QSP) we can then efficiently obtain a block encoding of the associated matrix exponential  $\exp(\pm ik\mathcal{A})$ . The overall error introduced from approximating the unitaries in the Gaussian-LCHS formula Eq. (28) to finite precision is analyzed in Appendix E 4. It is shown there that the query complexity for the block encoding of  $\mathcal{A}$  to approximate any term in the numerical quadrature scheme is upper bounded by

$$Q = O\left(\alpha \sqrt{t \log\left(\frac{1}{\epsilon}\right)} + \log\left(\frac{\alpha}{\epsilon}\right)\right). \quad (29)$$

Therefore, using Gaussian-LCHS with the Hamiltonian  $\mathcal{A}$ , we obtain an approximation to

$$e^{-\mathcal{A}^2 t} = \begin{pmatrix} e^{Ht} & 0 \\ 0 & * \end{pmatrix}, \quad (30)$$

using  $\tilde{O}\left(\alpha \sqrt{t \log\left(\frac{1}{\epsilon}\right)}\right)$  queries to the block encoding of  $\mathcal{A}$ . Combined with the lemmas of the previous sections, this leads to the following theorem, the proof of which is given Appendix E 4.

**Theorem 2.** *Let  $\mathcal{A}$  be an  $\mathcal{N} \times \mathcal{N}$  Hermitian matrix satisfying*

$$-\mathcal{A}^2 = H, \quad (31)$$

or

$$-\mathcal{A}^2 = \begin{pmatrix} H & 0 \\ 0 & * \end{pmatrix} \quad (32)$$

for  $H$  an  $N \times N$  negative definite or negative semi-definite Hermitian matrix with  $N \leq \mathcal{N}$ . Let  $U_{\mathcal{A}}$  be a block encoding of  $\mathcal{A}$  with subnormalization factor  $\alpha$  and let  $t > 0$ . Then, for any  $0 < \epsilon < \min\{\frac{1}{\alpha}, 1\}$ , there exists a quantum algorithm that queries  $U_{\mathcal{A}}$

$$O\left(\alpha \sqrt{t \log\left(\frac{1}{\epsilon}\right)} + \log\left(\frac{\alpha}{\epsilon}\right)\right) \quad (33)$$

times to produce a block encoding of a matrix  $\widetilde{e^{Ht}}$  satisfying

$$\|e^{Ht} - \widetilde{e^{Ht}}\| \leq \epsilon. \quad (34)$$

Moreover, the block encoding can be implemented using  $O\left(\log\left(\alpha \sqrt{t \log(1/\epsilon)}\right)\right)$  ancilla qubits and  $O\left(\alpha \sqrt{t \log(1/\epsilon)}\right)$  Toffoli or simpler gates in addition to those used in the block encoding of  $\mathcal{A}$ .

Applying this LCU to any tensor product state of the form  $|0\rangle |x\rangle$ , with  $|0\rangle, |x\rangle$  of appropriate dimensions, we will have  $e^{-\mathcal{A}^2 t} |0\rangle |x\rangle = |0\rangle e^{Ht} |x\rangle$ . We note that although each of the individual unitaries that make up the Gaussian-LCHS are realized with high probability, it is still the case that the preparation of a quantum state proportional to  $e^{-\mathcal{A}^2 t} |0\rangle |x\rangle$  can have vanishingly small success probability, as described in the introduction.

### C. Non-unitary overlap circuit

In this section we will explain the non-unitary overlap estimation circuit and the main operations that we perform in the algorithm. We will assume access to the following state preparation oracles which prepare normalized quantum states encoding the fixed ‘‘reactant’’ and ‘‘product’’ regions of the configuration space,  $R, P \subset [0, L]^{\eta d}$ . The corresponding oracles prepare the quantum states

$$\begin{aligned} O_R |0\rangle_{\text{sys}} &= \frac{1}{\sqrt{p_R}} \sum_{x \in R} \rho(x) |x\rangle \equiv |R\rangle \\ O_P |0\rangle_{\text{sys}} &= \frac{1}{\sqrt{p_P}} \sum_{x \in P} \rho(x) |x\rangle \equiv |P\rangle, \end{aligned} \quad (35)$$

where  $\rho(x) = \frac{e^{-\beta V(x)/2}}{\sqrt{Z}}$ . We shall also assume access to the controlled versions of both oracles (see Fig. 5) below.

For the purposes of demonstrating the main idea, in this section we will simply assume access to unitaries implementing  $\{e^{-ik_j \mathcal{A}}\}$  for  $j \in \{0, \dots, M_g - 1\}$  for  $\mathcal{A}$  corresponding to the dilated notion of matrix square root for the discretized  $\mathcal{H}_\beta$  operator given by Eq. (23). We will detail the implementation in later sections. Using the Gaussian-LCHS formulae, we obtain an expression for the non-unitary propagator in terms of a linear combination of unitaries,

$$e^{\mathcal{H}_\beta t} \approx \sum_{j=0}^{M_g-1} c_j(t) e^{-ik_j \mathcal{A}}. \quad (36)$$

For notational convenience we will write  $U_j \equiv e^{-ik_j \mathcal{A}T}$  to refer to the  $j$ th unitary, where  $k_j \in [-L_G, L_G]$  and  $c_j \in \mathbb{C}$  is the  $j$ th coefficient obtained from applying the quadrature scheme to the integrand.

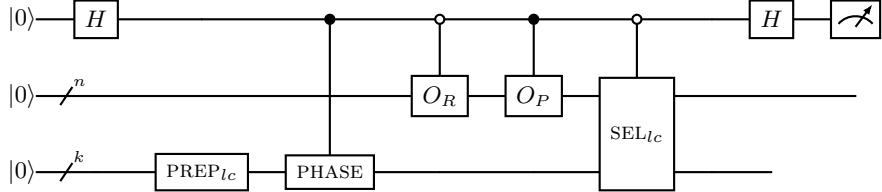


FIG. 5: Quantum circuit for non-unitary overlap estimation. This circuit uses the standard LCU PREP construction, a controlled version of the standard SEL routine, and an optional controlled PHASE oracle for complex and non-positive real coefficients. In conjunction with controlled state preparation, this circuit allows us to approximate  $\frac{1}{\alpha_g} \text{Re}(\langle P | e^{t\mathcal{H}_\beta} | R \rangle)$ .

Using the standard oracles from the LCU subroutine, we define

$$\text{PREP}_{lc} : |0\rangle \rightarrow \sum_j \sqrt{\frac{|c_j|}{\alpha_g}} |j\rangle, \quad \text{PHASE} : |j\rangle \rightarrow e^{-i\phi_j} |j\rangle \quad (37)$$

where  $\phi_j$  satisfies  $c_j = |c_j| e^{i\phi_j}$ , and the select oracle,

$$\text{SEL}_{lc} = \sum_j U_j \otimes |j\rangle \langle j|. \quad (38)$$

When all coefficients  $c_j$  in the formula are positive, the controlled-PHASE operation is unnecessary. As shown in Fig. 5, we make a simple modification to the Hadamard test and LCU circuits to obtain a quantum circuit that can be used for estimating overlaps of the non-unitary propagator. Analysis of this circuit shows that the expectation value of the Pauli-Z matrix on the top qubit satisfies

$$\langle \Phi | Z | \Phi \rangle = \frac{1}{\alpha_g} \text{Re}(\langle P | e^{\mathcal{H}_\beta t} | R \rangle). \quad (39)$$

We provide a detailed derivation of this result in Appendix G.

**Lemma 3.** *Let  $H$  be represented by the LCU*

$$H = \sum_{l=0}^{K-1} |c_l| e^{i\phi_l} U_l, \quad (40)$$

*with  $2^k \leq K \leq 2^{k+1}$  for some  $k \geq 1$ , and  $\alpha = \sum_l |c_l|$ . For any input states  $|\phi\rangle$  and  $|\psi\rangle$  constructed with oracles  $O_\psi$  and  $O_\phi$ , the quantum circuit in Fig. 5 can be used to estimate*

$$\langle \phi | \frac{H}{\alpha} |\psi\rangle, \quad (41)$$

*independent of the success probability of implementing the LCU, provided the  $U_l$  are unitaries.*

Surprisingly, even though the application of the block encoding of  $e^{\mathcal{H}_\beta t}$  to an arbitrary quantum state can have success probability that decays exponentially with  $t$ , the quantum circuit in Fig. 5 succeeds with high probability. This is because the unitaries  $U_j$  can be efficiently constructed with arbitrarily high success probability, since the circuit does not require any postselection on the ancilla qubits used to construct the linear combination of these unitaries. Therefore, even though the preparation of any particular quantum state of the form  $e^{\mathcal{H}_\beta t} |x\rangle$  may require many rounds of amplitude amplification, this circuit can estimate overlaps of the form,  $\langle y | e^{\mathcal{H}_\beta t} |x\rangle$  independent of the success probability of preparing a state proportional to  $e^{\mathcal{H}_\beta t} |x\rangle$ . This important fact highlights why the LCHS formulation of this problem is critical to this algorithm. Specifically, whereas using approaches based on direct polynomial approximation of the function  $e^{-|x|t}$  via QSP require post-selection on the success state of the block encoding, in contrast, the block encoding of the unitary operation made in our algorithm is realized with arbitrarily high success probability. We note that for the problem of preparing a quantum state proportional to  $e^{\mathcal{H}_\beta t} |u(0)\rangle$ , both LCHS and polynomial-based approaches have similar success probabilities, but they have very different complexities for the computation of overlaps.

#### D. Discussion on reactant state preparation

For the computation of reaction rates, we have assumed access to state preparation oracles encoding the Boltzmann weighted probability of being in the reactant and product regions of configuration space. In full generality, the preparation of these states is at least as difficult is likely harder in the generic non-convex setting we describe. The discerning reader may object that we have simply hid the complexity of our algorithm into these oracles and that quantum advantage is simply the result of our assumptions. However, we wish to establish at least one physically motivated scenario where the preparation of quantum states of the form

$$|R\rangle = \int_{x \in R} \frac{e^{-\beta V(x)/2}}{\sqrt{\mathcal{Z}_R}} |x\rangle, \quad \mathcal{Z}_R = \int_{x \in R} e^{-\beta V(x)} dx, \quad (42)$$

can be much more efficient than preparation of a quantum state encoding the (square root of) the full Boltzmann distribution.

In many problems of practical interest, one wishes to study the behavior of transitions between metastable configurations of the system. Such configurations correspond to local minima of the potential energy surface. Mathematically, this corresponds to the Hessian of the potential in that region being locally positive. Assume that the restriction  $V(x)|_{x \in R}$  is  $m$  strongly convex meaning,

$$\inf_{x \in R} \text{Hess}(V(x)) \succeq mI$$

for some  $m > 0$ . The approach we use to obtain an efficient algorithm is to augment the locally convex portion of the potential with a confining potential, and solving the problem with the augmented confining potential over the whole domain. One natural choice of an augmented potential  $V_R(x)$  is,

$$V_R(\mathbf{x}) = \begin{cases} V(\mathbf{x}) & \mathbf{x} \in R \\ V(\mathbf{x}) + \kappa \text{dist}(\mathbf{x}, \partial R)^2 & \mathbf{x} \in R^c, \end{cases} \quad (43)$$

where the parameter  $\kappa > 0$  controls the accuracy of the approximation. This construction is demonstrated in Fig. 6 below.

With these assumption and the above construction, we can establish that there exists a quantum algorithm that can produce a quantum state encoding of the local equilibrium  $|R\rangle$  with polynomial overhead.

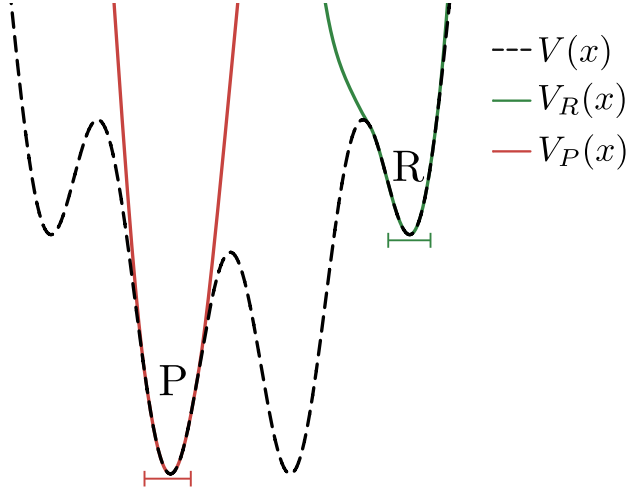


FIG. 6: The potential  $V(x) = \cos(2\pi x) + x^2$  is shown in dashed black lines. The reactant and product regions,  $R$  and  $P$ , are marked by the green and red lines under the graph respectively. The red and green curves are generated with a confining augmented potential having  $\kappa = 20$ : they preserve  $V(x)$  over  $R$  and  $P$ , and confine the particle trajectories to be within these initial and final regions, respectively. Under the dynamics generated by the Fokker-Planck equation with the convex potentials  $V_R$  and  $V_P$ , the system decays exponentially to the equilibrium distribution of  $V$  over  $R$  and  $P$  with controllable error determined by  $\kappa$ .

**Theorem 4.** *Fast thermal state preparation in locally convex region.* Let  $R$  be a convex open subset of  $[-L, L]^d$ . Assume that,

$$\inf_{x \in R} \text{Hess}(V(x)) \succeq mI.$$

Assume the warm start condition that an initial state  $|R_0\rangle$  has constant overlap with the target quantum state,

$$|R\rangle = \begin{cases} \int_{x \in R} \frac{e^{-\beta V(x)/2}}{\sqrt{\mathcal{Z}_R}} |x\rangle & x \in R, \\ 0 & \text{else} \end{cases}, \quad \mathcal{Z}_R = \int_{x \in R} e^{-\beta V(x)} dx. \quad (44)$$

Let  $V_R$  be the augmented potential from Eq. (43),  $\alpha_V = \max_{r \leq \sqrt{d}L} \frac{|V'(r)|}{r}$ , and  $\kappa \in O\left(\frac{1}{\epsilon^4 \mathcal{Z}_R^2 \beta}\right)$ , satisfying

$$\left\| e^{-\beta V_R/2} - |R\rangle \right\|_{L^2} \leq \epsilon.$$

Moreover, there exists a quantum algorithm preparing the state  $|\tilde{R}\rangle$  such that

$$\left\| |R\rangle - |\tilde{R}\rangle \right\|_{L^2} \leq \epsilon$$

using

$$\tilde{O}\left(\sqrt{\frac{\eta d}{2m}} \left(\beta \eta L(\alpha_V + \kappa) + \frac{N}{L}\right)\right),$$

queries to the block encoding of  $\mathcal{A}$ , where the  $\tilde{O}$  notation suppresses polylogarithmic factors in  $1/\epsilon$ .

The proof of this theorem is given in Appendix C.

#### IV. ANALYSIS AND CONSTRUCTION OF CORE SUBROUTINES

In this section we construct the core subroutines that are needed to realize the quantum circuit provided in Fig. 5. First, we show how to block encode a generic matrix satisfying Eq. (23). We then show how to block encode the

square root matrix  $\mathcal{A}$  for Schrödinger-type operators  $\mathcal{H}_\beta$  in the form of Eq. (14)) in first quantization and detail the block encodings of the individual terms that make up the block matrix encoding the square root. We then provide a scheme to efficiently construct the propagator using a multiplexed version of QSP combined with the Gaussian-LCHS method. To conclude this section, we bound the sampling costs as well as the sources of error in the method.

### A. Block encoding sum-of-squares Fokker-Planck operator

Recall the decomposition of the self-adjoint representation of the Fokker-Planck operator, Eq. (14), as

$$\begin{aligned}\mathcal{H}_\beta &= - \sum_{j \in [\eta]} A_j^\dagger A_j \\ A_j &= -i \left( \frac{1}{\sqrt{\beta}} \nabla_j + \sqrt{\beta} F_j \right),\end{aligned}\tag{45}$$

where  $F_j = -\nabla_j V$ . We will discretize the continuum operators in  $A_j$  using a plane-wave based spectral method. The differential operators become multiplication operators in the Fourier basis  $\nabla_j \rightarrow -ik_l |l\rangle \langle l|_j$ , and the diagonal multiplication operator  $F_j$  is treated by quantum Fourier transform. We will consider particles interacting via a radially symmetric pair-wise potential  $V = \sum_{i \in [\eta]} \sum_{j < i} V_{ij}$ , where  $V_{ij} = V(r_{ij})$  and  $r_{ij} = \|\mathbf{x}^i - \mathbf{x}^j\|$ . Under the assumption that the potential  $V$  is confining, the probability of the system occupying a state near the boundaries of the simulation box is exponentially small. Therefore, we may truncate the domain to some finite length  $L > 0$  that depends on the growth rate of the potential as  $\mathbf{x} \rightarrow \infty$  with minimal effect on the simulation accuracy, and enforce periodic boundary conditions so that the single-particle domain is defined over the  $d$ -dimensional torus  $[-L, L]^d$ .

**Theorem 5.** *Let  $N = 2^n$  be the number of plane wave modes per degree of freedom, for  $\eta$  particles occupying a  $d$ -dimensional reciprocal lattice  $\mathbf{G} = \mathbb{Z}_N^d$ , corresponding to a discretization of the real space  $[-L, L]^d$  for each particle. Let  $V$  be a potential function given by a polynomial of degree  $2k$  in the pair-wise distance between any distinct pairs particles  $i, j$ , with no term of degree 1, and let  $\alpha_V = \max_{\|r\| \leq \sqrt{d}L} \left| \frac{V'(r)}{r} \right|$ . Then there exists a quantum circuit that block encodes the plane wave representation of the operator*

$$\mathcal{A} = \sum_{j \in [\eta]} |0\rangle \langle j+1| \otimes A_j^\dagger + |j+1\rangle \langle 0| \otimes A_j\tag{46}$$

with subnormalization factor

$$\alpha_A \in O \left( \sqrt{\beta d} \eta^{3/2} L \alpha_V + \sqrt{\frac{\eta d}{\beta}} \frac{N}{L} \right),\tag{47}$$

using

$$\tilde{O}(\eta d n + 2k d n^2 + (nd)^2)\tag{48}$$

Toffoli or simpler gates, with the logarithmic factors hidden by the  $\tilde{O}$  notation arising from small overheads to compile finite precision rotation gates and multi-controlled operations.

The proof of Theorem 5 can be found in Appendix J.

### B. Block encoding propagator with Gaussian-LCHS

We now show how to implement the LCHS using  $\tilde{O}(\alpha_A \sqrt{t})$  queries to the block encoding of  $\mathcal{A}$ , which we denote as  $U_{\mathcal{A}}$ . Recall the expression for the propagator obtained by the Gaussian-LCHS formula

$$e^{-\mathcal{A}^2 t} \approx \sum_{j=0}^{M_q-1} w_j f_t(k(j)) e^{-ik(j)\mathcal{A}},\tag{49}$$

where  $k(j) \in [-L_G, L_G]$ ,  $j \in \{0, \dots, M_q - 1\}$  is the  $j$ th quadrature point,  $w_j$  is the  $j$ th weight in the Gauss quadrature, and  $f_t(k(j)) = \frac{e^{-\frac{k^2(j)}{4t}}}{2\sqrt{\pi t}}$ . This requires forming block encodings of each of the unitary matrices  $\mathcal{U}_j = e^{-ik(j)\mathcal{A}}$ . We use the Jacobi-Anger expansion to obtain a polynomial approximation to  $e^{i\mathcal{A}k}$  for  $k \in [-L_G, L_G]$ :

$$e^{ik\mathcal{A}} = J_0(k) + 2 \sum_{l \in \text{evens} > 0} (-1)^{l/2} J_l(k) T_l(\mathcal{A}) + 2i \sum_{l \in \text{odds} > 0} (-1)^{(l-1)/2} J_l(k) T_l(\mathcal{A}). \quad (50)$$

Therefore,  $k(j)$ , which can be thought of as the simulation time, is a function of the *coefficients* in the polynomial approximation, given by the Bessel  $J$  functions. For a fixed  $k$  and  $\epsilon$ , the polynomial degree  $D_k$  is chosen according to the bound

$$D_k = O\left(k\alpha_A + \log\left(\frac{1}{\epsilon}\right)\right). \quad (51)$$

We express the polynomial obtained by the Jacobi-Anger expansion abstractly as

$$P_k(\mathcal{A}) = \sum_{l=0}^{D_k-1} c_l(k) T_l(\mathcal{A}) \approx e^{ik\mathcal{A}}, \quad (52)$$

with the  $c_l(k)$ 's given explicitly by (50).

If we were to naively apply QSP to each term in the LCHS formula independently, we would require  $\tilde{O}(k(j)\alpha_A)$  queries to the block encoding of  $\mathcal{A}$  for each term. Since each term in the LCU has additive cost, this would entail an overall cost of  $\sim \sum_{j=0}^{M_q} k(j) \in O(L_G^2) \in O(t \log(\frac{1}{\epsilon}))$ . We will now demonstrate a block encoding of the above LCHS that uses only  $O(L_G)$  queries to  $U_{\mathcal{A}}$  and additionally does not require any controlled applications of  $U_{\mathcal{A}}$ , using a technique that we call *multiplexed QSP*.

**Lemma 6.** [Multiplexed QSP] Let  $U_A$  be an  $(\alpha, a)$  block encoding of  $A \in \mathbb{C}^{2^n \times 2^n}$ . Let  $\{P_0, \dots, P_{M-1}\}$  be a set of polynomials of degrees  $d_0, \dots, d_{M-1}$  respectively satisfying

1.  $|P_i(x)|^2 \leq 1 \forall x \in [-1, 1]$  and  $\forall i \in \{0, \dots, M-1\}$
2.  $\forall i \in \{0, \dots, M-1\}$ ,  $d_i \equiv p \pmod{2}$  for fixed  $p \in \{0, 1\}$ .

Then, for any  $|c\rangle = \sum_{j=0}^{M-1} c_j |j\rangle$  satisfying  $\langle c|c\rangle = 1$ , and any  $n$  qubit quantum state  $|\psi\rangle$ , there exists a quantum circuit using  $d_{\max} := \max\{d_0, \dots, d_{M-1}\}$  queries to  $U_A$  and  $\tilde{O}(M)$  additional Toffoli or simpler gates to implement the quantum state

$$\sum_{j=0}^{M-1} c_j P_j \left( \frac{A}{\alpha} \right) |\psi\rangle |0\rangle_{a+1} |j\rangle + |\perp\rangle. \quad (53)$$

The proof of this lemma is provided in Appendix F.

Remarkably, multiplexed QSP does not increase the overall query complexity to the block encoding, nor does it require controlled applications of the block encoding. Indeed, the total query complexity to  $U_{\mathcal{A}}$  for constructing the linear combination over  $U_{P_{k(j)}(\mathcal{A})}$  is  $D_{\max}$  (see Eq. (54) below) and is *independent* of  $M_q$ , the number of terms in the linear combination. Nevertheless, there is still a dependence of  $O(M_q \log(M_q))$  additional Toffoli gates needed to implement the control logic, which is subdominant to the block encoding cost.

Since  $k(j) \leq L_G \in O(\sqrt{t \log(1/\epsilon)})$  by Lemma 14 in Appendix E 1, the maximum polynomial degree that is needed to approximate any of the operators  $\{e^{ik(j)\mathcal{A}}\}_{j=0}^{M_q-1}$  is

$$D_{\max} = O\left(\alpha_A \sqrt{t \log(1/\epsilon)} + \log\left(\frac{1}{\epsilon}\right)\right). \quad (54)$$

For each of the polynomials  $P_{k(j)} \approx e^{ik(j)\mathcal{A}}$ , there is an associated set of phase factors  $\Phi^j \in \mathbb{R}^{D_{k(j)}+1}$ , where  $j \in \{0, \dots, M_q - 1\}$ . Let  $\Phi_i^j \in \mathbb{R}$  be the  $i$ th phase factor associated with the  $j$ th polynomial. Append a register of  $q = \lceil \log(M_q) \rceil$  ancilla qubits and let  $\mathcal{S}_i^j = e^{iZ_{\Pi} \Phi_i^j}$  be provided as an oracle which implements the  $i$ th rotation corresponding to the coefficients for the  $j$ th polynomial. The resulting quantum circuit implementation is provided as Fig. 7.

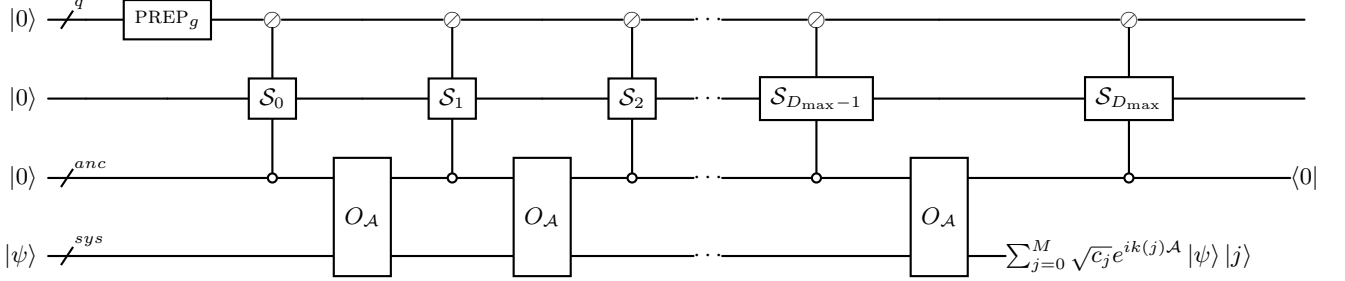


FIG. 7: Quantum circuit description of multiplexed QSP using the rotated block encoding  $O_A = U_A Z_{\Pi}$ . This circuit allows one to evaluate multiple polynomials of the block encoding of  $\mathcal{A}$  simultaneously by encoding the phases for the corresponding polynomial into the phase oracle  $\mathcal{S}$ , so that applying  $\mathcal{S}_i^j = e^{i\phi_i^j Z_{\Pi}}$  to the single ancilla qubit implements the  $i$ th phase factor for the  $j$ th polynomial. Remarkably, this circuit requires no controlled applications of the block encoding, and precisely  $D_{\max} = \max_l \{D_l\}$  queries to  $O_A$ . Here,  $q = \lceil \log(M_q) \rceil$  is the number of ancilla qubits needed to realize the coefficients for the Gaussian-LCHS formula.

Let  $\alpha_g = \sum_{j=0}^{M_q-1} |c_j(t)| \leq 1 + O(\epsilon)$  be the subnormalization factor associated with the quadrature function  $c_j(t)$ , which is given by the Gaussian-LCHS coefficients  $c_j(t) = w_j L_G \hat{f}_t(k(j))$ , with  $w_j$  the quadrature weight. Construct a superposition over the  $q = \lceil \log(M_q) \rceil$  qubit ancilla register,

$$\text{PREP}_g : |0\rangle_q \rightarrow \sum_{j=0}^{M_q-1} \sqrt{\frac{c_j(t)}{\alpha_g}} |j\rangle_q, \quad (55)$$

and apply the quantum circuit from Fig. 7 to obtain

$$\begin{aligned} |0\rangle_q |0\rangle_{m+1} |\psi\rangle_n &\rightarrow \sum_{j=0}^{M_q-1} \sqrt{\frac{c_j(t)}{\alpha_g}} |j\rangle_q (|0\rangle_{m+1} P_{k(j)}(\mathcal{A}) |\psi\rangle_n + |\perp\rangle) \\ &\approx \sum_{j=0}^{M_q-1} \sqrt{\frac{c_j(t)}{\alpha_g}} |j\rangle_q (|0\rangle_{m+1} e^{ik(j)A} |\psi\rangle_n + |\perp\rangle). \end{aligned} \quad (56)$$

By inspecting the circuit in Fig. 7 it is clear that the overall query complexity to  $U_A$  is

$$D_{\max} = O\left(\alpha_A \sqrt{t \log(1/\epsilon)}\right), \quad (57)$$

and the number of ancilla qubits used in addition to those used to construct  $U_A$  is  $\lceil \log(M_q) \rceil$ . Since the unitaries  $U_j$  can be implemented with success probability arbitrarily close to 1, the quantum circuit in Fig. 7 prepares a *superposition* of Hamiltonian simulations, which is distinct from a general linear combination, since the quantum state that we wish to sample from at the end of the circuit is approximately  $l_2$  normalized.

**Theorem 7** (Complexity to perform Gaussian-LCHS). *Let  $\mathcal{A}$  be given by its  $(\alpha_A, m)$  block encoding, and let  $t > 0$ . Then, for any  $\epsilon > 0$ , there exists a quantum algorithm that prepares an  $\epsilon$  approximation to the quantum state*

$$\sum_{j=0}^{M_q-1} \sqrt{\frac{c_j(t)}{\alpha_g}} |j\rangle_q (|0\rangle_{m+1} e^{ik(j)A} |\psi\rangle_n + |\perp\rangle), \quad (58)$$

in the  $l_2$  norm, using  $O\left(\alpha_A \sqrt{t \log\left(\frac{1}{\epsilon}\right)} + \log\left(\frac{1}{\epsilon}\right)\right)$  queries to  $\mathcal{A}$  and  $O(M_q \log(M_q) + \log\left(\frac{M_q}{\epsilon}\right))$  additional one and two qubit gates, with a normalization factor  $\alpha_g \in O(1)$  by Lemma 16.

*Proof.* Use Hamiltonian simulation to obtain an  $\epsilon$  block encoding of  $e^{ik(j)A}$  in the spectral norm. Since  $k(j) \leq L_G \in O\left(\sqrt{t \log\left(\frac{1}{\epsilon}\right)}\right)$ , this can be obtained with QSP and a polynomial of degree  $O\left(\alpha_A \sqrt{t \log\left(\frac{1}{\epsilon}\right)} + \log\left(\frac{1}{\epsilon}\right)\right)$ . By the construction of Lemma 6, the maximum polynomial is also the number of queries needed to form the superposition from above. The additional  $O(M_q \log(M_q) + \log\left(\frac{M_q}{\epsilon}\right))$  one and two qubit gates result from the state preparation of the coefficient state as well as the control logic needed to implement the multiplexed operations in the circuit of Fig. 7. This ensures that the quantum state Eq. (58) is  $\epsilon$  close in  $l_2$  norm and suffices to prove the theorem.  $\square$

**Corollary 1** (Gate complexity of Gaussian-LCHS applied to Fokker-Planck equation). *Let  $\mathcal{H}$  be the self-adjoint representation of the Fokker-Planck operator, and let  $t, \epsilon > 0$ . Assume that each particle is represented using  $nd$  qubits, corresponding to  $N^d$  plane wave modes. Assume that  $L, \alpha_V, d \in O(1)$ , and  $\sqrt{\beta} \gg \sqrt{\beta}^{-1}$ . Then the superposition of Hamiltonian simulations can be implemented using  $O\left((\sqrt{\beta}\eta^{5/2}n + \eta^{3/2}n^2)\sqrt{t\log(\frac{1}{\epsilon})}\right)$  Toffoli or simpler gates.*

*Proof.* Apply Theorem 7 to the block encoding from Theorem 5, and substitute the bounds for  $\alpha_A$  and the cost to perform the block encoding from the costs reported in Theorem 5.  $\square$

### C. Overlap estimation algorithm

With all of the core subroutines constructed, we now analyze the complexity of estimating the propagator overlaps needed to evaluate the rate constant, using the non-unitary overlap estimation circuit in Fig. 5 to approximate the reactive flux

$$\nu_{RP} \propto \langle P | e^{t\mathcal{H}_\beta} | R \rangle. \quad (59)$$

Post-selecting on the ancilla qubits used to form the block encoding of the unitary operation  $e^{-ik(j)\mathcal{A}}$ , the output of this circuit is a quantum state of the form

$$|\Phi\rangle := \frac{1}{2} \left( \sum_l \sqrt{\frac{c_l}{\alpha_g}} |0\rangle |0\rangle_{sys} \left( e^{-ik(l)\mathcal{A}} |R\rangle_{sys} + |P\rangle_{sys} \right) |l\rangle_k + \sum_l \sqrt{\frac{c_l}{\alpha_g}} |1\rangle |0\rangle_{sys} \left( e^{-ik(l)\mathcal{A}} |R\rangle_{sys} - |P\rangle_{sys} \right) |l\rangle_k \right). \quad (60)$$

The desired information is contained in a single qubit Pauli- $Z$  measurement,

$$\langle \Phi | Z_0 | \Phi \rangle = \frac{1}{2\alpha_g} \text{Re} \left( \langle P | e^{t\mathcal{H}_\beta} | P \rangle \right), \quad (61)$$

where  $Z_0$  is the Pauli- $Z$  operation on the top ancilla qubit in Fig. 5.

We can directly sample from the top ancilla qubit in Fig. 5, which attains the standard quantum limit and requires  $O(1/\epsilon^2)$  circuit repetitions, since  $\alpha_g$  and  $\text{Var}(\langle Z \rangle) \in O(1)$ . Sampling at this rate is sufficient if the desired error tolerance is reasonably large. On the other hand, if  $\epsilon \ll 1$ , it may be beneficial to use QAE or some variant thereof to estimate this quantity with  $O(1/\epsilon)$ . QAE essentially uses the quantum circuit in Fig. 5 in a quantum phase estimation circuit in a Grover iterate, which increases the circuit depth by a factor of  $O(1/\epsilon)$  and requires an additional  $O(\log(1/\epsilon))$  ancillae, but reduces the sample complexity to  $O(1)$ . We note that since amplitude estimation produces an  $\epsilon$  approximation of the *square root* of the probability, this does increase the query complexity by a factor of 2 due to the error propagation from squaring a number in  $(0, 1)$ . However, the detailed value of the desired error tolerance will determine whether the additional circuit overhead induced by adding QAE to achieve  $O(1/\epsilon)$  scaling is worthwhile for a specific instance. Theorem 8 below expresses the overall complexity for calculation of the reactive flux, including quantum amplitude estimation to arrive at the  $O(1/\epsilon)$  Heisenberg scaling.

**Theorem 8** (Complexity to compute reactive flux). *Let  $\epsilon, t > 0$ . Given access to quantum states  $|R\rangle$  and  $|P\rangle$  as defined in Eq. (19), and a block encoding of the matrix square root  $\mathcal{A}$ , with subnormalization factor  $\alpha_A \in O\left(\sqrt{\eta d} \left(\eta L \alpha_V \sqrt{\beta} + \sqrt{\beta^{-1}} N\right)\right)$ , with  $L, \alpha_V$  as in Theorem 5 and with a potential given by a polynomial of degree  $2k$ . There exists a quantum algorithm that outputs an approximation  $\tilde{\nu}_{RP}$  to the quantity*

$$\nu_{RP} = \langle P | e^{t\mathcal{H}_\beta} | R \rangle, \quad (62)$$

satisfying

$$|\tilde{\nu}_{RP} - \nu_{RP}| \leq \epsilon \quad (63)$$

that uses  $O\left(\frac{\sqrt{t}\alpha_A}{\epsilon} (\eta dn + 2kdn^2 + (nd)^2)\right)$  Toffoli or simpler gates and queries the state preparation oracles an additional  $O(1/\epsilon)$  times.

*Proof.* Simply apply amplitude estimation to the quantum circuit in Fig. 5, and implement the block encoding using the costs reported in Theorem 5 and the time evolutions using Corollary 1.  $\square$

Up to this point, our discussion has focused on achieving additive error in our estimates of the reactive flux. While relative error (requiring  $O(\frac{1}{P\epsilon^2})$  samples for a reaction occurring with probability  $P$ ) is necessary for precise quantification of reaction rates, many practical questions can be answered with additive error. For instance, determining whether a reaction rate falls below a safety threshold, comparing the relative efficiency of different catalysts, or determining if a reaction occurs with non-zero probability within some fixed time horizon, only require that our estimate has sufficient precision to distinguish the quantity from zero or from another value. For such additive-error questions, our quantum algorithm will achieve a sample complexity of  $O(\frac{1}{\epsilon})$  via amplitude estimation, independent of the actual magnitude of the reactive flux. For example, if we wish to determine whether the reaction occurs with probability  $< 10^{-6}$ , then we require only  $\Omega(10^3)$  queries to our quantum algorithm, while  $\Omega(10^6)$  queries to the classical algorithm are required to estimate the same quantity<sup>1</sup>

Finally, to obtain the time-dependent reaction rate we need only to combine our estimates of the reactive flux with the ratio of probabilities of being in the reactive and product states. Since

$$k_{RP}(T) = \frac{1}{T} \sqrt{\frac{\bar{p}_R}{\bar{p}_P}} \nu_{RP}(T),$$

with  $\bar{p}_R = \frac{Z_R}{Z}$ , we have  $\sqrt{\frac{\bar{p}_R}{\bar{p}_P}} = \sqrt{\frac{Z_R}{Z_P}}$  suffices to obtain estimates to the partition functions in the reactant and product regions. When  $R$  and  $P$  correspond to locally convex regions, these quantities can be efficiently obtained with a small additive overhead.

## V. DISCUSSION

We have constructed and analyzed a quantum algorithm that allows one to evaluate overlaps of the non-unitary propagator corresponding to the Kolmogorov equations using the method of Gaussian-LCHS, allowing calculation of classical correlation functions and hence of classical reaction rates. The quantum algorithm can estimate these overlaps to additive accuracy  $\epsilon$  using

$$\tilde{O} \left( (\eta dn + 2kdn^2 + (nd)^2) \sqrt{\eta d} \left( \eta L \alpha_V \sqrt{t\beta} + \sqrt{t\beta^{-1}} \frac{N}{L} \right) \epsilon^{-1} \right) \quad (64)$$

Toffoli or simpler quantum gates. In the regime where the dimension  $d$ , the polynomial degree  $2k$ , and the domain size  $L$  are all  $O(1)$ , this simplifies to

$$\tilde{O} \left( \frac{\eta^{5/2} \alpha_V \sqrt{t\beta} + \eta^{3/2} \sqrt{\frac{t}{\beta}} N}{\epsilon} \right), \quad (65)$$

with  $\alpha_V = \max_{\|r\| \leq \sqrt{d}L} \left| \frac{V'(r)}{r} \right|$ .

As evident from the scaling, our quantum algorithm has some favorable properties. First, it does not suffer from exponentially small success probabilities as we increase the simulation time  $t$ . Second, it achieves sub-linear dependence on both the simulation time and the inverse temperature  $\beta$ . Our approach is also extendable to more near-term approaches if the unitary evolution is implemented using splitting algorithms, such as Trotter, for the Hamiltonian simulation. The current work also shows a potentially *exponential* separation between the complexity of computing overlaps of generators with negative logarithmic norm and the complexity of preparing solution states and estimating the observables of a state. Thus, it is of general interest to find additional applications in dissipative high-dimensional PDEs that can be reduced to estimating such propagator overlaps, i.e., correlation functions between initial and time-evolved final states, rather than requiring the preparation of solution states. Furthermore, these propagator overlaps are directly related to experimentally relevant quantities such as transport coefficients and response functions.

We have provided a detailed analysis of the main costs that contribute to the overall complexity of the algorithm, including the block encoding of the square root matrix  $\mathcal{A}$  and the efficient implementation of the (Gaussian) LCHS approach using the construction of a new multiplexed QSP. Furthermore, we have analyzed the cost to estimate an observable of physical relevance in simulations of this type, namely, the reaction rate, providing an estimation for the

<sup>1</sup> More precisely, to determine if the probability that a reaction occurs is less than  $P$ , a quantum algorithm requires  $\Omega(\frac{1}{\sqrt{P}})$  queries, whereas  $\Omega(\frac{1}{P})$  queries are required classically.

cost of performing a realistic quantum computation of this type in an end-to-end fashion, with the block encoding, time evolution, and observable estimation costs all analyzed in detail. We also showed that this work can also be readily extended to the computation of hitting times and estimating the probability of particular transition states. We have analyzed one technique to efficiently construct quantum states encoding the reactant and product states when these correspond to local minima of the potential energy surface. However, we have left the detailed implementation of this subroutine as a subject for future work.

Under the assumptions of Theorem 1 and the sharpest known analytical bounds for time evolution of the stochastic dynamics of the corresponding overdamped Langevin in non-convex potentials, the classical complexity of estimating the reaction rate to additive error  $\epsilon$  using trajectory-based methods was shown in Ref. [47] to scale as

$$\mathcal{C} = O\left(\frac{t\eta^2 \log(\eta) e^L}{\epsilon^4}\right).$$

When the Lipschitz constant  $L$  scales linearly with  $\eta$  (as proven for radially symmetric pair potentials in this work (Theorem 1)), this classical bound becomes exponential in  $\eta$ . In contrast, our quantum algorithm scales polynomially in  $\eta$ , yielding an exponential separation in particle number with respect to these worst-case classical bounds, together with a quartic separation in accuracy  $\epsilon$ , and a quadratic separation in simulation time  $t$ . The classical exponential scaling with  $\eta$  is a result of the classical method requiring an exponentially small step size in the Lipschitz constant  $L$ , which is used as a measure of the non-convexity of the potential. In this context, it is remarkable that for finite time simulations, our quantum algorithm has negligible dependence on the convexity of the potential. However, we further note that for sampling from the equilibrium distribution, both quantum and classical algorithms must show a dependence on the convexity of the potential, which can be viewed as resulting from the long times required to escape from metastable configurations. It is therefore unlikely that an exponential quantum advantage persists for equilibrium sampling of general many-body states using the methods we propose in this work.

We also emphasize that these rigorous classical bounds are derived under general assumptions and may be overly pessimistic for specific problems, as noted earlier in this paper. Indeed, specialized classical heuristics often perform better in practice than the worst-case analytic treatment predicts. Consequently, direct empirical comparisons on concrete problem instances will be necessary to fully quantify the achievable quantum advantage in practice. Nevertheless, the polynomial-vs-exponential scaling in  $\eta$  found here for the calculation of reaction rates of classically interacting many-body systems as described by the Kolmogorov equations highlights a compelling route toward quantum advantage in regimes where classical methods are provably strained. This is particularly important because quadratic speedups alone are often insufficient for achieving practical advantage [78].

There are several avenues for practical improvements to the current quantum algorithm in this work. First, the  $\eta^{5/2}$  scaling presents a target for further optimization. There are two sources of this scaling. One factor of  $\eta^{3/2}$  comes from the subnormalization factor in the block encoding of  $\mathcal{A}$ . The other factor of  $\eta$  comes from the number of elementary operations we needed to realize a block encoding of the many-body potential. This is suboptimal when compared to classical methods, which achieve  $O(\eta^2)$  scaling for force evaluations, before applying optimizations such as the fast multipole method [73], which further reduce the scaling to  $O(\eta \log(\eta))$ . One reason for the difficulty in improving over the  $\eta^{5/2}$  quantum scaling is that the quantum algorithm, which is fundamentally discretizing a many-body differential operator, is evaluating the forces applied between particles occupying all possible configurations simultaneously. Thus, it is unclear how methods based on the fast-multipole method could be applied in the current framework.

Another avenue to potentially further improve these results is to develop methods that improve the convergence rate of the plane wave approximation to the  $A_j$  operators. Due to the non-periodic nature of the potential, one may require a large number of plane wave modes to discretize the system to the desired accuracy. Here we note that the efficiency of any plane-wave based algorithm for simulating continuum equations would be greatly improved if combined with a construction for a smooth periodic extension of the underlying potential. This could include the development of efficient quantum circuitry to perform a discrete circular convolution of the periodically extended potential with a mollifier, but additional work is needed to obtain efficient circuit constructions for mollified non-periodic potentials.

Finally, we note that this problem setting is likely amenable to the methods of Ref. [79], which achieve an asymptotic scaling of  $O(1/\sqrt{\epsilon})$  to estimate operator expectation values. In principle, this would further increase the asymptotic separation in  $\epsilon$  between the quantum and classical algorithm to a power of 8.

We conclude by noting that the construction of the generalized matrix square root given by  $\mathcal{A}$  mirrors the construction of a Hamiltonian of jump operators that has been proposed for quantum simulations of the Lindblad equation [80, 81]. Since the dynamics of the Fokker-Planck equation are purely dissipative, there is no coherent term in our problem. As was recently shown in Ref. [82], a coherent dynamical contribution can play an important role in improving the mixing time of open quantum systems. Noting the recent work of Ref. [83], where jump operators were constructed to induce dissipation to the ground state, it is an avenue of future work to investigate if the converse may be possible. That is, can one include a well-designed “coherent term” in  $\mathcal{A}$  so as to meaningfully accelerate the preparation of the equilibrium distribution? Here the recently designed “shortcut to Zeno” dynamics where a

system under continuous monitoring in a time-dependent basis is subjected to a coherent term designed to cancel out non-adiabatic transitions [84] offers one example. Another design route under continuous monitoring is offered by feedback, e.g., noise-cancelling quantum feedback [85]. It will be interesting to explore analogous methods for digital quantum algorithms.

## ACKNOWLEDGMENTS

T.D.K., A.M.A., K.K.M., and K.B.W. were supported by the U.S. Department of Energy, Office of Science, Office of Advanced Scientific Computing Research under Award Numbers DE-SC0023273 and DE-SC0025526. T.D.K. was also supported by a Siemens FutureMakers Fellowship. T.D.K. would also like to thank Aditya Singh for insightful discussions in the early portions of this work.

---

[1] William A. Eaton. Modern kinetics and mechanism of protein folding: A retrospective. *The Journal of Physical Chemistry B*, 125(14):3452–3467, March 2021. ISSN 1520-5207. doi:10.1021/acs.jpcb.1c00206. URL <http://dx.doi.org/10.1021/acs.jpcb.1c00206>.

[2] Hoi Sung Chung and William A Eaton. Protein folding transition path times from single molecule fret. *Current Opinion in Structural Biology*, 48:30–39, February 2018. ISSN 0959-440X. doi:10.1016/j.sbi.2017.10.007. URL <http://dx.doi.org/10.1016/j.sbi.2017.10.007>.

[3] S. Karthika, T. K. Radhakrishnan, and P. Kalaichelvi. A review of classical and nonclassical nucleation theories. *Crystal Growth & Design*, 16(11):6663–6681, October 2016. ISSN 1528-7505. doi:10.1021/acs.cgd.6b00794. URL <http://dx.doi.org/10.1021/acs.cgd.6b00794>.

[4] N. Dorsaz, C. De Michele, F. Piazza, P. De Los Rios, and G. Foffi. Diffusion-limited reactions in crowded environments. *Physical Review Letters*, 105(12), September 2010. ISSN 1079-7114. doi:10.1103/physrevlett.105.120601. URL <http://dx.doi.org/10.1103/PhysRevLett.105.120601>.

[5] Muhammad R. Hasyim and Kranthi K. Mandadapu. Emergent facilitation and glassy dynamics in supercooled liquids. *Proceedings of the National Academy of Sciences*, 121(23):e2322592121, 2024. doi:10.1073/pnas.2322592121. URL <https://www.pnas.org/doi/abs/10.1073/pnas.2322592121>.

[6] W. W. Heidbrink and R. B. White. Mechanisms of energetic-particle transport in magnetically confined plasmas. *Physics of Plasmas*, 27(3), March 2020. ISSN 1089-7674. doi:10.1063/1.5136237. URL <http://dx.doi.org/10.1063/1.5136237>.

[7] Zareer Dadachanji. *FX Barrier Options*. Palgrave Macmillan UK, 2015. ISBN 9781137462756. doi:10.1057/9781137462756. URL <http://dx.doi.org/10.1057/9781137462756>.

[8] Lingfei Li and Vadim Linetsky. Discretely monitored first passage problems and barrier options: an eigenfunction expansion approach. *Finance and Stochastics*, 19(4):941–977, August 2015. ISSN 1432-1122. doi:10.1007/s00780-015-0271-1. URL <http://dx.doi.org/10.1007/s00780-015-0271-1>.

[9] E. Vanden-Eijnden. *Transition Path Theory*, pages 453–493. Springer Berlin Heidelberg, Berlin, Heidelberg, 2006. ISBN 978-3-540-35273-0. doi:10.1007/3-540-35273-2\_13. URL [https://doi.org/10.1007/3-540-35273-2\\_13](https://doi.org/10.1007/3-540-35273-2_13).

[10] Weinan E and Eric Vanden-Eijnden. Transition-Path Theory and Path-Finding Algorithms for the Study of Rare Events. *Annual Review of Physical Chemistry*, 61(1):391–420, March 2010. ISSN 0066-426X, 1545-1593. doi:10.1146/annurev.physchem.040808.090412. URL <https://www.annualreviews.org/doi/10.1146/annurev.physchem.040808.090412>.

[11] Weinan E. and Eric Vanden-Eijnden. Towards a Theory of Transition Paths. *Journal of Statistical Physics*, 123(3):503–523, May 2006. ISSN 0022-4715, 1572-9613. doi:10.1007/s10955-005-9003-9. URL <http://link.springer.com/10.1007/s10955-005-9003-9>.

[12] Muhammad R. Hasyim, Clay H. Batton, and Kranthi K. Mandadapu. Supervised learning and the finite-temperature string method for computing committor functions and reaction rates. *The Journal of Chemical Physics*, 157(18):184111, November 2022. ISSN 0021-9606, 1089-7690. doi:10.1063/5.0102423. URL <https://aip.scitation.org/doi/10.1063/5.0102423>.

[13] Aditya N. Singh and David T. Limmer. Splitting probabilities as optimal controllers of rare reactive events, July 2024. URL <http://arxiv.org/abs/2402.05414>. arXiv:2402.05414 [cond-mat, physics:physics].

[14] Hannes Risken. *Fokker-planck equation*. Springer, 1996.

[15] Philipp Metzner, Christof Schütte, and Eric Vanden-Eijnden. Illustration of transition path theory on a collection of simple examples. *The Journal of Chemical Physics*, 125(8), August 2006. ISSN 1089-7690. doi:10.1063/1.2335447. URL <http://dx.doi.org/10.1063/1.2335447>.

[16] Yifei Sun and Mrinal Kumar. Numerical solution of high dimensional stationary fokker–planck equations via tensor decomposition and chebyshev spectral differentiation. *Computers & Mathematics with Applications*, 67(10):1960–1977, June 2014. ISSN 0898-1221. doi:10.1016/j.camwa.2014.04.017. URL <http://dx.doi.org/10.1016/j.camwa.2014.04.017>.

[17] Nan Chen, Andrew J. Majda, and Xin T. Tong. Rigorous analysis for efficient statistically accurate algorithms for solving fokker–planck equations in large dimensions. *SIAM/ASA Journal on Uncertainty Quantification*, 6(3):1198–1223, January 2018. ISSN 2166-2525. doi:10.1137/17m1142004. URL <http://dx.doi.org/10.1137/17M1142004>.

[18] Anton Bovier and Frank den Hollander. *Metastability: A Potential-Theoretic Approach*. Springer International Publishing, 2015. ISBN 9783319247779. doi:10.1007/978-3-319-24777-9. URL <http://dx.doi.org/10.1007/978-3-319-24777-9>.

[19] P A Markowich and C Villani. ON THE TREND TO EQUILIBRIUM FOR THE FOKKER-PLANCK EQUATION : AN INTERPLAY BETWEEN PHYSICS AND FUNCTIONAL ANALYSIS, 2000. URL <https://mc.sbm.org.br/wp-content/uploads/sites/9/sites/9/2021/12/19-1.pdf>.

[20] Rosalind J Allen, Chantal Valeriani, and Pieter Rein ten Wolde. Forward flux sampling for rare event simulations. *Journal of Physics: Condensed Matter*, 21(46):463102, October 2009. ISSN 1361-648X. doi:10.1088/0953-8984/21/46/463102. URL <http://dx.doi.org/10.1088/0953-8984/21/46/463102>.

[21] Thomas Dean and Paul Dupuis. Splitting for rare event simulation: A large deviation approach to design and analysis. *Stochastic Processes and their Applications*, 119(2):562–587, February 2009. ISSN 0304-4149. doi:10.1016/j.spa.2008.02.017. URL <http://dx.doi.org/10.1016/j.spa.2008.02.017>.

[22] Charles-Edouard Bréhier, Tony Lelièvre, and Mathias Rousset. Analysis of adaptive multilevel splitting algorithms in an idealized case. *ESAIM: Probability and Statistics*, 19:361–394, 2015. ISSN 1262-3318. doi:10.1051/ps/2014029. URL <http://dx.doi.org/10.1051/ps/2014029>.

[23] Haoya Li, Yuehaw Khoo, Yinuo Ren, and Lexing Ying. A semigroup method for high dimensional committor functions based on neural network. In *Proceedings of the 2nd Mathematical and Scientific Machine Learning Conference*, pages 598–618. PMLR, April 2022. URL <https://proceedings.mlr.press/v145/li22a.html>. ISSN: 2640-3498.

[24] Naoufal El Bekri, Lucas Drumetz, and Franck Vermet. FlowKac: An Efficient Neural Fokker-Planck solver using Temporal Normalizing flows and the Feynman Kac-Formula, March 2025. URL <http://arxiv.org/abs/2503.11427>. arXiv:2503.11427 [cs].

[25] Mark Ashbaugh, Evans Harrell, and Roman Svirsky. On minimal and maximal eigenvalue gaps and their causes. *Pacific Journal of Mathematics*, 147(1):1–24, January 1991. ISSN 0030-8730, 0030-8730. doi:10.2140/pjm.1991.147.1. URL <http://msp.org/pjm/1991/147-1/p01.xhtml>.

[26] Jonathan R Shewchuk. An Introduction to the Conjugate Gradient Method Without the Agonizing Pain. Technical Report, Carnegie Mellon University, USA, February 1994.

[27] Qisheng Wang and Zhicheng Zhang. Tight quantum depth lower bound for solving systems of linear equations. *Phys. Rev. A*, 110:012422, Jul 2024. doi:10.1103/PhysRevA.110.012422. URL <https://link.aps.org/doi/10.1103/PhysRevA.110.012422>.

[28] Davide Orsucci and Vedran Dunjko. On solving classes of positive-definite quantum linear systems with quadratically improved runtime in the condition number. *Quantum*, 5:573, November 2021. ISSN 2521-327X. doi:10.22331/q-2021-11-08-573. URL <http://arxiv.org/abs/2101.11868>. arXiv:2101.11868 [quant-ph].

[29] The MathWorks Inc. Matlab 23.2.0.2380103 (r2023b), 2023. URL <https://www.mathworks.com>.

[30] Oak Ridge National Laboratory. Frontier supercomputer hits new highs in third year of exascale. <https://www.ornl.gov/news/frontier-supercomputer-hits-new-highs-third-year-exascale>, 2024.

[31] Andrew M. Childs and Robin Kothari. Limitations on the simulation of non-sparse hamiltonians. *Quantum Info. Comput.*, 10(7):669–684, July 2010. ISSN 1533-7146.

[32] I. K. Razumov and Yu. N. Gornostyrev. Metastable Nanoprecipitates in Alloys: Phenomenology and Atomistic Simulation. *Physics of Metals and Metallography*, 125(11):1175–1182, November 2024. ISSN 1555-6190. doi:10.1134/S0031918X24601719. URL <https://doi.org/10.1134/S0031918X24601719>.

[33] Félix Therrien, Eric B. Jones, and Vladan Stevanović. Metastable materials discovery in the age of large-scale computation. *Applied Physics Reviews*, 8(3):031310, August 2021. ISSN 1931-9401. doi:10.1063/5.0049453. URL <https://doi.org/10.1063/5.0049453>.

[34] Debasish Kumar Ghosh and Akash Ranjan. The metastable states of proteins. *Protein Science: A Publication of the Protein Society*, 29(7):1559–1568, July 2020. ISSN 1469-896X. doi:10.1002/pro.3859.

[35] Lillian T. Chong, Ali S. Saglam, and Daniel M. Zuckerman. Path-sampling strategies for simulating rare events in biomolecular systems. *Current Opinion in Structural Biology*, 43:88–94, April 2017. ISSN 1879-033X. doi:10.1016/j.sbi.2016.11.019.

[36] Aaron R. Dinner and Martin Karplus. A metastable state in folding simulations of a protein model. *Nature Structural Biology*, 5(3):236–241, March 1998. ISSN 1545-9985. doi:10.1038/nsb0398-236. URL <https://www.nature.com/articles/nsb0398-236>. Publisher: Nature Publishing Group.

[37] Anton Bovier and Frank Den Hollander. *Metastability: A Potential-Theoretic Approach*, volume 351 of *Grundlehren der mathematischen Wissenschaften*. Springer International Publishing, Cham, 2015. ISBN 978-3-319-24775-5 978-3-319-24777-9. doi:10.1007/978-3-319-24777-9. URL <http://link.springer.com/10.1007/978-3-319-24777-9>.

[38] D. Nevins and F. J. Spera. Accurate computation of shear viscosity from equilibrium molecular dynamics simulations. *Molecular Simulation*, 33(15):1261–1266, December 2007. ISSN 0892-7022. doi:10.1080/08927020701675622. URL <https://doi.org/10.1080/08927020701675622>. Publisher: Taylor & Francis \_eprint: <https://doi.org/10.1080/08927020701675622>.

[39] R. Zwanzig. Time-Correlation Functions and Transport Coefficients in Statistical Mechanics. *Annual Review of Physical Chemistry*, 16(Volume 16,):67–102, October 1965. ISSN 0066-426X, 1545-1593. doi:10.1146/annurev.pc.16.100165.000435. URL <https://www.annualreviews.org/content/journals/10.1146/annurev.pc.16.100165.000435>. Publisher: Annual Reviews.

[40] Léon Van Hove. Correlations in Space and Time and Born Approximation Scattering in Systems of Interacting Particles. *Physical Review*, 95(1):249–262, July 1954. ISSN 0031-899X. doi:10.1103/PhysRev.95.249. URL <https://link.aps.org/doi/10.1103/PhysRev.95.249>.

[41] J.P. Hansen and I.R. McDonald. *Theory of simple liquids*. Academic Press, 2006. ISBN 978-0-08-045507-5. URL <https://books.google.com/books?id=Uhm87WZBnxEC>. tex.lccn: 2005055205.

[42] Ryogo Kubo. Statistical-Mechanical Theory of Irreversible Processes. I. General Theory and Simple Applications to Magnetic and Conduction Problems. *Journal of the Physical Society of Japan*, 12(6):570–586, June 1957. ISSN 0031-9015, 1347-4073. doi:10.1143/JPSJ.12.570. URL <https://journals.jps.jp/doi/10.1143/JPSJ.12.570>.

[43] Dong An, Jin-Peng Liu, and Lin Lin. Linear combination of Hamiltonian simulation for non-unitary dynamics with optimal state preparation cost, March 2023.

[44] Dong An, Andrew M. Childs, and Lin Lin. Quantum algorithm for linear non-unitary dynamics with near-optimal dependence on all parameters, December 2023.

[45] Guang Hao Low and Isaac L. Chuang. Optimal Hamiltonian Simulation by Quantum Signal Processing. *Physical Review Letters*, 118(1):1–5, 2017. ISSN 10797114. doi:10.1103/PhysRevLett.118.010501.

[46] Dong An, Jin-Peng Liu, Daochen Wang, and Qi Zhao. Quantum Differential Equation Solvers: Limitations and Fast-Forwarding. *Communications in Mathematical Physics*, 406(8):189, July 2025. ISSN 1432-0916. doi:10.1007/s00220-025-05358-7.

[47] Xiang Cheng, Niladri S. Chatterji, Yasin Abbasi-Yadkori, Peter L. Bartlett, and Michael I. Jordan. Sharp convergence rates for Langevin dynamics in the nonconvex setting, July 2020. URL <http://arxiv.org/abs/1805.01648>. arXiv:1805.01648 [stat].

[48] Dominic W. Berry. High-order quantum algorithm for solving linear differential equations. *Journal of Physics A: Mathematical and Theoretical*, 47(10):105301, March 2014. ISSN 1751-8113, 1751-8121. doi:10.1088/1751-8113/47/10/105301.

[49] Dong An, Akwum Onwunta, and Gengzhi Yang. Fast-forwarding quantum algorithms for linear dissipative differential equations, October 2024. URL <http://arxiv.org/abs/2410.13189>. arXiv:2410.13189.

[50] Di Fang, Lin Lin, and Yu Tong. Time-marching based quantum solvers for time-dependent linear differential equations. *Quantum*, 7:955, March 2023. doi:10.22331/q-2023-03-20-955. URL <https://quantum-journal.org/papers/q-2023-03-20-955/>. Publisher: Verein zur Förderung des Open Access Publizierens in den Quantenwissenschaften.

[51] Shi Jin, Nana Liu, and Yue Yu. Quantum simulation of partial differential equations via Schrodingerisation, December 2022.

[52] Pedro C. S. Costa, Stephen Jordan, and Aaron Ostrander. Quantum Algorithm for Simulating the Wave Equation. *Physical Review A*, 99(1):012323, January 2019. ISSN 2469-9926, 2469-9934. doi:10.1103/PhysRevA.99.012323. URL <http://arxiv.org/abs/1711.05394> [quant-ph].

[53] Efstratios Koukoutsis, Kyriakos Hizanidis, Abhay K. Ram, and George Vahala. Dyson Maps and Unitary Evolution for Maxwell Equations in Tensor Dielectric Media. *Physical Review A*, 107(4):042215, April 2023. ISSN 2469-9926, 2469-9934. doi:10.1103/PhysRevA.107.042215. URL <http://arxiv.org/abs/2209.08523>. arXiv:2209.08523 [physics].

[54] Pauline J. Ollitrault, Alexander Miessen, and Ivano Tavernelli. Molecular Quantum Dynamics: A Quantum Computing Perspective. *Accounts of Chemical Research*, 54(23):4229–4238, December 2021. ISSN 0001-4842. doi:10.1021/acs.accounts.1c00514. URL <https://doi.org/10.1021/acs.accounts.1c00514>. Publisher: American Chemical Society.

[55] Shi Jin, Nana Liu, and Yue Yu. Quantum simulation of the Fokker-Planck equation via Schrodingerization, April 2024.

[56] Ryan Babbush, Dominic W. Berry, Robin Kothari, Rolando D. Somma, and Nathan Wiebe. Exponential Quantum Speedup in Simulating Coupled Classical Oscillators. *Physical Review X*, 13(4):041041, December 2023. ISSN 2160-3308. doi:10.1103/PhysRevX.13.041041. URL <https://link.aps.org/doi/10.1103/PhysRevX.13.041041>.

[57] Jin-Peng Liu, Herman Øie Kolden, Hari K. Krovi, Nuno F. Loureiro, Konstantina Trivisa, and Andrew M. Childs. Efficient quantum algorithm for dissipative nonlinear differential equations. *Proceedings of the National Academy of Sciences of the United States of America*, 118(35):1–36, August 2021. ISSN 1091-6490. doi:10.1073/pnas.2026805118. URL <http://www.ncbi.nlm.nih.gov/pubmed/34446548>. arXiv: 2011.03185 Publisher: National Academy of Sciences.

[58] Shi Jin and Nana Liu. Quantum algorithms for computing observables of nonlinear partial differential equations, 2022. URL <http://arxiv.org/abs/2202.07834>. arXiv: 2202.07834.

[59] Dong An, Di Fang, Stephen Jordan, Jin-Peng Liu, Guang Hao Low, and Jiasu Wang. Efficient quantum algorithm for nonlinear reaction-diffusion equations and energy estimation, 2022. URL <http://arxiv.org/abs/2205.01141>. arXiv: 2205.01141.

[60] Pedro C. S. Costa, Philipp Schleich, Mauro E. S. Morales, and Dominic W. Berry. Further improving quantum algorithms for nonlinear differential equations via higher-order methods and rescaling, December 2023. URL <http://arxiv.org/abs/2312.09518>. arXiv:2312.09518 [math-ph, physics:quant-ph].

[61] Shi Jin, Nana Liu, and Yue Yu. Time complexity analysis of quantum difference methods for linear high dimensional and multiscale partial differential equations. *Journal of Computational Physics*, 471:111641, December 2022. ISSN 00219991. doi:10.1016/j.jcp.2022.111641. URL <http://arxiv.org/abs/2202.04537>. arXiv:2202.04537 [math-ph].

[62] David Jennings, Matteo Lostaglio, Robert B. Lowrie, Sam Pallister, and Andrew T. Sornborger. The cost of solving linear differential equations on a quantum computer: fast-forwarding to explicit resource counts, March 2024. URL <http://arxiv.org/abs/2309.07881>. arXiv:2309.07881 [quant-ph].

[63] Anirban Narayan Chowdhury and Rolando D. Somma. Quantum algorithms for Gibbs sampling and hitting-time estimation, March 2016.

[64] Zoe Holmes, Gopikrishnan Muraleedharan, Rolando D. Somma, Yigit Subasi, and Burak Şahinoğlu. Quantum algorithms from fluctuation theorems: Thermal-state preparation. *Quantum*, 6:825, October 2022. ISSN 2521-327X. doi:10.22331/q-2022-10-06-825. URL <http://arxiv.org/abs/2203.08882>. arXiv:2203.08882 [quant-ph].

[65] Jiaqi Leng, Zhiyan Ding, Zherui Chen, and Lin Lin. Operator-Level Quantum Acceleration of Non-Logconcave Sampling, May 2025. URL <http://arxiv.org/abs/2505.05301>. arXiv:2505.05301 [quant-ph].

[66] Edward Witten. Supersymmetry and Morse theory. *Journal of Differential Geometry*, 17(4):661 – 692, 1982. doi: 10.4310/jdg/1214437492. URL <https://doi.org/10.4310/jdg/1214437492>.

[67] Yian Chen, Jeremy Hoskins, Yuehaw Khoo, and Michael Lindsey. Committor functions via tensor networks. *Journal of Computational Physics*, 472:111646, January 2023. ISSN 00219991. doi:10.1016/j.jcp.2022.111646. URL <https://linkinghub.elsevier.com/retrieve/pii/S0021999122007094>.

[68] Yuehaw Khoo, Jianfeng Lu, and Lexing Ying. Solving for high-dimensional committor functions using artificial neural networks. *Research in the Mathematical Sciences*, 6(1):1, October 2018. ISSN 2197-9847. doi:10.1007/s40687-018-0160-2. URL <https://doi.org/10.1007/s40687-018-0160-2>.

[69] Yueyang Wang, Kejun Tang, Xili Wang, Xiaoliang Wan, Weiqing Ren, and Chao Yang. Estimating committor functions via deep adaptive sampling on rare transition paths. *Journal of Computational Physics*, 544:114439, January 2026. ISSN 0021-9991. doi:10.1016/j.jcp.2025.114439. URL <https://www.sciencedirect.com/science/article/pii/S0021999125007211>.

[70] Haoya Li, Yuehaw Khoo, Yinuo Ren, and Lexing Ying. A semigroup method for high dimensional committor functions based on neural network. In *Proceedings of the 2nd Mathematical and Scientific Machine Learning Conference*, pages 598–618. PMLR, April 2022. URL <https://proceedings.mlr.press/v145/li22a.html>. ISSN: 2640-3498.

[71] Rongjie Lai and Jianfeng Lu. Point Cloud Discretization of Fokker–Planck Operators for Committor Functions. *Multiscale Modeling & Simulation*, 16(2):710–726, January 2018. ISSN 1540-3459, 1540-3467. doi:10.1137/17M1123018. URL <https://pubs.siam.org/doi/10.1137/17M1123018>.

[72] Xun Tang and Lexing Ying. Solving high-dimensional Fokker-Planck equation with functional hierarchical tensor. *Journal of Computational Physics*, 511:113110, August 2024. ISSN 00219991. doi:10.1016/j.jcp.2024.113110. URL <https://linkinghub.elsevier.com/retrieve/pii/S0021999124003590>.

[73] Rick Beatson and Leslie Greengard. A short course on fast multipole methods, 2021. URL [https://math.nyu.edu/~greengar/shortcourse\\_fmm.pdf](https://math.nyu.edu/~greengar/shortcourse_fmm.pdf).

[74] Yi-An Ma, Yuansi Chen, Chi Jin, Nicolas Flammarion, and Michael I. Jordan. Sampling Can Be Faster Than Optimization. *Proceedings of the National Academy of Sciences*, 116(42):20881–20885, October 2019. ISSN 0027-8424, 1091-6490. doi: 10.1073/pnas.1820003116. URL <http://arxiv.org/abs/1811.08413>. arXiv:1811.08413 [stat].

[75] Robert L. Wolpert. Lecture notes on probability and measure theory: Spring 2009, March 2009. URL <https://www2.stat.duke.edu/courses/Spring09/sta205/lec/topics/stein/Lecture2.pdf>.

[76] B. Leimkuhler, C. Matthews, and M. V. Tretyakov. On the long-time integration of stochastic gradient systems. *Proceedings of the Royal Society A: Mathematical, Physical and Engineering Sciences*, 470(2170):20140120, October 2014. doi: 10.1098/rspa.2014.0120. URL <https://royalsocietypublishing.org/doi/10.1098/rspa.2014.0120>. Publisher: Royal Society.

[77] Matthew Pocanic, Peter D. Johnson, Amara Katabarwa, and Nathan Wiebe. Constant-Factor Improvements in Quantum Algorithms for Linear Differential Equations, June 2025. URL <http://arxiv.org/abs/2506.20760>. arXiv:2506.20760 [quant-ph].

[78] Ryan Babbush, Jarrod R. McClean, Michael Newman, Craig Gidney, Sergio Boixo, and Hartmut Neven. Focus beyond Quadratic Speedups for Error-Corrected Quantum Advantage. *PRX Quantum*, 2(1):010103, March 2021. ISSN 2691-3399. doi:10.1103/PRXQuantum.2.010103. URL <https://link.aps.org/doi/10.1103/PRXQuantum.2.010103>.

[79] Sophia Simon, Matthias Degroote, Nikolaj Moll, Raffaele Santagati, Michael Streif, and Nathan Wiebe. Amplified Amplitude Estimation: Exploiting Prior Knowledge to Improve Estimates of Expectation Values, March 2024. URL <http://arxiv.org/abs/2402.14791>. arXiv:2402.14791 [quant-ph].

[80] Richard Cleve and Chunhao Wang. Efficient Quantum Algorithms for Simulating Lindblad Evolution, January 2019.

[81] Zhiyan Ding, Xiantao Li, and Lin Lin. Simulating Open Quantum Systems Using Hamiltonian Simulations, November 2023.

[82] Di Fang, Jianfeng Lu, and Yu Tong. Mixing Time of Open Quantum Systems via Hypocoercivity, April 2024.

[83] Zhiyan Ding, Chi-Fang Chen, and Lin Lin. Single-ancilla ground state preparation via Lindbladians, August 2023.

[84] Philippe Lewalle, Yipei Zhang, and K Birgitta Whaley. Optimal zeno dragging for quantum control: a shortcut to zeno with action-based scheduling optimization. *PRX Quantum*, 5(2):020366, 2024.

[85] Tathagata Karmakar, Philippe Lewalle, Yipei Zhang, and K Birgitta Whaley. Noise-canceling quantum feedback: non-hermitian dynamics with applications to state preparation and magic state distillation. *arXiv preprint arXiv:2507.05611*, 2025.

[86] Neha S. Wadia, Ryan V. Zarcone, and Michael R. DeWeese. Solution to the Fokker-Planck equation for slowly driven Brownian motion: Emergent geometry and a formula for the corresponding thermodynamic metric. *Physical Review E*, 105(3):034130, March 2022. ISSN 2470-0045, 2470-0053. doi:10.1103/PhysRevE.105.034130. URL <https://link.aps.org/doi/10.1103/PhysRevE.105.034130>.

[87] David Tong. University of Cambridge Graduate Course on kinetic theory, 2025. URL <https://www.damtp.cam.ac.uk/user/tong/kinetic.html>.

[88] D. Bakry and M. Émery. Diffusions hypercontractives. In Jacques Azéma and Marc Yor, editors, *Séminaire de Probabilités XIX 1983/84*, volume 1123, pages 177–206. Springer Berlin Heidelberg, Berlin, Heidelberg, 1985. ISBN 978-3-540-15230-9 978-3-540-39397-9. doi:10.1007/BFb0075847. URL <http://link.springer.com/10.1007/BFb0075847>. Series Title: Lecture Notes in Mathematics.

[89] Guang Hao Low and Isaac L. Chuang. Hamiltonian simulation by qubitization. *Quantum*, 3:1–23, 2019. ISSN 2521327X. doi:10.22331/q-2019-07-12-163.

[90] András Gilyén, Yuan Su, Guang Hao Low, and Nathan Wiebe. Quantum singular value transformation and beyond:

Exponential improvements for quantum matrix arithmetics. In *Proceedings of the 51st Annual ACM SIGACT Symposium on Theory of Computing*, pages 193–204, June 2019. doi:10.1145/3313276.3316366.

[91] Danial Motagh and Nathan Wiebe. Generalized Quantum Signal Processing, August 2023.

[92] Lin Lin. Lecture Notes on Quantum Algorithms for Scientific Computation, 2022. URL <http://arxiv.org/abs/2201.08309>. arXiv: 2201.08309.

[93] Yulong Dong, Xiang Meng, K Birgitta Whaley, and Lin Lin. Efficient phase-factor evaluation in quantum signal processing. *Physical Review A*, 103(4), 2021. ISSN 24699934. doi:10.1103/PhysRevA.103.042419. arXiv: 2002.11649.

[94] Lexing Ying. Stable factorization for phase factors of quantum signal processing. *Quantum*, 6:842, October 2022. ISSN 2521-327X. doi:10.22331/q-2022-10-20-842. URL <https://doi.org/10.22331/q-2022-10-20-842>.

[95] L.N. Trefethen. *Approximation Theory and Approximation Practice*. Other Titles in Applied Mathematics. Society for Industrial and Applied Mathematics, 2013. ISBN 9781611972399. URL <https://books.google.com/books?id=En41UGQ6YXsC>.

[96] Yuan Su, Dominic W Berry, Nathan Wiebe, Nicholas Rubin, and Ryan Babbush. Fault-Tolerant Quantum Simulations of Chemistry in First Quantization. *PRX Quantum*, 2(4):1–96, 2021. ISSN 26913399. doi:10.1103/PRXQuantum.2.040332. arXiv: 2105.12767v2 ISBN: 2105.12767v3.

[97] Yuval R. Sanders, Guang Hao Low, Artur Scherer, and Dominic W. Berry. Black-Box Quantum State Preparation without Arithmetic. *Physical Review Letters*, 122(2):1–5, 2019. ISSN 10797114. doi:10.1103/PhysRevLett.122.020502. arXiv: 1807.03206.

### Appendix A: Bound on Lipschitz constant (Proof of Theorem 1)

We will first perform some elementary computations. Let

$$V_{\text{pair}} = \frac{1}{2} \sum_{i=0}^{\eta-1} \sum_{j \neq i} V(r_{ij}) \quad (\text{A1})$$

First, denote the partial derivative with respect to particle  $i$ 's  $k$ 'th direction as  $\partial_{i,k} := \partial_{x_{i,k}}$ . Then, the derivatives satisfy

$$\begin{aligned} \partial_{i,k} V(r_{ij}) &= V'(r_{ij}) \frac{x_{i,k} - x_{j,k}}{r_{ij}} \\ \partial_{i,k} V_{\text{pair}} &= \sum_{j \neq i} V'(r_{ij}) \frac{x_{i,k} - x_{j,k}}{r_{ij}}. \end{aligned}$$

For the second derivatives, we have

$$\partial_{i,l} \partial_{i,k} V(r_{ij}) = \partial_{i,l} \left( V'(r_{ij}) \frac{x_{i,k} - x_{j,k}}{r_{ij}} \right),$$

where

$$\partial_{i,l} \left( V'(r_{ij}) \frac{x_{i,k} - x_{j,k}}{r_{ij}} \right) = \frac{(x_{i,k} - x_{j,k})(x_{i,l} - x_{j,l})V''(r_{ij})}{r_{ij}^2} - \frac{(x_{i,k} - x_{j,k})(x_{i,l} - x_{j,l})V'(r_{ij})}{r_{ij}^3}.$$

We also have

$$\begin{aligned} \partial_{j,l} \partial_{i,k} V_{\text{pair}} &= -\frac{(x_{i,k} - x_{j,k})(x_{i,l} - x_{j,l})V''(r_{ij})}{r_{ij}^2} + \frac{(x_{i,k} - x_{j,k})(x_{i,l} - x_{j,l})V'(r_{ij})}{r_{ij}^3} \\ &= -\partial_{i,l} \partial_{i,k} V(r_{ij}). \end{aligned}$$

Therefore, the Hessian for a single  $V(r_{ij})$  takes the form,

$$H(V(r_{ij})) = \begin{pmatrix} \nabla_i \nabla_i^T V(r_{ij}) & \nabla_i \nabla_j^T V(r_{ij}) \\ \nabla_j \nabla_i^T V(r_{ij}) & \nabla_j \nabla_j^T V(r_{ij}) \end{pmatrix} \quad (\text{A2})$$

$$= \begin{pmatrix} A_{ij} & -A_{ij} \\ -A_{ij} & A_{ij} \end{pmatrix}, \quad (\text{A3})$$

where,

$$A_{ij} = V''(r_{ij}) \frac{(x_i - x_j)(x_i - x_j)^T}{r_{ij}^2} + \frac{V'(r_{ij})}{r_{ij}} \left( I_d - \frac{(x_i - x_j)(x_i - x_j)^T}{r_{ij}^2} \right).$$

Due to the assumption the  $\nabla V$  is  $\gamma$ -Lipschitz, we also have

$$\sup_{r_{ij} < \infty} \|H(V(r_{ij}))\| = \gamma. \quad (\text{A4})$$

Now, let us also find the matrix elements of the Hessian for the full potential. Consider the case for  $\eta = 3$ . Then, the Hessian will take the form

$$\begin{aligned} H_{\text{pair}} &= \begin{pmatrix} \nabla_0 \nabla_0^T (V_{01} + V_{02}) & \nabla_0 \nabla_1^T V_{01} & \nabla_0 \nabla_2^T V_{02} \\ \nabla_0 \nabla_1^T V_{01} & \nabla_1 \nabla_1^T (V_{01} + V_{12}) & \nabla_1 \nabla_2^T V_{12} \\ \nabla_0 \nabla_2^T V_{02} & \nabla_1 \nabla_2^T V_{12} & \nabla_2 \nabla_2^T (V_{02} + V_{12}) \end{pmatrix} \\ &= \begin{pmatrix} \nabla_0 \nabla_0^T V_{01} & \nabla_0 \nabla_1^T V_{01} & 0 \\ \nabla_1 \nabla_0^T V_{01} & \nabla_1 \nabla_1^T V_{01} & 0 \\ 0 & 0 & 0 \end{pmatrix} + \begin{pmatrix} \nabla_0 \nabla_0^T V_{02} & 0 & \nabla_0 \nabla_2^T V_{02} \\ 0 & 0 & 0 \\ \nabla_2 \nabla_0^T V_{02} & 0 & \nabla_2 \nabla_2^T V_{02} \end{pmatrix} + \begin{pmatrix} 0 & 0 & 0 \\ 0 & \nabla_1 \nabla_1^T V_{1,2} & \nabla_1 \nabla_2^T V_{1,2} \\ 0 & \nabla_2 \nabla_1^T V_{1,2} & \nabla_2 \nabla_2^T V_{1,2} \end{pmatrix}. \end{aligned}$$

Now, consider some arbitrary vector  $\mathbf{u} = \begin{pmatrix} u_0 & u_1 & u_2 \end{pmatrix}^T \in \mathbb{R}^{3d}$  (i.e. each  $u_j \in \mathbb{R}^d$ ). Then, it is straightforward to observe that

$$H_{\text{pair}} \begin{pmatrix} u_0 \\ u_1 \\ u_2 \end{pmatrix} = H_{0,1} \begin{pmatrix} u_0 \\ u_1 \end{pmatrix} + H_{0,2} \begin{pmatrix} u_0 \\ u_2 \end{pmatrix} + H_{1,2} \begin{pmatrix} u_1 \\ u_2 \end{pmatrix},$$

where  $H_{i,j}$  is the  $2d \times 2d$  Hessian for  $V(r_{ij})$  in Eq. (A2). This pattern persists for arbitrary  $\eta$ , in particular, for any  $\mathbf{u} = \begin{pmatrix} u_0 & \dots & u_{\eta-1} \end{pmatrix}^T \in \mathbb{R}^{\eta d}$  with  $u_i \in \mathbb{R}^d$  we have

$$H_{\text{pair}} \mathbf{u} = \frac{1}{2} \sum_{i=0}^{\eta-1} \sum_{j \neq i} H_{i,j} \begin{pmatrix} u_i \\ u_j \end{pmatrix}.$$

Then,

$$\begin{aligned} \mathbf{u}^T H_{\text{pair}} \mathbf{u} &= \frac{1}{2} \sum_{i=0}^{\eta-1} \sum_{j \neq i} \begin{pmatrix} u_i^T & u_j^T \end{pmatrix} \begin{pmatrix} A_{ij} & -A_{ij} \\ -A_{ij} & A_{ij} \end{pmatrix} \begin{pmatrix} u_i \\ u_j \end{pmatrix} \\ &= \frac{1}{2} \sum_{i=0}^{\eta-1} \sum_{j \neq i} u_i^T A_{ij} u_i - u_i^T A_{ij} u_j + u_j^T A_{ij} u_j - u_j^T A_{ij} u_i, \end{aligned}$$

which, due to the symmetry of  $A_{ij} \in \mathbb{R}^{d \times d}$  resulting from the equality of mixed partials, gives

$$\begin{aligned} \mathbf{u}^T H_{\text{pair}} \mathbf{u} &= \frac{1}{2} \sum_{i=0}^{\eta-1} \sum_{j \neq i} u_i^T A_{ij} u_i - 2u_i^T A_{ij} u_j + u_j^T A_{ij} u_j \\ &= \frac{1}{2} \sum_{i=0}^{\eta-1} \sum_{j \neq i} (u_i^T - u_j^T) A_{ij} (u_i - u_j). \end{aligned} \tag{A5}$$

We now construct a particular configuration to obtain the lower bound and prove the following theorem.

**Theorem 1.** *Let  $V : \mathbb{R} \rightarrow \mathbb{R}$  and assume that  $\nabla V$  is Lipschitz continuous with Lipschitz constant  $\gamma > 0$ . Further assume that  $\nabla V$  is everywhere differentiable. Let  $r_{ij} = \|\mathbf{x}_i - \mathbf{x}_j\|$  for all  $\mathbf{x}_i, \mathbf{x}_j$ . For  $\eta > 2$ , define the pair potential*

$$V_{\text{pair}} = \sum_{i=0}^{\eta-1} \sum_{j < i} V(r_{ij}).$$

*Then, the Lipschitz constant  $\text{Lip}(\nabla V_{\text{pair}}) \in \Omega(\eta\gamma)$ .*

*Proof.* Let  $V : [0, \infty) \rightarrow \mathbb{R}$  be a twice differentiable function with bounded derivatives. Assume that  $V'$  is Lipschitz continuous with Lipschitz constant  $\gamma > 0$ ,

$$|V'(r) - V'(s)| \leq L|r - s| \quad \forall r, s \geq 0.$$

Since  $V''$  is continuous, this implies  $\sup_{r \geq 0} |V''(r)| = \gamma$ , and there exists  $r_0 > 0$  such that  $V''(r_0) \geq \gamma/2$ .

Consider a system of  $\eta$  particles in  $\mathbb{R}^d$ , with positions  $\mathbf{x} = (x_0, \dots, x_{\eta-1}) \in \mathbb{R}^{\eta d}$ . Define the pairwise potential

$$V_{\text{pair}}(\mathbf{x}) = \frac{1}{2} \sum_{i \neq j} V(r_{ij}), \quad \text{where } r_{ij} = \|\mathbf{x}_i - \mathbf{x}_j\|.$$

The gradient  $\nabla V_{\text{pair}} : \mathbb{R}^{\eta d} \rightarrow \mathbb{R}^{\eta d}$  is Lipschitz continuous if there exists  $\gamma' > 0$  such that

$$\|\nabla V_{\text{pair}}(\mathbf{x}) - \nabla V_{\text{pair}}(\mathbf{y})\| \leq \gamma' \|\mathbf{x} - \mathbf{y}\| \quad \forall \mathbf{x}, \mathbf{y} \in \mathbb{R}^{\eta d}.$$

Since  $V_{\text{pair}}$  is  $C^2$ , the optimal  $\gamma'$  is the supremum of the operator norm of the Hessian

$$\gamma' = \sup_{\mathbf{x}} \|H(\mathbf{x})\| \text{ where,}$$

$$H(\mathbf{x}) = \nabla \nabla^T V_{\text{pair}}(\mathbf{x}).$$

From Eq. (A5) at the beginning of this section, for any vector  $\mathbf{u} \in \mathbb{R}^{\eta d}$  with  $u_i \in \mathbb{R}^d$ , the quadratic form

$$\mathbf{u}^T H(\mathbf{x}) \mathbf{u} = \frac{1}{2} \sum_{i=0}^{\eta-1} \sum_{j \neq i} (u_i^T - u_j^T) A_{ij} (u_i - u_j).$$

The following argument can be made much simpler if one is allowed to place multiple particles at the same position. Indeed, nothing in our stated assumptions prevents this from being the case. Nevertheless, it is quite common to restrict particles from occupying the same location, and so we proceed with an argument lower bounding the Lipschitz constant in this case.

Assume  $\eta$  is even. The case for  $\eta$  odd is similar.

Let  $r_0$  such that  $|V''(r_0)| \geq \gamma/2$ . Such an  $r_0$  exists because  $\sup_{r \geq 0} |V''(r)| = \gamma$  and  $V''$  is continuous. Let  $r_0 = A - B$ , with  $A, B \in \mathbb{R}^d$ . Place  $\eta/2$  particles co-linearly with  $\mathbf{r}_0$  within a radius  $\delta$  of  $r_0$  surrounding the point  $A \in \mathbb{R}^d$  and the remaining  $\eta/2$  particles co-linearly with  $\mathbf{r}_0$  in a  $\delta$  ball surrounding the point  $B \in \mathbb{R}^d$ . In addition, we assume  $\delta$  is chosen such that  $\delta < r_0/2$ . Define  $B_\delta(A) = \{\mathbf{x} : \|\mathbf{x} - A\| \leq \delta\}$ , and  $B_\delta(B)$  analogously.

Notice that for any  $\mathbf{x} \in B_\delta(A)$  and  $\mathbf{y} \in B_\delta(B)$ , that

$$r_0 - 2\delta \leq \|\mathbf{x} - \mathbf{y}\| \leq r_0 + 2\delta.$$

Fix an  $\epsilon \leq \gamma/4$ . We now wish to show that we can choose a  $\delta > 0$  so that  $|V''(r_0 \pm 2\delta)| \geq \gamma/2 - \epsilon \geq \gamma/4$ . This follows from the continuity of  $V''$ . In particular, there exists  $\delta > 0$  such that for all  $y$  satisfying  $|y - r_0| \leq \delta$ , we have

$$|V''(y) - V''(r_0)| < \epsilon,$$

thus,

$$-\epsilon + \frac{\gamma}{2} < V''(y).$$

With the guarantee of such a  $\delta$ , we can proceed with lower bounding the Lipschitz constant.

Define a test vector  $\mathbf{v} = (v_0, \dots, v_{\eta-1})$  by

$$v_i = \begin{cases} e, & \text{if particle } i \text{ is in } B_\epsilon(A) \\ -e, & \text{if particle } i \text{ is in } B_\epsilon(B), \end{cases}$$

where  $e = \frac{A - B}{\|A - B\|}$  is a unit vector. Then,  $\|v_i\| = 1 \ \forall i$ , so  $\|\mathbf{v}\|^2 = \sum_{i=0}^{\eta-1} \|v_i\|^2 = \eta$ .

Now, evaluating the quadratic form,

$$\mathbf{v}^T H(\mathbf{x}) \mathbf{v} = \frac{1}{2} \sum_{i=0}^{\eta-1} \sum_{j \neq i} (v_i^T - v_j^T) A_{ij} (\mathbf{x}) (v_i - v_j),$$

we can see that if  $i$  and  $j$  are in the same cluster that  $v_i - v_j = 0$ , whereas if  $i$  and  $j$  are in different clusters,  $v_i - v_j = \pm 2e$ . Thus, in this case

$$\begin{aligned} (v_i^T - v_j^T) A_{ij} (\mathbf{x}) (v_i - v_j) &= (v_i^T - v_j^T) \left( V''(r_{ij}) \frac{(x_i - x_j)(x_i - x_j)^T}{\|x_i - x_j\|^2} + \frac{V'(r_{ij})}{\|x_i - x_j\|} \left( I_d - \frac{(x_i - x_j)(x_i - x_j)^T}{\|x_i - x_j\|^2} \right) \right) (v_i - v_j) \\ &= \frac{4r_0^T}{\|r_0\|^2} \left( V''(r_{ij}) \frac{(x_i - x_j)(x_i - x_j)^T}{\|x_i - x_j\|^2} + \frac{V'(r_{ij})}{\|x_i - x_j\|} \left( I_d - \frac{(x_i - x_j)(x_i - x_j)^T}{\|x_i - x_j\|^2} \right) \right) r_0 \\ &= \frac{4}{\|r_0\|^2} \left( V''(r_{ij}) \frac{r_0^T (x_i - x_j)(x_i - x_j)^T r_0}{\|x_i - x_j\|^2} + \frac{V'(r_{ij})}{\|x_i - x_j\|} \left( \|r_0\|^2 - \frac{r_0^T (x_i - x_j)(x_i - x_j)^T r_0}{\|x_i - x_j\|^2} \right) \right) \\ &= \frac{4}{\|r_0\|^2} \left( V''(r_{ij}) \frac{\|r_0\|^2 \|x_i - x_j\|^2}{\|x_i - x_j\|^2} + \frac{V'(r_{ij})}{\|x_i - x_j\|} \left( \|r_0\|^2 - \frac{\|r_0\|^2 \|x_i - x_j\|^2}{\|x_i - x_j\|^2} \right) \right) \\ &= 4V''(r_{ij}). \end{aligned}$$

Since  $r_0 - \delta_0 \leq r_{ij} \leq r_0 + \delta_0$ , we know that

$$V''(\|\mathbf{x}_i - \mathbf{x}_j\|) \geq \frac{\gamma}{4}.$$

There are  $\eta^2/4$  such terms. Thus,

$$\gamma' \geq \frac{\mathbf{v}^T H(\mathbf{x}) \mathbf{v}}{\|\mathbf{v}\|^2} \geq \frac{\gamma \eta^2}{4\eta} = \frac{\gamma \eta}{4} \in \Omega(\gamma \eta).$$

□

## Appendix B: Technical Background on Kolmogorov Equations

Recall the Fokker-Planck operator,

$$\mathcal{F}[\rho] = \nabla \cdot (\rho \nabla V + \beta^{-1} \nabla \rho). \quad (\text{B1})$$

$F = -\nabla V$  is the force generated by the potential  $V$ , and  $\beta$  is the inverse temperature. The operator is the dynamical generator for the forward Kolmogorov equation

$$\mathcal{F}[P](\mathbf{x}, t | \mathbf{x}', 0) = \partial_t P(\mathbf{x}, t | \mathbf{x}', 0). \quad (\text{B2})$$

Therefore, the operator  $\mathcal{F}$  generates diffusive and convective dynamics, and is closely related to the convection-diffusion equation. The differential operator  $\mathcal{F}$  is negative semi-definite and the eigenfunction associated to the zero-mode is the equilibrium Boltzmann distribution,

$$\mu(\mathbf{x}) = \frac{e^{-\beta V(\mathbf{x})}}{\mathcal{Z}}, \quad (\text{B3})$$

where  $\mathcal{Z}$  is the associated normalization factor or partition function,

$$\mathcal{Z} = \int e^{-\beta V(\mathbf{x})} d\mathbf{x}. \quad (\text{B4})$$

$\mathcal{F}$  is self-adjoint with respect to the measure generated by  $\mu$ , that is, for any smooth functions  $u$  and  $v$  the following holds,

$$\langle u, \mathcal{F}[v] \rangle_\mu \equiv \frac{1}{\mathcal{Z}} \int e^{-\beta V(\mathbf{x})} u(\mathbf{x}) \mathcal{F}[v](\mathbf{x}) d\mathbf{x} = -\langle \nabla u, \nabla v \rangle_\mu, \quad (\text{B5})$$

with the last equality resulting from applying integration by parts and using the confining property of  $V$  to evaluate the boundary term. If we instead enforced homogeneous Neumann conditions on the boundary of a domain of finite volume, one obtains the same result without requiring  $V$  to be confining. As the operator  $\mathcal{F}$  is not self-adjoint under the standard  $L^2$  inner product, its adjoint is given by

$$\mathcal{F}^\dagger = \nabla V \cdot \nabla + \beta^{-1} \Delta, \quad (\text{B6})$$

and is the generator for the closely related backward Kolmogorov equation

$$-\mathcal{F}^\dagger[Q](\mathbf{x}', t' | \mathbf{x}, t) = \partial_t Q(\mathbf{x}', t' | \mathbf{x}, t). \quad (\text{B7})$$

The operator  $\mathcal{F}$  (and its adjoint) can be related to an explicitly self-adjoint operator via a similarity transformation generated by the square root of the equilibrium measure,

$$\rho_\beta(\mathbf{x}) = \sqrt{\mu(\mathbf{x})}. \quad (\text{B8})$$

We define

$$\mathcal{H}_\beta[u] = \rho_\beta^{-1} \mathcal{F}[\rho_\beta u], \quad (\text{B9})$$

and through straightforward calculations find that the resulting operator can be expressed as

$$\mathcal{H}_\beta = \beta^{-1} \Delta + U_\beta(\mathbf{x}), \quad (\text{B10})$$

where

$$U_\beta(\mathbf{x}) = -\frac{\beta}{4} \|\nabla V\|^2(\mathbf{x}) + \frac{1}{2} \Delta V(\mathbf{x}). \quad (\text{B11})$$

As a result,  $\mathcal{H}_\beta$  is a *Schrödinger*-type operator, and we thereby refer to this as the self-adjoint representation of  $\mathcal{F}$ . Since the spectrum of any operator is preserved under similarity transformation, and we know that  $\mathcal{F}$  is negative semi-definite,  $\mathcal{H}_\beta$  inherits this property as well. We note that this relationship between the Fokker-Planck operator and Schrödinger-type operator is somewhat well known, see e.g. Refs. [65, 86, 87].

For a many-body potential  $V_{\text{tot}}$ , expressed in terms of the joint variable  $\mathbf{x} = (\mathbf{x}^0, \mathbf{x}^2, \dots, \mathbf{x}^{\eta-1})$  given by a summation over pair-wise interactions governed by  $V$ , we have,

$$V_{\text{tot}}(\mathbf{x}) = \sum_{i=0}^{\eta-1} \sum_{j < i} V(\mathbf{x}^i, \mathbf{x}^j), \quad (\text{B12})$$

where  $\mathbf{x}^i \in \mathbb{R}^d$ . We will consider functions  $V$  that are symmetric functions of their arguments, so that  $\partial_{\mathbf{x}^i} V(\mathbf{x}^i, \mathbf{x}^j) = \partial_{\mathbf{x}^j} V(\mathbf{x}^j, \mathbf{x}^i)$ . In particular, we assume spherically symmetric pair-wise interactions of the form  $V(r_{ij})$  where  $r_{ij} = \|\mathbf{x}^i - \mathbf{x}^j\|$  is the Euclidean distance in  $d$  dimensions. The terms in the effective potential for the self-adjoint representation of the Fokker-Planck operator  $U_\beta$  take the form,

$$\begin{aligned} \|\nabla V_{\text{tot}}\|^2(\mathbf{x}) &= \sum_{k=0}^{\eta-1} \sum_{j < k} \|\partial_{\mathbf{x}^k} V(\mathbf{x}^k, \mathbf{x}^j)\|^2 = \sum_{k=0}^{\eta-1} \sum_{j < k} \sum_{i=0}^{d-1} \left| \partial_{x_i^k} V(\mathbf{x}^k, \mathbf{x}^j) \right|^2 \\ \Delta V(\mathbf{x}) &= \sum_{k=0}^{\eta-1} \sum_{j < k} \sum_{i=0}^{d-1} \partial_{x_i^k}^2 V(\mathbf{x}^k, \mathbf{x}^j), \end{aligned} \quad (\text{B13})$$

where we write  $\partial_{\mathbf{x}^k}$  to mean the  $d$ -dimensional gradient vector of partial derivatives for particle  $k$  and  $\partial_{x_i^k}^{(2)}$  to mean the first (second) derivative of particle  $k$  with respect to its  $i$ th dimension.

The effective potential for the self-adjoint representation of the Fokker-Planck operator is explicitly written as,

$$U_\beta(\mathbf{x}) = \frac{-\beta}{4} \sum_{i=0}^{\eta-1} \|\partial_{\mathbf{x}^k} V(\mathbf{x}^k, \mathbf{x}^j)\|^2 + \frac{1}{2} \sum_{k=0}^{\eta-1} \sum_{j < k} \sum_{i=0}^{d-1} \partial_{x_i^k}^2 V(\mathbf{x}^k, \mathbf{x}^j), \quad (\text{B14})$$

and the two particle and many-body interaction terms are

$$\begin{aligned} U_{ij} &= \frac{-\beta}{4} \|\partial_{\mathbf{x}^i} V(\mathbf{x}^i, \mathbf{x}^j)\|^2 + \frac{1}{2} \sum_{k=0}^{d-1} \partial_{x_k^i}^2 V(\mathbf{x}^i, \mathbf{x}^j) \\ U_{\text{tot}} &= \sum_{i=0}^{\eta} \sum_{j < i} U_{ij} \end{aligned} \quad (\text{B15})$$

An important quantity of interest is the so-called *reaction rate*, which describes the probability of trajectories beginning in some region of configuration space ending in another region of configuration space. This describes an abstract notion of “reactant” and “product” states, e.g. in a chemical reaction, and we refer to the set of states where the trajectories start ( $R$ ) and terminate ( $P$ ) as the reactants and products. Although the reaction rate is typically defined as a steady state property, there exists a related time-dependent quantity that is more useful for this work. The time-dependent reaction rate  $k_{RP}(T)$  between subsets of the configuration space,  $R$  and  $P$  is defined as the time-average quantity

$$k_{RP}(T) := \frac{1}{T \bar{p}_R} \int dx \int dx' 1_P(x') P(x', T|x, 0) \mu(x) 1_R(x), \quad (\text{B16})$$

with

$$1_R(x) = \begin{cases} 1 & x \in R \\ 0 & \text{else} \end{cases}, \quad (\text{B17})$$

and

$$\bar{p}_R = \int dx 1_R(x) \mu(x). \quad (\text{B18})$$

$P(x', T|x, 0)$  is the probability of being in state  $x'$  at time  $T$  given the state  $x$  at time 0 and is obtained by the propagator for the FPE,

$$P(x', T|x, 0) = \langle x' | e^{T\mathcal{F}} | x \rangle. \quad (\text{B19})$$

The time-dependent reaction rate can be interpreted as the probability of a trajectory starting in  $R$  to terminate in  $P$  at time  $T$ .

We may define an analogous expression for the time-dependent reaction rate  $k_{RP}(T)$  in terms of the propagator in the self-adjoint representation,  $\tilde{P}(x', t|x, 0) = \langle x' | e^{\mathcal{H}_\beta t} | x \rangle$ . By applying (B9) and (B16) it is straightforward to show that,

$$k_{RP}(T) = \frac{1}{T \bar{p}_R} \int dx \int dx' \langle x' | 1_P(x') \rho(x') e^{T\mathcal{H}_\beta} \rho(x) 1_R(x) | x \rangle. \quad (\text{B20})$$

We define the normalized quantum states

$$|R\rangle = \int 1_R(x) \frac{e^{-\beta V(x)/2}}{\sqrt{\bar{p}_R}} |x\rangle, \quad (\text{B21})$$

and see that

$$k_{RP}(T) = \frac{1}{T} \sqrt{\frac{\bar{p}_P}{\bar{p}_R}} \langle P | e^{T\mathcal{H}_\beta} | R \rangle.$$

From the above, we extract the reactive flux

$$\nu_{RP}(T) := \langle P | e^{T\mathcal{H}_\beta} | R \rangle. \quad (\text{B22})$$

### Appendix C: Equilibrium state preparation in locally convex region

Before we begin our discussion of the particular construction that we use to demonstrate efficient state preparation, we briefly review some elementary results on the rate of convergence to equilibrium in the convex setting. First, we establish exponential decay rate  $\lambda$  to the steady state  $(e^{-\beta V})$  when the steady state satisfies a Poincaré inequality with constant  $\lambda$ .

**Lemma 9** (Convergence rate is Poincaré constant (adapted from Ref. [19])). *Let  $L$  be the generator for the Fokker-Planck equation with steady state  $\mu = e^{-\beta V}$ , a suitably normalized distribution. Denote  $L^2(\mu)$  as the weighted  $L^2$  norm. Suppose  $\mu$  satisfies a Poincaré inequality with constant  $\lambda\beta$ , i.e.*

$$\forall g \in L^2(\mu), \quad \int g(x) e^{-\beta V(x)} dx = 0 \implies \int \|\nabla g(x)\|^2 \mu dx \geq \lambda\beta \int g^2(x) \mu dx. \quad (\text{C1})$$

Then, for any  $L^1$  normalized initial state  $\rho_0 = h_0 e^{-\beta V} = u_0 e^{-\beta V/2}$  the following inequalities hold,

$$\begin{aligned} \|h(t) - 1\|_{L^2(\mu)} &\leq e^{-2\lambda t} \|h_0 - 1\|_{L^2(\mu)} \\ \chi^2(\rho(t), \mu) &\leq e^{-2\lambda t} \chi^2(\rho_0, \mu) \\ \|u(t) - e^{-\beta V/2}\|_2^2 &\leq e^{-2\lambda t} \|u_0 - e^{-\beta V/2}\|_2^2. \end{aligned} \quad (\text{C2})$$

*Proof.* The Fokker-Planck equation (B1) under the change of variable  $\rho = he^{-\beta V}$ , reads

$$\frac{\partial h}{\partial t}(x, t) = -\nabla V \cdot \nabla h + \beta^{-1} \Delta h, \quad (\text{C3})$$

where we extract  $L = -\nabla V \cdot \nabla + \beta^{-1} \Delta$ . For confining potentials  $V$ , the operator  $L$  is self-adjoint with respect to the equilibrium measure, and in particular, it can be shown that

$$\langle f, L[g] \rangle_\mu := \int f(x) L[g](x) e^{-\beta V(x)} dx = -\beta^{-1} \langle \nabla f, \nabla g \rangle_\mu,$$

for any  $f, g \in C^2 \cap L^2(\mu)$ .

Using Eq. (C3) one can perform the computation,

$$\frac{d}{dt} \int (h(x, t) - 1)^2 \mu(x) dx = -2\beta^{-1} \int \|\nabla h\|^2(x, t) \mu(x) dx.$$

Now for  $\rho = he^{-\beta V}$  with  $\int \rho(x) dx = 1$ , we have that  $\int (h(x) - 1) e^{-\beta V(x)} dx = 0$ , therefore  $h - 1$  satisfies the Poincaré inequality (C1)

$$\int \|\nabla h\|^2(x, t) \mu(x) dx \geq \lambda \beta \int (h(x, t) - 1)^2 \mu(x) dx.$$

This entails the estimate,

$$-\frac{d}{dt} \int (h(x, t) - 1)^2 \mu(x) dx = 2\beta^{-1} \int \|\nabla h\|^2(x, t) \mu(x) dx \geq 2\lambda \int (h(x, t) - 1)^2 \mu(x) dx$$

or that

$$\int (h(x, t) - 1)^2 \mu(x) dx \leq e^{-2\lambda t} \int (h(x, 0) - 1)^2 \mu(x) dx.$$

Thus, for any initial state  $\rho_0 = h_0 e^{-\beta V}$ , with  $\int \rho_0 dx = 1$ , we have by Grönwall's inequality

$$\|h(x, t) - 1\|_{L^2(\mu)} \leq e^{-2\lambda t} \|h(x, 0) - 1\|_{L^2(\mu)}.$$

Equivalently,

$$\begin{aligned} \chi^2(\rho, e^{-\beta V}) &= \int |\rho - e^{-\beta V}|^2 e^{\beta V} dx \\ &= \int |he^{-\beta V} - 1e^{-\beta V}|^2 e^{\beta V} dx \\ &= \int |h - 1|^2 e^{-\beta V} dx \\ &= \|h - 1\|_{L^2(\mu)}^2. \end{aligned}$$

, We further have, that for  $\rho = e^{-\beta V/2} u$ ,

$$\begin{aligned} \chi^2(\rho, e^{-\beta V}) &= \int |\rho - e^{-\beta V}|^2 e^{\beta V} dx \\ &= \int |e^{-\beta V/2} u - e^{-\beta V}|^2 e^{\beta V} dx \\ &= \int |u - e^{-\beta V/2}|^2 dx \\ &= \|u - e^{-\beta V/2}\|_2^2, \end{aligned}$$

thus, convergence of  $h$  to 1 is equivalent to the convergence of  $\rho$  to  $e^{-\beta V}$  in  $\chi^2$  divergence, and convergence of  $\rho$  to  $e^{-\beta V}$  in  $\chi^2$  divergence is equivalent to convergence of  $u$  to  $\sqrt{e^{-\beta V}}$  in the standard  $L^2$  norm.  $\square$

The above lemma guarantees that when the measure  $L^2(e^{-\beta V})$  supports a space of functions with a positive Poincaré constant  $\lambda$  that an exponential convergence rate of  $\lambda$  to equilibrium can be established. An equivalent condition, provided by the Bakry-Emery criteria [88], shows that the Poincaré constant can be related to the convexity of the potential  $V$ . In particular, Theorems 1 and 2 of Ref. [19] establish that if  $V$  satisfies

$$\text{Hess}(V) \geq \lambda I,$$

then  $e^{-\beta V}$  satisfies the Poincaré inequality (C1) with constant  $\frac{\lambda}{\beta}$ . Thus, the assumption that the potential is  $m$ -strongly convex is sufficient to prove that the dynamics converge to the equilibrium distribution at a rate of  $O(e^{-tm})$ , and thus establishes a mixing time estimate  $t_{\text{mix}} \in O(\frac{1}{m})$ .

### 1. Quantum reactant (product) state preparation

Our goal is to prepare a quantum state corresponding to  $\sqrt{\pi_R(x)}$  where  $\pi_R(x) \propto e^{-\beta V(x)} 1_R(x)$ , where the restriction of the potential  $V(x)|_{x \in R}$  is  $m$ -strongly convex. We remark that weaker conditions can also be used to obtain exponential convergence. Throughout this section,  $R$  can be replaced with  $P$  for the preparation of the product distribution. We would like to establish that even if the potential  $V(x)$  has no global convex structure that the mixing in the region  $R$  is exponentially fast, and that there exists a quantum algorithm that prepares an encoding of  $\pi_R(x)$  into a quantum state with complexity proportional to the mixing time  $t_{\text{mix}} \in O(\frac{1}{m})$ .

Consider the Fokker-Planck operator restricted to the region  $R$ , an open subset of  $\mathbb{R}^{nd}$ , endowed with homogeneous Neumann boundary conditions,

$$\begin{aligned} \nabla \cdot (\rho \nabla V + \beta^{-1} \nabla \rho) &= \partial_t \rho \\ \mathbf{n} \cdot (\nabla V \rho(\mathbf{x}) + \beta^{-1} \nabla \rho(\mathbf{x})) &= 0 \text{ for } \mathbf{x} \in \partial R \end{aligned} \quad (\text{C4})$$

where  $\mathbf{n}$  is an outward pointing unit vector on  $\partial R$ . Under the change of variable  $\rho = e^{-\beta V/2} \psi$ , we obtain a Robin boundary value problem with the self-adjoint operator  $\mathcal{H}_\beta$ ,

$$\begin{aligned} (\beta^{-1} \Delta - \frac{\beta}{4} \|\nabla V\|^2 + \frac{1}{2} \Delta V) \psi &= \partial_t \psi \\ \mathbf{n} \cdot \left( \frac{1}{2} \psi(\mathbf{x}) \nabla V(\mathbf{x}) + \frac{1}{\beta} \nabla \psi(\mathbf{x}) \right) &= 0 \text{ for } \mathbf{x} \in \partial R. \end{aligned} \quad (\text{C5})$$

Since  $V$  is not necessarily confining on  $R$ , more effort is needed to enforce the Robin boundary conditions using the plane wave discretization we employ in the full configuration space. One straightforward method is to introduce an auxiliary confining potential,

$$V_R(\mathbf{x}) = \begin{cases} V(\mathbf{x}) & \mathbf{x} \in R \\ V(\mathbf{x}) + \kappa \text{dist}(\mathbf{x}, \partial R)^2 & \mathbf{x} \in R^c, \end{cases} \quad (\text{C6})$$

where  $\kappa > 1$  is a stiffness parameter that improves the accuracy of the Robin boundary value problem as  $\kappa \rightarrow \infty$ .

A demonstration of this construction is provided in Fig. 6 below. Since  $V_R$  and  $V$  match at  $\partial R$ , we know that  $V_R$  is at least a  $C^0$  extension of  $V$ , however, we also have that  $\nabla V$  and  $\nabla V_R$  match at  $\partial R$ ,

$$\nabla V_R(\mathbf{x}) = \begin{cases} \nabla V(\mathbf{x}) & \mathbf{x} \in R \\ \nabla V(\mathbf{x}) + 2\kappa(\mathbf{x} - \partial R) & \mathbf{x} \in R^c. \end{cases}$$

Thus as  $\mathbf{x} \rightarrow \partial R$ ,  $\nabla V_R \rightarrow \nabla V(\mathbf{x})$  and we have continuity in the first derivative, and  $V_R$  is a  $C^1$  extension of  $V$ . This in turn allows us to at least establish a convergence rate of  $O(N^{-1})$  in the plane wave discretization and avoid problematic Gibbs phenomenon.

With this augmented potential, we now wish to solve the problem

$$\begin{aligned} \left( \beta^{-1} \Delta - \frac{\beta}{4} V_R(\mathbf{x}) + \frac{1}{2} \Delta V_R \right) \psi &= \partial_t \psi \\ \psi(0) &= \psi_0. \end{aligned} \quad (\text{C7})$$

In the following Lemma 10, we establish bounds on how large  $\kappa$  needs to be to ensure that the steady state of Eq. (C7) well approximates the steady state of Eq. (C5). The result takes as a simplifying assumption that  $R$  defines

a spherical open subset of  $\mathbb{R}^{\eta d}$ , but this is not strictly necessary, and serves as an example where bounds can be explicitly computed. We expect similar results would hold in less symmetric settings. With a well-behaved enough potential, for example, we may be able extend  $R$  onto a larger, but simpler, domain.

**Lemma 10.** *Let  $V_R$  and  $V$  be as above. Let  $R$  define a spherical subset of  $\mathbb{R}^{\eta d}$ . That is for some  $\mathbf{x}_0 \in \mathbb{R}^{\eta d}$  and some  $r_0 > 0$ ,*

$$R = \{\mathbf{x} \in \mathbb{R}^{\eta d} : \|\mathbf{x} - \mathbf{x}_0\| < r_0\}.$$

*Then, for any  $\epsilon > 0$ , we can choose  $\kappa \in O\left(\frac{1}{\mathcal{Z}_R^2 \beta \epsilon^4}\right)$ , to ensure that*

$$\left\| e^{-\beta V_R(\mathbf{x})} - e^{-\beta V(\mathbf{x})} \right\|_2 \leq \epsilon,$$

*where  $\|\cdot\|_2$  is the  $L^2$  norm over  $\mathbb{R}^{\eta d}$ .*

*Proof.* Let  $\rho_R(\mathbf{x}) = \frac{e^{-\beta V_R(\mathbf{x})/2}}{\sqrt{\mathcal{Z}}}$  and  $\rho(\mathbf{x}) = \frac{e^{-\beta V(\mathbf{x})/2}}{\sqrt{\mathcal{Z}_R}}$ , where

$$\begin{aligned} \mathcal{Z} &= \int e^{-\beta V_R(\mathbf{x})} d\mathbf{x} \\ \mathcal{Z}_R &= \int_R e^{-\beta V(\mathbf{x})} d\mathbf{x} \end{aligned}$$

are normalizing factors. We also write  $\mathcal{Z} = \mathcal{Z}_R + \mathcal{Z}_{R^c}$ . Trivially extend  $\rho$  as,

$$\rho(\mathbf{x}) = \begin{cases} \rho(\mathbf{x}) & \mathbf{x} \in R \\ 0 & \text{else} \end{cases}.$$

And compute the  $L_2$  norm of their difference

$$\begin{aligned} \|\rho_R - \rho\|_2^2 &= \int |\rho_R(\mathbf{x}) - \rho(\mathbf{x})|^2 d\mathbf{x} \\ &= \int_{x \in R} \left| \frac{e^{-\beta V(\mathbf{x})/2}}{\sqrt{\mathcal{Z}}} - \frac{e^{-\beta V(\mathbf{x})/2}}{\sqrt{\mathcal{Z}_R}} \right|^2 d\mathbf{x} + \int_{x \in R^c} \frac{e^{-\beta V_R(\mathbf{x})}}{\mathcal{Z}} d\mathbf{x} \\ &= \left| \frac{1}{\sqrt{\mathcal{Z}}} - \frac{1}{\sqrt{\mathcal{Z}_R}} \right|^2 \int_{x \in R} e^{-\beta V(\mathbf{x})} d\mathbf{x} + \frac{1}{\mathcal{Z}} \int_{x \in R^c} e^{-\beta V_R(\mathbf{x})} d\mathbf{x} \\ &= \left| \frac{1}{\sqrt{\mathcal{Z}}} - \frac{1}{\sqrt{\mathcal{Z}_R}} \right|^2 \mathcal{Z}_R + \frac{\mathcal{Z}_{R^c}}{\mathcal{Z}} \\ &= 1 - 2\sqrt{\frac{\mathcal{Z}_R}{\mathcal{Z}}} + \frac{\mathcal{Z}_R}{\mathcal{Z}} + \frac{\mathcal{Z}_{R^c}}{\mathcal{Z}} \\ &= 2 \left( 1 - \sqrt{\frac{\mathcal{Z}_R}{\mathcal{Z}}} \right). \end{aligned}$$

Thus, in order to ensure that

$$\|\rho_R - \rho\|_2^2 \leq \epsilon^2,$$

we require

$$\frac{\mathcal{Z}_R}{\mathcal{Z}_R + \mathcal{Z}_{R^c}} \geq \left( 1 - \frac{\epsilon^2}{2} \right)^2.$$

Expanding the left hand side around  $\mathcal{Z}_{R^c} = 0$ , we have

$$\frac{\mathcal{Z}_R}{\mathcal{Z}_R + \mathcal{Z}_{R^c}} = 1 - \frac{\mathcal{Z}_{R^c}}{\mathcal{Z}} + O\left(\left(\frac{\mathcal{Z}_{R^c}}{\mathcal{Z}}\right)^2\right).$$

Now, we obtain a lower bound on  $\mathcal{Z}_{R^c}$ . Assume that  $\min_{\mathbf{x} \in \partial R} e^{-\beta V(\mathbf{x})} \geq C > 0$ .

$$\mathcal{Z}_{R^c} \geq C \int_{R^c} e^{-\beta \kappa \operatorname{dist}(\mathbf{x}, \partial R)^2} d\mathbf{x},$$

since the point  $\mathbf{x}_0$  defining the center of the spherical region  $R$  entails an overall translation of the coordinates, and the above integral is invariant under this translation, we may take  $\mathbf{x}_0 = 0$  without loss of generality. Therefore,

$$\int_{R^c} e^{-\beta \kappa \operatorname{dist}(\mathbf{x}, \partial R)^2} d\mathbf{x} = \omega_{\eta d} \int_{r_0}^{\infty} e^{-\beta \kappa (r-r_0)^2} r^{\eta d-1} dr,$$

and  $\omega_n = \frac{2\pi^{n/2}}{\Gamma(n/2)}$ . Let  $u = r - r_0$ , then

$$\int_{r_0}^{\infty} e^{-\beta \kappa (r-r_0)^2} r^{\eta d-1} dr = \int_0^{\infty} e^{-\beta \kappa u^2} (u + r_0)^{\eta d-1} du.$$

The term  $(u + r_0)^{\eta d-1}$  can be expanded using the binomial theorem, and using standard Gaussian integrals we can obtain an exact expression for the integral

$$\int_{R^c} e^{-\beta \kappa \operatorname{dist}(\mathbf{x}, \partial R)^2} d\mathbf{x} = \frac{\omega_{\eta d}}{2} \sum_{k=0}^{\eta d-1} \binom{\eta d-1}{k} r_0^{\eta d-1-k} (\beta \kappa)^{-(k+1)/2} \Gamma\left(\frac{k+1}{2}\right). \quad (\text{C8})$$

For  $\beta \kappa$  large and  $r_0$  some constant, we have the following asymptotic bound on the integral in terms of the dimension-dependent constant  $C_{\eta d}$ ,

$$\frac{\pi^{(\eta d+1)/2}}{\Gamma(\eta d/2)} (\beta \kappa)^{-1/2} r_0^{\eta d-1} = C_{\eta d} (\kappa \beta)^{-1/2} \in O\left(\sqrt{\kappa \beta}\right). \quad (\text{C9})$$

With this asymptotic bound  $\mathcal{Z}_R$ , it therefore suffices to choose

$$\kappa \in O\left(\frac{1}{\mathcal{Z}_R^2 \beta \epsilon^4}\right), \quad (\text{C10})$$

with constants depending on the behavior of the potential on  $\partial R$  and the dimension  $\eta d$ .  $\square$

The  $\kappa \sim O\left(\frac{1}{\epsilon^4}\right)$  scaling from Lemma 10 entails a complexity of  $\Omega(\epsilon^{-2})$  for quantum state preparation algorithms employing the sum-of-squares decomposition we use in this work, as the block encoding subnormalization factor for the potential will scale with this factor. Thus, the procedure based on augmenting the potential to obtain a confining potential is likely suboptimal. Nevertheless, it satisfies our purpose of demonstrating a method that prepares the initial reactant and product states with polynomial complexity in the locally convex setting.

Finally, it remains to establish the convexity of the augmented potential  $V_R(x)$  given the original potential  $V(x)$  restricted to  $R$  is  $m$ -strongly convex. By the following Lemma, the augmented potential  $V_R$  has Poincaré constant  $m + 2\kappa$ , and has a corresponding mixing time of  $t_{\text{mix}} \sim \frac{\beta}{m+2\kappa}$ .

**Lemma 11.** *Suppose  $V$  is  $m$ -strongly convex for all  $x \in R$ , for a convex set  $R$ . Then with  $V_R$  defined as in Eq. (43), we have that  $\operatorname{Hess}(V_R) \geq mI$  for any  $\kappa \geq 1/2$ .*

*Proof.* The assumption that  $V$  is  $m$ -strongly convex on  $R$  is equivalent to the statement that for all  $x, y \in R$ ,

$$(\nabla V(\mathbf{x}) - \nabla V(\mathbf{y}))^T (\mathbf{x} - \mathbf{y}) \geq \frac{m}{2} \|\mathbf{x} - \mathbf{y}\|^2.$$

Clearly, for all  $\mathbf{x}, \mathbf{y} \in R^c$ ,  $V_R$  satisfies

$$(\nabla V_R(\mathbf{x}) - \nabla V_R(\mathbf{y}))^T (\mathbf{x} - \mathbf{y}) \geq \left(\frac{m}{2} + \kappa\right) \|\mathbf{x} - \mathbf{y}\|^2. \quad (\text{C11})$$

Thus, it remains to show that for  $\mathbf{x} \in R$  and  $\mathbf{y} \in R^c$  that

$$(\nabla V(\mathbf{x}) - \nabla V(\mathbf{y}))^T (\mathbf{x} - \mathbf{y}) \geq \frac{m}{2} \|\mathbf{x} - \mathbf{y}\|^2.$$

Noting that,

$$\nabla V_R(\mathbf{x}) = \begin{cases} \nabla V(\mathbf{x}) & \mathbf{x} \in R \\ \nabla V(\mathbf{x}) + 2\kappa(\mathbf{x} - \partial R) & \mathbf{x} \in R^c. \end{cases}$$

We have,

$$\begin{aligned} & (\nabla V(\mathbf{x}) - \nabla V(\mathbf{y}) - 2\kappa(\mathbf{y} - \partial R))^T(\mathbf{x} - \mathbf{y}) \\ &= (\nabla V(\mathbf{x}) - \nabla V(\mathbf{y}))^T(\mathbf{x} - \mathbf{y}) - 2\kappa(\mathbf{y} - \partial R)^T(\mathbf{x} - \mathbf{y}) \\ &= (\nabla V(\mathbf{x}) - \nabla V(\mathbf{y}))^T(\mathbf{x} - \mathbf{y}) - 2\kappa(\mathbf{y} - \mathbf{x})^T(\mathbf{x} - \mathbf{y}) - 2\kappa(\mathbf{x} - \partial R)^T(\mathbf{x} - \mathbf{y}) \\ &\geq \frac{m}{2} \|\mathbf{x} - \mathbf{y}\|^2 + 2\kappa \|\mathbf{x} - \mathbf{y}\|^2 - 2\kappa(\mathbf{x} - \partial R)^T(\mathbf{x} - \mathbf{y}). \end{aligned}$$

Then, since  $\|\mathbf{x} - \mathbf{y}\| \geq \|\mathbf{x} - \partial R\|$ , we have

$$(\nabla V(\mathbf{x}) - \nabla V(\mathbf{y}) - 2\kappa(\mathbf{y} - \partial R))^T(\mathbf{x} - \mathbf{y}) \geq (m + 2\kappa - 1) \|\mathbf{x} - \mathbf{y}\|^2, \quad (\text{C12})$$

Thus for any  $\kappa \geq 1/2$ , we obtain the desired result.  $\square$

Under the given assumption that  $V(x)$  is strongly convex on  $R$ , and the construction of Lemma 10, we can use our block encoding of the Witten Laplacian (see Appendix J) with the augmented potential to efficiently prepare the equilibrium distribution over reactant and product regions that correspond to local minima of the potential energy surface. The state preparation can be performed by either performing direct dynamics under the Witten Laplacian, or by applying the eigenstate filtering algorithm of Ref. [65].

**Theorem 4.** *Fast thermal state preparation in locally convex region.* Let  $R$  be a convex open subset of  $[-L, L]^d$ . Assume that,

$$\inf_{x \in R} \text{Hess}(V(x)) \succeq mI.$$

Assume the warm start condition that an initial state  $|R_0\rangle$  has constant overlap with the target quantum state,

$$|R\rangle = \begin{cases} \int_{x \in R} \frac{e^{-\beta V(x)/2}}{\sqrt{\mathcal{Z}_R}} |x\rangle & x \in R, \\ 0 & \text{else} \end{cases}, \quad \mathcal{Z}_R = \int_{x \in R} e^{-\beta V(x)} dx. \quad (44)$$

Let  $V_R$  be the augmented potential from Eq. (43),  $\alpha_V = \max_{r \leq \sqrt{d}L} \frac{|V'(r)|}{r}$ , and  $\kappa \in O\left(\frac{1}{\epsilon^4 \mathcal{Z}_R^2 \beta}\right)$ , satisfying

$$\left\| e^{-\beta V_R/2} - |R\rangle \right\|_{L^2} \leq \epsilon.$$

Moreover, there exists a quantum algorithm preparing the state  $|\tilde{R}\rangle$  such that

$$\left\| |R\rangle - |\tilde{R}\rangle \right\|_{L^2} \leq \epsilon$$

using

$$\tilde{O}\left(\sqrt{\frac{\eta d}{2m}} \left(\beta \eta L(\alpha_V + \kappa) + \frac{N}{L}\right)\right),$$

queries to the block encoding of  $\mathcal{A}$ , where the  $\tilde{O}$  notation suppresses polylogarithmic factors in  $1/\epsilon$ .

*Proof.* First, we employ Lemma 10, to obtain a construction of the augmented confining potential  $V_R$ , where  $\kappa \sim \frac{1}{\mathcal{Z}_R^2 \beta \epsilon^4}$ . Then, using the technique described in Lemma 9 of Ref. [65], we can choose an isometry  $I_N$  that acts as an embedding from  $\mathbb{C}^{N^{nd}}$  into  $L^2$ , thus translating error in  $\ell^2[\mathbb{C}^{N^{nd}}]$  into error in the standard  $L^2$  norm. Thus, with this construction and Lemmas 9 and 11, then the dynamics generated by  $\mathcal{H}_\beta$  satisfy,

$$\left\| I_N e^{\mathcal{H}_\beta t} |R_0\rangle - |R\rangle \right\|_2 \leq e^{-2t\frac{m}{\beta}} \|I_N |R_0\rangle - |R\rangle\|_{L^2} \leq e^{-2t\frac{m}{\beta}} C, \quad (\text{C13})$$

for some constant  $C \in O(1)$ . Thus, for any  $\epsilon > 0$ , we can ensure

$$\|I_N e^{\mathcal{H}_\beta t} |R_0\rangle - |R\rangle\|_2 \leq \epsilon, \quad (\text{C14})$$

by choosing

$$t \geq \frac{\beta}{2m} O\left(\log\left(\frac{1}{\epsilon}\right)\right). \quad (\text{C15})$$

The subnormalization factor associated with the block encoding of the matrix square root  $\mathcal{A}$  is shown in Theorem 5 from Appendix J, to be  $\alpha_A = O\left(\sqrt{\beta d} \eta^{3/2} L \alpha_V + \sqrt{\frac{\eta d}{\beta}} \frac{N}{L}\right)$ . This, combined with a query complexity of  $\tilde{O}(\alpha_A \sqrt{t})$  where  $\sqrt{t} \in \tilde{O}\left(\sqrt{\frac{\beta}{2m}}\right)$  leads to an overall complexity of

$$\tilde{O}\left(\sqrt{\frac{\eta d}{2m}} \left(\beta \eta L(\alpha_V + \kappa) + \frac{N}{L}\right)\right),$$

queries to the block encoding of  $\mathcal{A}$  as desired.  $\square$

## Appendix D: Background on quantum algorithms

### 1. Block encoding

Block encoding is a quantum subroutine that implements the action of a non-unitary matrix in a subspace of a unitary matrix. We will exclusively use the linear combination of unitaries (LCU) approach to constructing block encodings, which we describe here. Suppose we have a matrix operation  $A$  where we have an expression for  $A$  as

$$A = \sum_{l=0}^{M-1} c_l U_l \quad (\text{D1})$$

where the  $U_l$  are unitary matrices of the same dimension as  $A$  and the  $c_l \in \mathbb{C}$  are the coefficients in the expansion. We first define the PREP routine on an ancilla register with  $m = \lceil \log_2(M) \rceil$  ancilla qubits,

$$\text{PREP} : |0\rangle_m \rightarrow \sum_{l=0}^{M-1} \sqrt{\frac{c_l}{\alpha}} |l\rangle_m \quad (\text{D2})$$

with  $\alpha = \sum_{l=0}^{M-1} |c_l|$ , the so-called *subnormalization factor*. Then, we apply the unitaries  $U_l$  in a controlled manner using the SEL routine

$$\text{SEL} = \sum_{l=0}^{M-1} U_l \otimes |l\rangle\langle l|. \quad (\text{D3})$$

In a quantum circuit we may sometimes express the SEL operation using the  $\otimes$  notation, which is to be interpreted as a controlled operation applied on all relevant bitstrings in the control register. Combining these routines, we define the block encoding operation

$$U_A = (I \otimes \text{PREP}^\dagger) \text{SEL} (I \otimes \text{PREP}). \quad (\text{D4})$$

We say that  $U_A$  is an  $(\alpha, m, \epsilon)$  block encoding of the matrix  $A$ , if it satisfies

$$\|A - \alpha(I \otimes |0\rangle\langle 0|) U_A (I \otimes |0\rangle\langle 0|)\| \leq \epsilon. \quad (\text{D5})$$

## 2. Quantum Signal Processing

Quantum signal processing (QSP) and its variants [45, 89–91] provides a systematic procedure for implementing a class of polynomial transformations to block encoded matrices. For Hermitian matrices  $A$ , the action of a scalar function  $f$  can be determined by the eigendecomposition of  $A = UDU^\dagger$ , as

$$f(A) := U \sum_i f(\lambda_i) |i\rangle \langle i| U^\dagger, \quad (\text{D6})$$

where  $\lambda_i$  is the  $i$ th eigenvalue, and  $U|i\rangle$  is the  $i$ th eigenvector. When  $A$  is not Hermitian, a generalized procedure based on the singular value transform [90] can be used to implement these functions. To implement a degree  $d$  polynomial, QSP uses  $O(d)$  applications of the block encoding and therefore its efficiency depends closely on the rate at which a given polynomial approximation converges to the function of interest, as well as on the circuit complexity required to implement the block encoding.

The following, originally from Ref. [89], characterizes the complexity of performing Hamiltonian simulation with QSP in terms of the number of queries to the block encoding of the Hamiltonian matrix.

**Lemma 12** (Polynomial degree for Hamiltonian simulation (adapted from Ref.[89] Theorem 1) ). *Let  $A$  be a Hermitian matrix accessed via a block encoding  $U_A$  with subnormalization factor  $\alpha \geq \|A\|$ . Then, for any  $t$  we can construct a block encoding of  $U_{e^{iAt}}$  using a polynomial of degree*

$$O(\alpha t + \log(1/\epsilon)). \quad (\text{D7})$$

QSP uses repeated applications of the block encoding circuit to implement a polynomial of the block encoded matrix. We assume that  $A$  is a Hermitian matrix that has been suitably subnormalized by some factor  $\lambda$  so that  $\|A/\lambda\| \leq 1$ . QSP exploits the fact that the block encoding  $U_A$  can be expressed as a direct sum over one and two-dimensional invariant subspaces which correspond directly to the eigensystem of  $A$ , without knowledge of the eigendecomposition. For each eigenvector  $|x\rangle$  of  $A$ , there is a  $2 \times 2$  rotation matrix  $O_x$  representing the  $2d$  subspace associated with  $|x\rangle$ . In turn this allows one to *obliviously* apply a class of polynomial functions to the eigenvalues in each subspace, which builds up the polynomial transformation of the block encoded matrix  $A/\lambda$ . QSP is characterized by the following theorem, which is a rephrasing of Theorem 4 of Ref. [45].

**Lemma 13** (Quantum Signal Processing (Theorem 7.21 [92])). *There exists a set of phase factors  $\Phi := (\phi_0, \dots, \phi_d) \in \mathbb{R}^{d+1}$  such that*

$$\begin{aligned} U_\phi(x) &= e^{i\phi_0 Z} \prod_{j=1}^d [O(x) e^{i\phi_j Z}] \\ &= \begin{pmatrix} P(x) & -Q(x)\sqrt{1-x^2} \\ Q^*(x)\sqrt{1-x^2} & P^*(x) \end{pmatrix}, \end{aligned} \quad (\text{D8})$$

where

$$O(x) = \begin{pmatrix} x & -\sqrt{1-x^2} \\ \sqrt{1-x^2} & x \end{pmatrix}, \quad (\text{D9})$$

if and only if  $P, Q \in \mathbb{C}[x]$  satisfy

1.  $\deg(P) \leq d, \deg(Q) \leq d-1$ ,
2.  $P$  has parity  $d \bmod 2$  and  $Q$  has parity  $d-1 \bmod 2$ , and
3.  $|P(x)|^2 + (1-x^2)|Q(x)|^2 = 1 \ \forall x \in [-1, 1]$ .

Given a scalar function with  $\|f(x)\| \leq 1$ , we can use QSP to approximately implement  $f(A/\lambda)$  by using the block encoding of  $A$ , a polynomial approximation to the desired scalar function, and a set of phase factors corresponding to the approximating polynomial. If  $f$  is not of definite parity, we can use the technique of linear combination of block encodings to obtain a polynomial approximation to  $f$  that is also of indefinite parity, or use generalized QSP from Ref. [91].

We note that there are efficient algorithms for computing the phase factors of QSP for very high degree polynomials. Algorithms for finding phase factors for polynomials of degree  $d = O(10^7)$  have been reported in the literature (see e.g. [91, 93, 94]) and are surprisingly numerically stable even to such high degree. Given that it is straightforward to obtain polynomial approximations to scalar functions and to obtain the corresponding phase factors for QSP, the block encoding circuitry combined with the QSP framework immediately provides a nearly fully explicit circuit description of the block encodings in this work.

### 3. The original LCHS method

The original LCHS method [43] describes the non-unitary propagator  $e^{-tH}$ , for  $H \succeq 0$ , in terms of the expectation value over a family of unitaries  $e^{-itkH}$ , where the probability measure can be obtained in terms of the normalized Fourier coefficients of the exponential function  $e^{-t|x|}$ . This is described by the following relationship

$$e^{-t|x|} = \frac{1}{\pi} \int_{-\infty}^{\infty} dk \frac{e^{itk|x|}}{1+k^2}, \quad (\text{D10})$$

which is a Cauchy distribution over the Fourier modes. Although the LCHS method can accommodate both time-dependent and non-Hermitian matrices, our work is restricted to the case of approximating the propagator for a time-independent Hermitian matrix, which greatly simplifies its usage. Analogously, the LCHS method represents the dissipative, non-unitary propagator  $e^{-tH}$  as a summation over the set of unitaries  $\{e^{itHk}\}$ , over the variable  $k$ ,

$$e^{-tH} = \frac{1}{\pi} \int_{-\infty}^{\infty} dk \frac{e^{-itkH}}{1+k^2}. \quad (\text{D11})$$

One then truncates the infinite interval to a finite interval  $[-K, K]$ , choosing  $K = O(1/\epsilon)$  and approximating the truncated integral using a quadrature scheme to obtain an  $\epsilon$  accurate approximation D10 in the spectral norm.

The follow-up work of Ref. [44] showed that there exists a generalized family of weight functions which can be used instead of the Cauchy distribution, some of which exhibit rapid decay properties away from the origin. In turn, this leads to an improved bound with respect to the cutoff parameter  $K$ . For a function  $f$  satisfying the conditions of Theorem 5 of [44], the LCHS formula can be expressed in the more general form

$$e^{-tH} = \int_{-\infty}^{\infty} dk \frac{f(k)}{1-ik} e^{-itkH}, \quad (\text{D12})$$

where a near-optimal choice of  $f$  was shown to be

$$f_{\sigma}(k) = \frac{1}{2\pi e^{-2\sigma} e^{(1+ik)\sigma}} \quad (\text{D13})$$

for a parameter  $\sigma$  satisfying  $0 < \sigma < 1$ . As discussed in Appendix C of the same work, a practical choice is  $\sigma \in [.7, .8]$ .

The integral (D12) can be approximated using numerical quadrature. First the range of integration is truncated to  $[-K, K]$ , where  $K$  is chosen to be  $O(\log^{1/\sigma}(1/\epsilon))$  when using the near-optimal choice of kernel function (D13). Then one employs a composite Gaussian quadrature scheme, where the large interval  $[-K, K]$  is broken-up into a sequence of small intervals  $[mh, (m+1)h]$ , with  $m \in \{-K/h, \dots, K/h - 1\}$ , then we perform Gaussian quadrature with  $Q$  Gauss points on each sub-interval. Ultimately, this provides an expression for the non-unitary propagator in terms of an LCU

$$e^{-tH} = \sum_{m=-K/h}^{K/h-1} \sum_{q=0}^{Q-1} g_q w(k_{q,m}) e^{-itk_{q,m}H}, \quad (\text{D14})$$

where  $k_{q,m}$  is the  $q$ th quadrature point on the  $m$ th sub-interval,  $w$  the weight function, and  $g_q$  is quadrature weight on the  $q$ th point for Gaussian quadrature on  $Q$  points. Lemmas 9 and 10 of [44] bound the size of each sub-interval  $h = \frac{1}{\epsilon t \|H\|}$  and the number of quadrature points  $Q = O(\log(1/\epsilon))$ . Therefore, the total number of unitaries in the LCU (D14) is

$$M = \frac{2KQ}{h} = O\left(t \|H\| \log^{1+1/\sigma}(1/\epsilon)\right). \quad (\text{D15})$$

## Appendix E: Error Bounds on Gaussian-LCHS

We now perform the error estimates on the Gaussian-LCHS formula introduced from domain truncation and quadrature. We analyze error introduced at nearly every stage of the algorithm, sans errors in preparation of any coefficient states that are used to prepare LCUs. We first analyze the error from truncating the domain of integration in the Gaussian-LCHS formula in Sec. E 1. We then bound the error introduced by applying the quadrature scheme on the truncated integration domain in Sec. E 2. Then we bound the error introduced by approximating the unitaries in the LCHS to finite precision in Sec. E 4.

### 1. Truncation error bounds

The error from truncating the domain of integration is characterized by the following lemma.

**Lemma 14** (Truncation Error). *For any  $\epsilon > 0$  there exists a  $K > 2\sqrt{t}$  such that*

$$\left| \int_{-\infty}^{\infty} \frac{e^{-k^2/4t}}{2\sqrt{\pi t}} e^{ikx} dk - \int_{-K}^{K} \frac{e^{-k^2/4t}}{2\sqrt{\pi t}} e^{ikx} dk \right| \leq \epsilon,$$

where  $K$  can be chosen  $O\left(\sqrt{t \log\left(\frac{1}{\epsilon}\right)}\right)$ .

*Proof.* Let

$$E_K = \left| \int_{-\infty}^{\infty} \frac{e^{-k^2/4t}}{2\sqrt{\pi t}} e^{ikx} dk - \int_{-K}^{K} \frac{e^{-k^2/4t}}{2\sqrt{\pi t}} e^{ikx} dk \right|, \quad (\text{E1})$$

be the error introduced from truncating the integral. We have that

$$\begin{aligned} E_K &= \left| \int_K^{\infty} \frac{e^{-k^2/4t}}{2\sqrt{\pi t}} (e^{-ikx} + e^{ikx}) dk \right| \\ &\leq \frac{1}{\sqrt{\pi t}} \int_K^{\infty} |e^{-k^2/4t}| dk \\ &= \text{erfc}\left(\frac{K}{2\sqrt{t}}\right). \end{aligned}$$

We would like this to be less than some  $\epsilon > 0$ . To simplify the notation let  $x = \sqrt{K^2/4t}$ ,  $K, t > 0$ . For  $x > 0$ , the complimentary error function satisfies the inequalities

$$\frac{2e^{-x^2}}{\sqrt{\pi}(x + \sqrt{x^2 + 2})} \leq \text{erfc}(x) \leq \frac{2e^{-x^2}}{\sqrt{\pi}\left(x + \sqrt{x^2 + \frac{4}{\pi}}\right)},$$

therefore,

$$\begin{aligned} E_K &\leq \frac{2e^{-x^2}}{\sqrt{\pi}\left(x + \sqrt{x^2 + \frac{4}{\pi}}\right)} \Big|_{x=\sqrt{\frac{K^2}{4t}}} \\ &\leq \frac{2e^{-K^2/4t}}{\sqrt{\pi}\left(\frac{K}{2\sqrt{t}} + \sqrt{\frac{K^2\pi + 16t}{4\pi t}}\right)} \\ &\leq 4 \frac{e^{-K^2/4t}}{\sqrt{\pi}} \end{aligned}$$

where the last inequality results from the assumption that  $K \geq 2\sqrt{t}$ . Therefore, if we wish to have this quantity be less than some  $\epsilon > 0$ , it suffices to choose

$$\begin{aligned} K &\geq 2\sqrt{t \log\left(\frac{4}{\sqrt{\pi}\epsilon}\right)} \\ &\in O\left(\sqrt{t \log(1/\epsilon)}\right), \end{aligned} \tag{E2}$$

as desired.  $\square$

## 2. Quadrature Error Bounds

Now, we would like to bound the size of the error introduced from the quadrature scheme on  $M$  grid points. This is characterized by the following lemma.

**Lemma 15** (Quadrature Error). *For any  $\epsilon > 0$ , there exists a positive integer  $M \geq 2$ , a set of weights  $w_j \in \{0, \dots, M\}$ , and quadrature points  $k(j) \subset [-K, K]$  for  $j \in \{0, \dots, M\}$  such that*

$$\left| \sum_{j=0}^M w_j f_t(k(j)) - \int_{-K}^K f_t(k) e^{ikx} dk \right| \leq \epsilon,$$

where

$$f_t(k) = \frac{e^{-k^2/4t}}{2\sqrt{\pi t}} e^{ikx}.$$

Furthermore, for a block encoding with subnormalization factor  $\alpha$  of the square root matrix,  $M$  can be chosen

$$M \in O\left(\alpha \sqrt{t \log(1/\epsilon)}\right).$$

*Proof.* By Theorem 19.3 of Ref. [95], for a number of quadrature points  $M \geq 2$ , we have the error estimates for the Gauss quadrature

$$\left| I_M - \int_{-K}^K \frac{e^{-k^2/4t}}{2\sqrt{\pi t}} e^{-ikx} dk \right| \leq \frac{144}{35} \frac{\Gamma \rho^{-2M}}{\rho^2 - 1}, \tag{E3}$$

where  $\rho$  controls the size of the Bernstein ellipse and  $\Gamma$  is the maximum that the integrand attains on the ellipse. With

$$g(z) = \frac{K}{2} (z + z^{-1}), \tag{E4}$$

parameterizing the Bernstein ellipse over  $[-K, K]$  with  $z \in \mathbb{C}$ , we have that

$$\frac{\partial}{\partial \bar{z}} e^{-g^2(z)/4t} e^{-ig(z)x} = 0, \tag{E5}$$

so the integrand satisfies the Cauchy-Riemann equations and is analytic for any  $\rho$ . Therefore, we can choose  $\rho$  arbitrarily large, but this also causes  $\Gamma$  to grow correspondingly. For some fixed  $\rho > 1$  we have

$$\Gamma = \frac{1}{2\sqrt{\pi t}} \max_{\theta, x \in [-\alpha, \alpha]} e^{-g^2(\rho e^{i\theta})/4t - ig(\rho e^{i\theta})x}, \tag{E6}$$

which is maximized when  $-\frac{g^2(\rho e^{i\theta})}{4t} - ig(\rho e^{i\theta})x$  is maximized. Furthermore, we only need to maximize the real part of the expression.

It can be shown that

$$\operatorname{Re}\left(-\frac{g^2(\rho e^{i\theta})}{4t} - ig(\rho e^{i\theta})x\right) = \frac{-K \left(K \operatorname{Re}(e^{-2i\theta}(1 + e^{i\theta}\rho)^4) + 16tx\rho(\rho^2 - 1)\sin(\theta)\right)}{64t\rho^2}, \tag{E7}$$

which achieves its maximum at  $\theta = -\pi/2$ . At  $\theta = -\pi/2$ , we have

$$\frac{K(16tx\rho(\rho^2 - 1) + K(1 - 6\rho^2 + \rho^4))}{64t\rho^2}. \quad (\text{E8})$$

Now, we can see that for  $1 < \rho \leq 1 + \sqrt{2}$  that

$$\delta\rho(\rho^2 - 1) + 1 - 6\rho^2 + \rho^4 \leq \delta\rho(\rho^2 - 1) \quad (\text{E9})$$

for any  $\delta > 0$ , as  $\rho = 1 + \sqrt{2}$  is a zero of  $(1 - 6\rho^2 + \rho^4)$  and is strictly negative on  $[1, 1 + \sqrt{2}]$ . Therefore, with the choice of  $\rho = 1 + \sqrt{2}$ , we have that the exponent is upper bounded by

$$\frac{Kx}{2}, \quad (\text{E10})$$

or that

$$\Gamma \geq \frac{e^{K\alpha/2}}{2\sqrt{\pi t}}. \quad (\text{E11})$$

Then, for any  $\epsilon > 0$ , we choose  $M$  such that

$$\frac{144\Gamma\rho^{-2M}}{35(\rho^2 - 1)} \leq \epsilon, \quad (\text{E12})$$

where it can be shown that it suffices to choose

$$M \geq \frac{1}{2\log(1 + \sqrt{2})} \left( \frac{K\alpha}{2} + \log\left(\frac{10}{\epsilon\sqrt{t}}\right) \right), \quad (\text{E13})$$

since  $K \sim \sqrt{t\log(1/\epsilon_K)}$ , and  $\epsilon_K \sim \epsilon$ , we have the estimate

$$M \in O\left(\alpha\sqrt{t\log(1/\epsilon)}\right), \quad (\text{E14})$$

as desired.  $\square$

### 3. Bound on LCHS subnormalization factor

The following lemma characterizes the subnormalization factor from implementing the Gaussian-LCHS using Gauss quadrature as a linear combination of unitaries.

**Lemma 16** (Bound on subnormalization factor). *The subnormalization factor  $\alpha_g$  resulting from applying the Gaussian-LCHS formula using Gauss quadrature satisfies*

$$\alpha_g \in O(1).$$

*Proof.* We have

$$I_M = \sum_{j=0}^M w_j f_t(k(j)), \quad (\text{E15})$$

where  $k(j)$  is a Gaussian quadrature point and

$$f_t(k) = \frac{e^{-k^2/4t}}{2\sqrt{\pi t}} e^{ikx}. \quad (\text{E16})$$

Then the subnormalization factor

$$\begin{aligned}
\alpha_g &= \sum_{j=0}^M \left| w_j \frac{e^{-k(j)^2/4t}}{2\sqrt{\pi t}} \right| \\
&= \frac{1}{2\sqrt{\pi t}} \sum_{j=0}^M \left| w_j e^{-k(j)^2/4t} \right| \\
&= \frac{1}{2\sqrt{\pi t}} \sum_{j=0}^M w_j e^{-k(j)^2/4t} \\
&\leq \frac{1}{2\sqrt{\pi t}} \int_{-\infty}^{\infty} e^{-k^2} 4t + O(\epsilon) \\
&= 1 + O(\epsilon) \\
&\in O(1).
\end{aligned}$$

The third equality results from the fact that the Gauss quadrature weights satisfy  $w_j > 0$ , and the last equality completes the lemma.  $\square$

#### 4. Simulation error bounds

Now we will bound the effect of implementing the unitary terms to finite error in the Gaussian-LCHS formula.

**Lemma 17** (Bound on simulation error and polynomial degree). *Let  $\mathcal{A}$  be provided as a block encoding with subnormalization factor  $\alpha$  and let  $K$  and  $M$  be as in Lemmas 14 and 15 respectively. Let  $\widetilde{e^{ik(j)\mathcal{A}}}$  be an approximate block encoding of the true unitary evolution  $e^{ik(j)\mathcal{A}}$  obtained via polynomial approximation. For any  $\epsilon > 0$ , there exists  $K > 1$ ,  $M \geq 2$  and  $\{\epsilon_j > 0\}_{j=0}^M$  satisfying*

$$\left\| e^{ik(j)\mathcal{A}} - \widetilde{e^{ik(j)\mathcal{A}}} \right\| \leq \epsilon_j,$$

such that

$$\left\| e^{-t\mathcal{A}^2} - \sum_{j=0}^M w_j f_t(k(j)) \widetilde{e^{ik(j)\mathcal{A}}} \right\| \leq \epsilon. \quad (\text{E17})$$

Moreover, there exists a polynomial approximation to  $e^{ik(j)\mathcal{A}}$  of degree

$$O\left(\alpha \sqrt{t \log\left(\frac{1}{\epsilon}\right)} + \log\left(\frac{\alpha}{\epsilon}\right)\right) \quad (\text{E18})$$

such that the inequalities Eqs. (E17) and (E18) hold.

*Proof.* Let

$$U_j = e^{ik(j)\mathcal{A}}. \quad (\text{E19})$$

When each  $U_j$  is implemented with zero error, choosing  $K$  and  $M$  according to the bounds in E 1 and E 2 with error  $\epsilon/4$ , in the spectral norm we have

$$\begin{aligned}
\left\| e^{\mathcal{H}_\beta t} - \sum_{j=0}^M f_t(k(j)) e^{ik(j)\mathcal{A}} \right\| &\leq \left\| e^{\mathcal{H}_\beta t} - \int_{-K}^K f_t(k) e^{ik(j)\mathcal{A}} dk \right\| + \left\| \int_{-K}^K f_t(k) e^{ik(j)\mathcal{A}} dk - \sum_{j=0}^M f_t(k(j)) e^{ik(j)\mathcal{A}} \right\| \\
&\leq \frac{\epsilon}{4} + \frac{\epsilon}{4} \\
&= \frac{\epsilon}{2}.
\end{aligned} \quad (\text{E20})$$

Now suppose each  $U_j$  is approximated with a unitary  $\tilde{U}_j$  to error  $\epsilon_j > 0$  in the spectral norm

$$\|U_j - \tilde{U}_j\| \leq \epsilon_j. \quad (\text{E21})$$

Then,

$$\begin{aligned} E &= \left\| \sum_{j=0}^M w_j f_t(k_j) (U_j - \tilde{U}_j) \right\| \\ &\leq \sum_{j=0}^M w_j f_t(k_j) \|U_j - \tilde{U}_j\| \\ &\leq \sum_{j=0}^M w_j f_t(k_j) \epsilon_j. \end{aligned}$$

If we desire,  $E < \epsilon'$  for some  $0 < \epsilon' \leq \epsilon/2$ , it is sufficient to choose each  $\epsilon_j \leq \frac{\epsilon'}{(M+1)w_j f_t(k_j)}$ , as

$$\begin{aligned} E &\leq \sum_{j=0}^M w_j f_t(k(j)) \epsilon_j \\ &\leq \sum_{j=0}^M w_j f_t(k(j)) \frac{\epsilon'}{(M+1)w_j f_t(k(j))} \\ &= \sum_{j=0}^M \frac{\epsilon'}{(M+1)} \\ &= \epsilon'. \end{aligned}$$

With  $K$  and  $M$  chosen as above and  $\epsilon' < \epsilon/2$ , we see that

$$\begin{aligned} &\left\| e^{-t\mathcal{A}^2} - \sum_{j=0}^M w_j f_t(k(j)) e^{ik(j)\mathcal{A}} \right\| \\ &\leq \frac{\epsilon}{2} + \left\| \sum_{j=0}^M w_j f_t(k_j) (U_j - \tilde{U}_j) \right\| \\ &\leq \epsilon \end{aligned} \quad (\text{E22})$$

and find that the error in the Gaussian-LCHS formula with finite precision implementation of the  $U_j$  is bounded by  $\epsilon$ .

Now, for any  $\epsilon_j$  we have by Lemma 12 that  $e^{ik(j)\mathcal{A}}$  can be approximated by a polynomial of degree

$$O\left(\alpha k(j) + \log\left(\frac{1}{\epsilon_j}\right)\right). \quad (\text{E23})$$

Now, substitute  $\epsilon_j \sim \frac{\epsilon}{Mw_j f_t(k(j))}$  into the above logarithm,

$$\begin{aligned} \log\left(\frac{1}{\epsilon_j}\right) &= \log\left(\frac{Mw_j f_t(k(j))}{\epsilon'}\right) \\ &= \log\left(\frac{Mw_j e^{-k^2(j)/4t}}{\sqrt{t}\epsilon}\right). \end{aligned}$$

From Eq. (E14), we have

$$M \in O\left(\alpha\sqrt{t\log(1/\epsilon)}\right). \quad (\text{E24})$$

Therefore,

$$\begin{aligned}
\log \left( \frac{M w_j e^{-k^2(j)/4t}}{\sqrt{t}\epsilon'} \right) &\sim \log \left( \frac{\alpha \sqrt{t \log(1/\epsilon)} w_j e^{-k^2(j)/4t}}{\sqrt{t}\epsilon} \right) \\
&= \log \left( \frac{\alpha \sqrt{\log(1/\epsilon)} w_j e^{-k^2(j)/4t}}{\epsilon} \right) \\
&\sim \log \left( \frac{\alpha w_j e^{-k^2(j)/4t}}{\epsilon} \right) \\
&= \log \left( \frac{\alpha w_j}{\epsilon} \right) - \frac{k^2(j)}{4t} \\
&\leq \log \left( \frac{\alpha w_j}{\epsilon} \right) \\
&\in O \left( \log \left( \frac{\alpha}{\epsilon} \right) \right).
\end{aligned}$$

Then, with  $k(j) \leq K \in O \left( \sqrt{t \log \left( \frac{1}{\epsilon} \right)} \right)$  per Lemma 14, the polynomial degree  $n$  can be chosen

$$n \in O \left( \alpha \sqrt{t \log \left( \frac{1}{\epsilon} \right)} + \log \left( \frac{\alpha}{\epsilon} \right) \right) \quad (\text{E25})$$

□

Lemmas 14, 15, and 17 prove the following theorem.

**Theorem 2.** *Let  $\mathcal{A}$  be an  $\mathcal{N} \times \mathcal{N}$  Hermitian matrix satisfying*

$$-\mathcal{A}^2 = H, \quad (31)$$

or

$$-\mathcal{A}^2 = \begin{pmatrix} H & 0 \\ 0 & * \end{pmatrix} \quad (32)$$

for  $H$  an  $N \times N$  negative definite or negative semi-definite Hermitian matrix with  $N \leq \mathcal{N}$ . Let  $U_{\mathcal{A}}$  be a block encoding of  $\mathcal{A}$  with subnormalization factor  $\alpha$  and let  $t > 0$ . Then, for any  $0 < \epsilon < \min\{\frac{1}{\alpha}, 1\}$ , there exists a quantum algorithm that queries  $U_{\mathcal{A}}$

$$O \left( \alpha \sqrt{t \log \left( \frac{1}{\epsilon} \right)} + \log \left( \frac{\alpha}{\epsilon} \right) \right) \quad (33)$$

times to produce a block encoding of a matrix  $e^{\widetilde{H}t}$  satisfying

$$\left\| e^{Ht} - e^{\widetilde{H}t} \right\| \leq \epsilon. \quad (34)$$

Moreover, the block encoding can be implemented using  $O \left( \log \left( \alpha \sqrt{t \log(1/\epsilon)} \right) \right)$  ancilla qubits and  $O \left( \alpha \sqrt{t \log(1/\epsilon)} \right)$  Toffoli or simpler gates in addition to those used in the block encoding of  $\mathcal{A}$ .

#### Appendix F: Multiplexed QSP (Proof of Lemma 6)

**Lemma 6.** *[Multiplexed QSP] Let  $U_A$  be an  $(\alpha, a)$  block encoding of  $A \in \mathbb{C}^{2^n \times 2^n}$ . Let  $\{P_0, \dots, P_{M-1}\}$  be a set of polynomials of degrees  $d_0, \dots, d_{M-1}$  respectively satisfying*

1.  $|P_i(x)|^2 \leq 1 \ \forall x \in [-1, 1]$  and  $\forall i \in \{0, \dots, M-1\}$

2.  $\forall i \in \{0, \dots, M-1\}$ ,  $d_i \equiv p \pmod{2}$  for fixed  $p \in \{0, 1\}$ .

Then, for any  $|c\rangle = \sum_{j=0}^{M-1} c_j |j\rangle$  satisfying  $\langle c|c\rangle = 1$ , and any  $n$  qubit quantum state  $|\psi\rangle$ , there exists a quantum circuit using  $d_{\max} := \max\{d_0, \dots, d_{M-1}\}$  queries to  $U_A$  and  $\tilde{O}(M)$  additional Toffoli or simpler gates to implement the quantum state

$$\sum_{j=0}^{M-1} c_j P_j \left( \frac{A}{\alpha} \right) |\psi\rangle |0\rangle_{a+1} |j\rangle + |\perp\rangle. \quad (53)$$

*Proof.* By QSP (Lemma 13) there exists a set of phases  $\Phi^j \in \mathbb{R}^{d_j+1}$  for each  $P_j$  such that

$$e^{i\Phi_0^j Z_{\Pi}} \prod_{k=1}^{d_j} \left[ O_A e^{i\Phi_k^j Z_{\Pi}} \right] = U_{P_j(A/\alpha)}, \quad (\text{F1})$$

where  $Z_{\Pi} = 2|0\rangle\langle 0|_a - I$  and  $O_A = U_A Z_{\Pi}$ .  $Z_{\Pi}$  can be implemented with an additional ancilla qubit controlled on the ancilla register of the block encoding (see e.g. Fig. 7.7 of Ref. [92]). Note that since each  $d_j$  are of the same parity, we have that  $d_{\max} - d_j \in 2\mathbb{N}$ . Additionally, notice that

$$O_A^{-1} = O_A^{\dagger} = e^{-i\pi/2Z_{\Pi}} O_A e^{i\pi/2Z_{\Pi}}, \quad (\text{F2})$$

thus, we may extend the phases  $\Phi^j \in \mathbb{R}^{d_j+1} \hookrightarrow \mathbb{R}^{d_{\max}+1}$  by setting  $\Phi_k^j = (-1)^k \frac{\pi}{2}$  for all  $k \in \{d_j+1, \dots, d_{\max}+1\}$ . With this choice of phases we have,

$$\begin{aligned} & e^{i\Phi_0^j Z_{\Pi}} \prod_{k=1}^{d_{\max}} \left[ O_A e^{i\Phi_k^j Z_{\Pi}} \right] \\ &= e^{i\Phi_0^j Z_{\Pi}} \prod_{k=1}^{d_j} \left[ O_A e^{i\Phi_k^j Z_{\Pi}} \right] \prod_{k=d_j+1}^{d_{\max}} \left[ O_A e^{i\Phi_k^j Z_{\Pi}} \right] \\ &= U_{P_j(A)} \prod_{k=1}^{d_{\max}-d_j} \left[ O_A e^{i(-1)^k \frac{\pi}{2} Z_{\Pi}} \right], \end{aligned}$$

Notice that since  $d_{\max} - d_j \in 2\mathbb{Z}$ , write  $d_{\max} - d_j = 2d$

$$\begin{aligned} & \prod_{k=1}^{2d} \left[ O_A e^{i(-1)^k \frac{\pi}{2} Z_{\Pi}} \right] \\ &= \left( O_A e^{-i\frac{\pi}{2} Z_{\Pi}} O_A e^{i(-1)^k \frac{\pi}{2} Z_{\Pi}} \right)^d \\ &= \left( e^{i\frac{\pi}{2} Z_{\Pi}} O_A^{\dagger} O_A e^{i(-1)^k \frac{\pi}{2} Z_{\Pi}} \right)^d \\ &= I. \end{aligned}$$

Thus, the construction of the quantum state can be achieved as follows. Introduce an ancilla register of  $m = \lceil \log(M) \rceil$  qubits and prepare the  $m$  qubit quantum state  $|c\rangle$ . Additionally, introduce the controlled operation

$$c\mathcal{S}_i^j : |0\rangle_{a+1} |j\rangle \rightarrow e^{i\Phi_i^j} |0\rangle_{a+1} |j\rangle. \quad (\text{F3})$$

Then,

$$\begin{aligned}
& c\mathcal{S}_i^j \prod_{k=1}^{d_{\max}} \left[ O_A c\mathcal{S}_i^j \right] |\psi\rangle |0\rangle_{a+1} |c\rangle \\
&= \sum_j c_j c\mathcal{S}_i^j \prod_{k=1}^{d_{\max}} \left[ O_A c\mathcal{S}_i^j \right] |\psi\rangle |0\rangle_{a+1} |j\rangle \\
&= \sum_j c_j c\mathcal{S}_i^j \prod_{k=1}^{d_{\max}} \left[ O_A |\psi\rangle |0\rangle_{a+1} e^{i\Phi_i^j} \right] |j\rangle \\
&= \sum_j c_j U_{P_j(A)} |\psi\rangle |0\rangle_{a+1} |j\rangle \\
&= \sum_j c_j P_j(A) |\psi\rangle |0\rangle_{a+1} |j\rangle + |\perp\rangle.
\end{aligned}$$

A circuit diagram describing these operations is provided as Fig. 7. The controlled operations require  $O(m)$  Toffoli gates to implement, which are queried  $O(M)$  times. The state preparation of  $|c\rangle$  also requires no more than  $\tilde{O}(M)$  Toffoli or simpler gates, thus achieving the stated complexities.  $\square$

#### Appendix G: Non-unitary overlap circuit

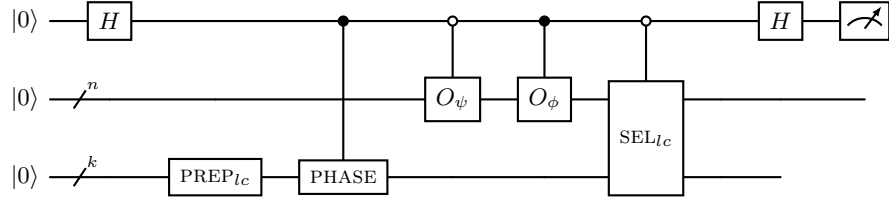


FIG. 8: Quantum circuit for estimating overlaps of the form  $\langle \phi | A | \psi \rangle$  for non-unitary matrices  $A$  using the oracles for the block encoding of  $A$ . This circuit also neglects possible ancilla qubits used in the construction of  $SEL_{lc}$ , i.e. by using a block encoding and quantum signal processing to construct the Hamiltonian simulation unitaries.

We now show how the circuit in non-unitary overlap circuit (reproduced as fig. 8 above for convenience) can be used to estimate these overlaps. Given some matrix  $H$  that we have written as an LCU  $H = \sum_l |c_l| e^{i\phi_l} U_l$  with subnormalization factor  $\alpha = \sum_l |c_l|$ . We show by direct computation how the above circuit can be used to approximate  $\text{Re}(\langle \phi | H | \psi \rangle)$ . The imaginary part can also be obtained using the standard method by applying an additional  $S$  gate on the ancilla qubit prior to the application of the final Hadamard gate. First, observe that the circuit performs the following sequence of transformations

$$\begin{aligned}
& |0\rangle |0\rangle_n |0\rangle_k \xrightarrow{H \otimes I_n \otimes I_k} \frac{1}{\sqrt{2}} (|0\rangle |0\rangle_n |0\rangle_k + |1\rangle |0\rangle_n |0\rangle_k) \\
& \xrightarrow{\text{PREP}_{lc} \text{C-PHASE}} \frac{1}{\sqrt{2}} \left( |0\rangle |0\rangle_n \sum_l \sqrt{\frac{|c_l|}{\alpha}} |l\rangle_k + |1\rangle |0\rangle_n \sum_l e^{-i\phi_l} \sqrt{\frac{|c_l|}{\alpha}} |l\rangle_k \right) \\
& \xrightarrow{\text{C-}\psi, \text{C-}\phi} \frac{1}{\sqrt{2}} \left( |0\rangle |\psi\rangle_n \sum_l \sqrt{\frac{|c_l|}{\alpha}} |l\rangle_k + |1\rangle |\phi\rangle_n \sum_l e^{-i\phi_l} \sqrt{\frac{|c_l|}{\alpha}} |l\rangle_k \right) \\
& \xrightarrow{\text{c-SEL}_{lc}} \frac{1}{\sqrt{2}} \left( \sum_l \sqrt{\frac{|c_l|}{\alpha}} |0\rangle U_l |\psi\rangle_n |l\rangle_k + \sum_l e^{-i\phi_l} \sqrt{\frac{|c_l|}{\alpha}} |1\rangle |\phi\rangle_n |l\rangle_k \right) \\
& \xrightarrow{H \otimes I_n \otimes I_k} \frac{1}{2} \left( \sum_l \sqrt{\frac{|c_l|}{\alpha}} |0\rangle (U_l |\psi\rangle_n + e^{-i\phi_l} |\phi\rangle_n) |l\rangle_k + \sum_l \sqrt{\frac{|c_l|}{\alpha}} |1\rangle (U_l |\psi\rangle_n - e^{-i\phi_l} |\phi\rangle_n) |l\rangle_k \right).
\end{aligned}$$

The probability of measuring the ancilla qubit at the top of the circuit in  $|0\rangle$ ,  $P(0)$ , is

$$P(0) = \frac{1}{4} \left\| \sum_l \sqrt{\frac{|c_l|}{\alpha}} |0\rangle (U_l |\psi\rangle_n + e^{-i\phi_l} |\phi\rangle_n) |l\rangle_k \right\|^2. \quad (\text{G1})$$

Where

$$\begin{aligned} & \left\| \sum_l \sqrt{\frac{|c_l|}{\alpha}} |0\rangle (U_l |\psi\rangle_n + e^{-i\phi_l} |\phi\rangle_n) |l\rangle_k \right\|^2 \\ &= \sum_{l'} \sqrt{\frac{|c_{l'}|}{\alpha}} \langle 0| \left( {}_n\langle \psi | U_{l'}^\dagger + {}_n\langle \phi | e^{i\phi_{l'}} \right)_k \langle l' | \sum_l \sqrt{\frac{|c_l|}{\alpha}} |0\rangle (U_l |\psi\rangle_n + e^{-i\phi_l} |\phi\rangle_n) |l\rangle_k \\ &= \sum_l \frac{|c_l|}{\alpha} \left( {}_n\langle \psi | U_l^\dagger + {}_n\langle \phi | e^{i\phi_l} \right) (U_l |\psi\rangle_n + e^{-i\phi_l} |\phi\rangle_n) \\ &= \sum_l \frac{|c_l|}{\alpha} \left( e^{-i\phi_l} \langle \psi | U_l^\dagger |\phi\rangle + e^{i\phi_l} \langle \phi | U_l |\psi\rangle + 2 \right) \\ &= \sum_l \left( \frac{|c_l|}{\alpha} e^{-i\phi_l} \langle \psi | U_l^\dagger |\phi\rangle + \frac{|c_l|}{\alpha} e^{i\phi_l} \langle \phi | U_l |\psi\rangle \right) + 2, \end{aligned} \quad (\text{G2})$$

where in the second to last line above we used that  $\sum_l \frac{|c_l|}{\alpha} = 1$ . Now,

$$\begin{aligned} & \sum_l \left( \frac{|c_l|}{\alpha} e^{-i\phi_l} \langle \psi | U_l^\dagger |\phi\rangle + \frac{|c_l|}{\alpha} e^{i\phi_l} \langle \phi | U_l |\psi\rangle \right) \\ &= \frac{1}{\alpha} \langle \psi | \sum_l c_l^* U_l^\dagger |\phi\rangle + \frac{1}{\alpha} \langle \phi | \sum_l c_l U_l |\psi\rangle \\ &= \langle \phi | \frac{H}{\alpha} |\psi\rangle + \langle \psi | \frac{H^\dagger}{\alpha} |\phi\rangle \\ &= \langle \phi | \frac{H}{\alpha} |\psi\rangle + \left( \langle \phi | \frac{H}{\alpha} |\psi\rangle \right)^* \\ &= \frac{2}{\alpha} \text{Re}(\langle \phi | H |\psi\rangle). \end{aligned} \quad (\text{G3})$$

So that overall (G1) simplifies to

$$P(0) = \frac{1}{2} \left( 1 + \frac{1}{\alpha} \text{Re}(\langle \phi | H |\psi\rangle) \right). \quad (\text{G4})$$

We also note that the imaginary part of the overlap can be obtained in the standard way, by applying a phase gate to the top ancilla qubit as the penultimate gate prior to the application of the final Hadamard gate.

Notice that there is no post-selection on the qubits used to form the linear combination of unitaries. This is significant, since without using amplitude amplification and sampling at the standard limit and assuming the success probability scales inversely with  $\alpha$ , one would need to repeat the circuit  $\sim \alpha^2$  times to obtain a successful outcome, and additionally obtain  $O(\alpha^2/\epsilon^2)$  samples from the circuit to obtain an approximation with additive error less than  $\epsilon$ , so that the total number of queries to the quantum circuit becomes  $O(\alpha^4/\epsilon^2)$ . On the other hand, we can directly sample from the output of the above quantum circuit only  $O(\alpha^2/\epsilon^2)$  times to obtain the same error, obtaining a quadratic improvement in the  $\alpha$  parameter. We formalize this result with the following lemma.

**Lemma 3.** *Let  $H$  be represented by the LCU*

$$H = \sum_{l=0}^{K-1} |c_l| e^{i\phi_l} U_l, \quad (\text{40})$$

*with  $2^k \leq K \leq 2^{k+1}$  for some  $k \geq 1$ , and  $\alpha = \sum_l |c_l|$ . For any input states  $|\phi\rangle$  and  $|\psi\rangle$  constructed with oracles  $O_\psi$  and  $O_\phi$ , the quantum circuit in Fig. 5 can be used to estimate*

$$\langle \phi | \frac{H}{\alpha} |\psi\rangle, \quad (\text{41})$$

independent of the success probability of implementing the LCU, provided the  $U_l$  are unitaries.

*Proof.* The above calculation is sufficient to prove the lemma.  $\square$

### Appendix H: Block encoding dilated matrix square root

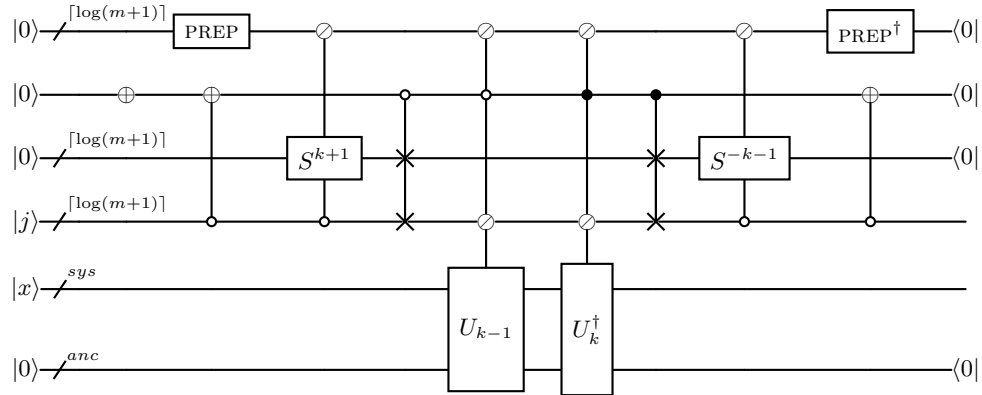


FIG. 9: Quantum circuit for an  $(2s + \max_{j=0}^{m-1} \{m_j\}, \alpha = \sum_{j=0}^{m-1} \alpha_j)$  – block encoding of  $\mathcal{A}$ . Here  $S^j$  is the modular increment-by- $j$  unitary matrix and each  $U_k$  is an  $(\alpha_k, m_k)$  block encoding of  $A_k$ .

Let, PREP  $|0\rangle_s = \sum_{k=0}^{M-1} \sqrt{\frac{\alpha_k}{\alpha}} |k\rangle$ . We now verify that this produces a block encoding of  $\mathcal{A}$ . For  $j > 0$  this circuit performs the operations,

$$\begin{aligned}
|0\rangle_s |1\rangle |0\rangle_s |j\rangle_s |x\rangle |0\rangle &\rightarrow \sum_{k=0}^{M-1} \sqrt{\frac{\alpha_k}{\alpha}} |k\rangle |1\rangle |0\rangle_s |j\rangle_s |x\rangle \\
&\rightarrow \sum_{k=0}^{M-1} \sqrt{\frac{\alpha_k}{\alpha}} |k\rangle |1\rangle |0\rangle_s |j\rangle_s \left( \delta_{j,k} \frac{A_k^\dagger}{\alpha_k} + (1 - \delta_{j,k}) I \right) |x\rangle + |\perp\rangle \\
&\rightarrow \sum_{k=0}^{M-1} \sqrt{\frac{\alpha_k}{\alpha}} |k\rangle |1\rangle |j\rangle_s |0\rangle_s \left( \delta_{j,k} \frac{A_k^\dagger}{\alpha_k} + (1 - \delta_{j,k}) I \right) |x\rangle + |\perp\rangle \\
&\rightarrow \sum_{k=0}^{M-1} \sqrt{\frac{\alpha_k}{\alpha}} |k\rangle |0\rangle |j - (k+1)\rangle_s |0\rangle_s \left( \delta_{j,k} \frac{A_k^\dagger}{\alpha_k} + (1 - \delta_{j,k}) I \right) |x\rangle + |\perp\rangle \\
&\rightarrow \sum_{k=0}^{M-1} \frac{\alpha_k}{\alpha} |0\rangle |0\rangle |j - (k+1)\rangle_s |0\rangle_s \left( \delta_{j,k} \frac{A_k^\dagger}{\alpha_k} + (1 - \delta_{j,k}) I \right) |x\rangle + |\perp\rangle \\
&= |0\rangle |0\rangle |0\rangle_s |0\rangle_s \frac{A_{j-1}^\dagger}{\alpha_{j-1}} |x\rangle + |\perp\rangle
\end{aligned}$$

For  $j = 0$ , the circuit in Fig. 9 performs the operations,

$$\begin{aligned}
|0\rangle_s |1\rangle |0\rangle_s |0\rangle_s |x\rangle |0\rangle &\rightarrow \sum_{k=0}^{M-1} \sqrt{\frac{\alpha_k}{\alpha}} |k\rangle |1\rangle |0\rangle_s |0\rangle_s |x\rangle \\
&\rightarrow \sum_{k=0}^{M-1} \sqrt{\frac{\alpha_k}{\alpha}} |k\rangle |0\rangle |0\rangle_s |0\rangle_s |x\rangle \\
&\rightarrow \sum_{k=0}^{M-1} \sqrt{\frac{\alpha_k}{\alpha}} |k\rangle |0\rangle |k+1\rangle_s |0\rangle_s |x\rangle \\
&\rightarrow \sum_{k=0}^{M-1} \sqrt{\frac{\alpha_k}{\alpha}} |k\rangle |0\rangle |0\rangle_s |k+1\rangle_s \frac{A_k}{\alpha_k} |x\rangle + |\perp\rangle \\
&\rightarrow \sum_{k=0}^{M-1} \frac{\alpha_k}{\alpha} |0\rangle |0\rangle |0\rangle_s |k+1\rangle_s \frac{A_k}{\alpha_k} |x\rangle + |\perp\rangle, \\
&= \frac{1}{\alpha} |0\rangle |0\rangle |0\rangle_s \sum_{k=0}^{M-1} |k+1\rangle_s A_k |x\rangle + |\perp\rangle
\end{aligned}$$

as desired. Note that the single ancilla qubit is actually reset to  $|0\rangle$  deterministically.

We now compare estimates of the subnormalization factors to block encode  $\mathcal{A}$  and  $H$ .

**Lemma 18** (Quadratic improvement in subnormalization).

*Proof.* Assume that each  $A_j$  and  $A_j^\dagger$  are provided as block encodings with subnormalization  $\alpha_j$  and that the product terms  $A_j^\dagger A_j$  are provided as block encodings with subnormalization factors  $\beta_j$  and that  $\beta_j \in O(\alpha_j^2)$ . Let  $\gamma_1$  and  $\gamma_2$  be the subnormalization factors for the block encodings of  $\mathcal{A}$  and  $H$  respectively.  $\mathcal{A}$  is obtained using a linear combination of block encodings as,

$$\mathcal{A} = \sum_{j=0}^{M-1} \alpha_j \left( |j+1\rangle \langle 0| \otimes_{m_j} \langle 0| U_j |0\rangle_{m_j} + |0\rangle \langle j+1| \otimes_{m_j} \langle 0| U_j^\dagger |0\rangle_{m_j} \right). \quad (\text{H1})$$

Therefore, the subnormalization  $\gamma_1$  for the block encoding of  $\mathcal{A}$  is

$$\gamma_1 = \sum_{j=0}^{M-1} \alpha_j. \quad (\text{H2})$$

If we proceed in a similar fashion for the block encoding of  $H$ , by writing it as a linear combination of block encodings of  $A_j^\dagger A_j$ , we find

$$\gamma_2 = \sum_{j=0}^{M-1} \beta_j = O \left( \sum_{j=0}^{M-1} \alpha_j^2 \right) = O(\gamma_1^2). \quad (\text{H3})$$

Therefore, we can conclude that the subnormalization  $\gamma_1$  for the block encoding of  $\mathcal{A}$  can be quadratically smaller than that of  $H$  given access to similar oracles.  $\square$

## Appendix I: Consistency of plane wave discretization

We have the decomposition of the continuum operator  $\mathcal{H}_\beta$  into a summation of terms

$$\mathcal{H}_\beta = - \sum_{j \in [\eta d]} A_j^\dagger A_j \quad (\text{I1})$$

where

$$A_j = -i(\partial_{x_j} + F_j). \quad (\text{I2})$$

Now, we would like to construct a discretization of  $A_j$  induces a consistent finite-dimensional approximation of the continuum operators  $A_j^\dagger A_j$ . We will construct such a discretization using a plane wave basis in one dimension, the generalization to higher dimensional problems holds by the underlying tensor product structure of the  $A_j$ .

Consider the domain  $[0, L]$ , that we discretize with  $N$  plane wave modes. In this representation, the derivative operator becomes  $\partial_x \rightarrow \frac{iN}{2L} \sum_{j \in [N]} j |j\rangle \langle j|$ , and the diagonal force matrix  $F \rightarrow QFQ^\dagger = \hat{F}$ . Now the operator decomposition becomes

$$A = \frac{iN}{L} \sum_{k \in [N]} k |k\rangle \langle k| + \hat{F}.$$

Then,

$$\begin{aligned} & (-ik |k\rangle \langle k| + \hat{F}) (ik' |k'\rangle \langle k'| + \hat{F}) \\ &= k^2 |k\rangle \langle k| - ik |k\rangle \langle k| \hat{F} + ik \hat{F} |k\rangle \langle k| + \hat{F}^2. \end{aligned}$$

The first term corresponds to the negative Laplacian, the last term the squared gradient, therefore, we now need to show that the terms

$$-ik |k\rangle \langle k| \hat{F} + ik \hat{F} |k\rangle \langle k|$$

provide an approximation for the operation of multiplication by  $-\Delta V$  in the computational basis. This is provided by the following lemma.

**Lemma 19** (Validity of discrete approximation to  $-\Delta V$ ).

*Proof.* First, let us evaluate the term  $\partial_x(F|\phi\rangle)$ , for some initial state  $|\phi\rangle$ , where  $\hat{\phi}$  and  $\hat{F}$  are the corresponding Fourier transformed quantities. In the Fourier basis, the diagonal multiplication operator  $F$  becomes

$$\hat{F} = \sum_{j,k} \hat{F}_{j-k} |j\rangle \langle k|,$$

therefore, the  $n$ th entry for any state  $|\hat{\phi}\rangle$  is,

$$\langle n | \hat{F} | \hat{\phi} \rangle = \sum_k \hat{\phi}_k \hat{F}_{n-k}$$

Then, application of the operator  $\partial_x$  in the plane wave basis yields

$$\langle n | \partial_x \hat{F} | \hat{\phi} \rangle = ik_n \sum_j \hat{\phi}_n \hat{F}_{n-j}.$$

Similarly, the term  $F \partial_x \phi$  in the plane wave basis gives,

$$\langle n | \hat{F} \partial_x | \hat{\phi} \rangle = i \sum_m k_m \hat{F}_{n-m} \hat{\phi}_m.$$

Thus,

$$\langle n | (-\partial_x \hat{F} + \hat{F} \partial_x) | \hat{\phi} \rangle = i \sum_j (k_j - k_n) \hat{F}_{n-j} \hat{\phi}_j. \quad (\text{I3})$$

Now, let us consider how the multiplication operator  $\partial_x F = F'$  acts in the plane wave basis,

$$\hat{F}' = \sum_{n,m} \hat{F}'_{m-n} |m\rangle \langle n|.$$

Now,  $\hat{F}'_{m-n}$  is the  $(m-n)$ th Fourier coefficient of  $F'$ , which is just  $ik_{n-m}\hat{F}_{n-m}$ , therefore,

$$\langle n | \hat{F}' | \hat{\phi} \rangle = i \sum_j k_{n-j} \hat{F}_{n-j} \hat{\phi}_j.$$

Now, in order for these to be equal, we must have

$$i \sum_j (k_j - k_n) \hat{F}_{n-j} \hat{\phi}_j = -i \sum_j k_{n-j} \hat{F}_{n-j} \hat{\phi}_j,$$

and thusly,

$$-k_{n-j} = k_j - k_n,$$

but recall that  $-k_{n-j} = -\frac{2\pi(n-j)}{L} = \frac{2\pi j}{L} - \frac{2\pi n}{L} = k_j - k_n$  as desired.  $\square$

Therefore, the above calculation guarantees that the finite dimensional discretization with plane waves mimics the desired continuum operator.

## Appendix J: Detailed construction of block encoding

### 1. Block Encoding Potential Gradient

We will assume that the potential functions take the form of polynomials, which, due to the assumption of  $V$  being confining implies that the polynomial must be of even degree. For symmetric pair wise potentials,  $V_{ij} = V(r_{ij})$ , the gradients can be simply expressed,

$$\nabla_i V_{ij} = V'(r_{ij}) \frac{\mathbf{x}^i - \mathbf{x}^j}{r_{ij}} = -\nabla_j V_{ij}.$$

For simplicity, we will also assume that  $V$  contains no terms of order 1 in  $r_{ij}$  as this would necessitate the computation of the inverse square root, which we wish to avoid. Nevertheless, this assumption can be removed by applying the methods developed in Appendix K of [96] to prepare the inverse square root with overall  $O(n^2)$  complexity.

To block encode the gradient operator, we will use a combination of arithmetic operations, the inequality testing method of [97], and QSP. First, we compute the difference between each distinct pair of registers

$$|\mathbf{r}_i\rangle_i |\mathbf{r}_j\rangle_j \rightarrow |\mathbf{r}_i\rangle_i |\mathbf{r}_i - \mathbf{r}_j\rangle_j.$$

Then, we will calculate the sum of squares of these differences into a work register of  $2n + \lceil \log(d) \rceil$  qubits, which prepares the state

$$|\mathbf{r}_i\rangle_i |\mathbf{r}_i - \mathbf{r}_j\rangle_j |0\rangle \rightarrow |\mathbf{r}_i\rangle_i |\mathbf{r}_i - \mathbf{r}_j\rangle_j |r_{ij}^2\rangle.$$

Next, we apply the technique from Ref. [97] to kickback an amplitude  $\propto \sqrt{r_{ij}^2}$ .

To apply this method, we append another  $n_d = 2n + \lceil \log(d) \rceil$  qubit ancilla register plus one additional ancilla qubit and prepare the uniform superposition over the  $n_d$  qubit register. This prepares the state

$$|\mathbf{r}_i\rangle_i |\mathbf{r}_i - \mathbf{r}_j\rangle_j |r_{ij}^2\rangle \frac{1}{\sqrt{2^{n_d}}} \sum_{m \in [2^{n_d}]} |m\rangle |0\rangle.$$

Then, we perform an inequality test between  $m$  and  $r_{ij}^2$ ,

$$\text{COMP} : |n\rangle |m\rangle |0\rangle \rightarrow \begin{cases} |n\rangle |m\rangle |0\rangle & n < m \\ |n\rangle |m\rangle |1\rangle & n \geq m. \end{cases}$$

This can be performed through a subtraction circuit, and results in the state

$$|\mathbf{r}_i\rangle_i |\mathbf{r}_i - \mathbf{r}_j\rangle_j |r_{ij}^2\rangle \frac{1}{\sqrt{2^{n_d}}} \sum_{m < r_{ij}^2} |m\rangle |0\rangle + |\perp\rangle.$$

We will forgo uncomputing the subtraction at this stage, as we will use this information in a forthcoming calculation. Now, we perform the operation  $\text{unif}^{-1}$ , which is defined implicitly via

$$\text{unif} : |x\rangle |0\rangle \rightarrow \frac{1}{\sqrt{x}} |x\rangle \sum_{j < x} |j\rangle .$$

Applying  $\text{unif}^{-1}$  to the  $|r_{ij}^2\rangle$  and  $|m\rangle$  registers, we obtain

$$\sqrt{\frac{r_{ij}^2}{2^{n_d}}} |\mathbf{r}\rangle_i |\mathbf{r}_i - \mathbf{r}_j\rangle_j |r_{ij}^2\rangle |0\rangle |0\rangle + |\perp\rangle .$$

Then, uncomputing the sum of squares and the the difference of positions, we obtain

$$U_r : |\mathbf{r}\rangle_i |\mathbf{r}\rangle_j |0\rangle \rightarrow \frac{r_{ij}}{\sqrt{2^{n_d}}} |\mathbf{r}\rangle_i |\mathbf{r}\rangle_j |0\rangle |0\rangle + |\perp\rangle , \quad (\text{J1})$$

which is a block encoding of symmetric Euclidean distance between particles  $i$  and  $j$  with subnormalization factor  $\alpha_r = \sqrt{2^{n_d}}$ . The cost to perform this block encoding is characterized by Lemma 20.

**Lemma 20** (Complexity of block encoding inter-particle distance). *There exists a quantum circuit which outputs an  $(\alpha_r, 2n + \lceil \log(d) \rceil + 1)$  block encoding of the Euclidean distance matrix  $U_r$  in Eq. (J1), with  $\alpha_r = O(N^{d/2})$  using approximately*

$$2dn^2 + 4nd + 4n + O\left((2n + 2 \lceil \log(d) \rceil) \log\left(\frac{1}{\epsilon}\right)\right) + O(d) + 2 \lceil \log(d) \rceil \quad (\text{J2})$$

Toffoli gates and

$$2n + \lceil \log(d) \rceil \quad (\text{J3})$$

work qubits in addition to those that flag the success of the block encoding.

*Proof.* This operation requires the usage of  $2d$   $n$  qubit subtraction circuits to compute and uncompute the difference. The Toffoli complexity of  $n$  qubit subtraction is  $2n + O(1)$ , therefore, the Toffoli complexity of the  $d n$  qubit subtractions is  $2nd + O(d)$ . The summation of  $d n$  qubit states can be performed with  $dn^2$  Toffoli gates per Lemma 9 of Ref. [96] and requires  $n_d = 2n + \lceil \log(d) \rceil$  qubits to store the output. This is then followed by the subtraction circuit to compute INEQ, which uses an addition  $2nd + O(d)$  Toffoli gates. We then, append an additional  $n_d$  qubits and prepare the uniform superposition over them. Preparation of the uniform superposition over a power of 2 has zero Toffoli cost, the antecedent inequality test requires  $n_d$  Toffoli gates.  $\text{unif}^{-1}$  can be performed with  $n_d$  controlled Hadamard gates and a round of fixed point amplitude amplification with  $\sim O(n_d \log(\frac{1}{\epsilon}))$ , Toffoli gates. The controlled Hadamard gates can be implemented with a single catalytically used  $|T\rangle$  state, for a Toffoli complexity of  $n_d$ . Finally, we conclude by uncomputing the sum of squares which incurs an additional  $dn^2$  Toffoli gates. In total, these operations entail

$$2dn^2 + 4nd + 4n + O\left((2n + 2 \lceil \log(d) \rceil) \log\left(\frac{1}{\epsilon}\right)\right) + O(d) + 2 \lceil \log(d) \rceil$$

Toffoli gates, and  $2n + \lceil \log(d) \rceil$  additional work qubits.  $\square$

For  $V(r)$  a polynomial of degree  $2k$  with coefficients  $c_j$  with no term of degree 1, then  $\frac{V'(r)}{r}$  is a polynomial of degree  $2(k-1)$  of the form  $\sum_{j=2}^{2k-2} j c_j r^{j-2}$ . Using, QSP we can query the block encoding of  $r_{ij}$   $2k-2$  times to obtain the desired block encoding, with subnormalization factor  $\alpha_V = \max_{\|r\| \leq \sqrt{dL}} \frac{V'(r)}{r}$ .

The last stage requires us to multiply by the difference of the shared degrees of freedom for the pair of particles. Fixing some  $l \in [d]$ , we seek to block encode the operation  $|r_{ij}\rangle \rightarrow r_{ij}^{(l)} |r_{ij}\rangle$ , where  $r_{ij}^{(l)} \in [0, 1]$ . This can once again be accomplished using the techniques presented in Ref. [97] and a product of block encodings. In total, we perform the operations

$$\begin{aligned} |\mathbf{r}_i - \mathbf{r}_j\rangle |0\rangle |0\rangle &\xrightarrow{\text{UNIF}} \frac{1}{\sqrt{N}} |\mathbf{r}_i - \mathbf{r}_j\rangle \sum_{k=0}^{N-1} |k\rangle |0\rangle \\ &\xrightarrow{\text{INEQ}} \frac{1}{\sqrt{N}} |\mathbf{r}_i - \mathbf{r}_j\rangle \sum_{k \leq r_{ij}^{(l)}} |k\rangle |0\rangle + |\perp\rangle \\ &\xrightarrow{\text{UNIF}^\dagger} r_{ij}^{(l)} |\mathbf{r}_i - \mathbf{r}_j\rangle |0\rangle |0\rangle + |\perp\rangle . \end{aligned}$$

The inequality in the second summation is calculated in two's complement arithmetic to account for the sign information in  $r_{ij}^{(l)}$ . Since we have already included the cost of performing the subtraction in the Euclidean distance operator in Lemma 20, the only additional non-Clifford cost is in performing the INEQ operation, which requires  $n$  Toffoli gates. Using the compression gadget described in Ref. [50], we can perform the product of these block encodings with a single additional ancilla qubit,  $n + n_d$  additional Toffoli gates to control on the all zero state of the ancilla register, and one use of each of the block encodings. Overall, this entails a non-Clifford cost of

$$2dn^2 + 4nd + 7n + O\left((2n + 2\lceil\log(d)\rceil)\log\left(\frac{1}{\epsilon}\right)\right) + O(d) + 4\lceil\log(d)\rceil + 2. \quad (\text{J4})$$

Now, to construct a block encoding of the full potential gradient operator, we will control swaps into an ancilla register and apply the above routines. The algorithm proceeds as follows. We prepare two quantum states encoding the uniform superposition over  $\eta$  states using two registers of  $n_\eta = \lceil\log(\eta)\rceil$  ancilla qubits, we also prepare a uniform superposition over  $d$  states with a register of  $n_d = \lceil\log(d)\rceil$  ancilla. Then, we perform a comparison test which is flagged by another ancilla qubit to mark if the two particle indices are the same. This entails the bulk of the prepare construction,

$$\text{PREP} : |0\rangle_{n_\eta} |0\rangle_{n_\eta} |0\rangle_{n_d} |0\rangle \rightarrow \frac{1}{\eta\sqrt{d}} \sum_{i \neq j \in [\eta]} \sum_{l \in [d]} |i\rangle |j\rangle |l\rangle |0\rangle + |\perp\rangle. \quad (\text{J5})$$

Then, controlling on the two  $n_\eta$  qubit registers, as well as the flag indicating the particle indices are unequal, we will swap the registers of particles  $i$  and  $j$  into ancilla. Then, we will perform two  $nd$  qubit quantum Fourier transforms on the two  $nd$  qubit registers that hold the degrees of freedom of particles  $i$  and  $j$ . Then, we will apply the block encoding of the gradient operator, controlling on the  $n_d$  qubit register indexing over the dimension index. Then, we will uncompute the  $n_d$  qubit and one of the  $n_\eta$  qubit registers encoding the uniform superpositions. We will use the notation  $p_i$  to refer to the encoding of particle  $i$ 's degrees of freedom in the momentum representation and  $r_i$  to refer to particle  $i$ 's degrees of freedom in the position representation. In all, the operations are as follows

$$\begin{aligned} |0\rangle_{temp0} |0\rangle_{temp1} |0\rangle_{n_\eta} |0\rangle_{n_\eta} |0\rangle_{n_d} |0\rangle &\xrightarrow{\text{PREP}} |0\rangle_{temp0} |0\rangle_{temp1} \frac{1}{\eta\sqrt{d}} \sum_{i \in [\eta]} \sum_{j \neq i} \sum_{k \in [d]} |i\rangle_{n_\eta} |j\rangle_{n_\eta} |k\rangle_{n_d} |0\rangle + |\perp\rangle \\ &\xrightarrow{\text{CSWAP}_{ij}} |p_i\rangle_{temp0} |p_j\rangle_{temp1} \frac{1}{\eta\sqrt{d}} \sum_{i \in [\eta]} \sum_{j \neq i} \sum_{k \in [d]} |i\rangle_{n_\eta} |j\rangle_{n_\eta} |k\rangle_{n_d} |0\rangle + |\perp\rangle \\ &\xrightarrow{Q_{nd} \otimes Q_{nd}} \sum_{i \in [\eta]} \sum_{j \neq i} \sum_{k \in [d]} |r_i\rangle_{temp0} |r_j\rangle_{temp1} \frac{1}{\eta\sqrt{d}} |i\rangle_{n_\eta} |j\rangle_{n_\eta} |k\rangle_{n_d} |0\rangle + |\perp\rangle \\ &\xrightarrow{U_F} \sum_{i \in [\eta]} \sum_{j \neq i} \sum_{k \in [d]} \frac{F_k^i(r_{ij})}{\alpha_F} |r_i\rangle_{temp0} |r_j\rangle_{temp1} \frac{1}{\eta\sqrt{d}} |i\rangle_{n_\eta} |j\rangle_{n_\eta} |k\rangle_{n_d} |0\rangle + |\perp'\rangle \\ &\xrightarrow{Q_{nd}^\dagger \otimes Q_{nd}^\dagger} \sum_{i \in [\eta]} \sum_{j \neq i} \sum_{k \in [d]} \widehat{F_k^i(r_{ij})} |p_i\rangle_{temp0} |p_j\rangle_{temp1} \frac{1}{\eta\sqrt{d}} |i\rangle_{n_\eta} |j\rangle_{n_\eta} |k\rangle_{n_d} |0\rangle + |\perp'\rangle \\ &\xrightarrow{\text{CSWAP}_{ij}^\dagger} |0\rangle_{temp0} |0\rangle_{temp1} \sum_{i \in [\eta]} \sum_{j \neq i} \sum_{k \in [d]} \frac{\widehat{F_k^i(r_{ij})}}{\alpha_F} \frac{1}{\eta\sqrt{d}} |i\rangle_{n_\eta} |j\rangle_{n_\eta} |k\rangle_{n_d} |0\rangle + |\perp'\rangle \\ &\xrightarrow{I \otimes \text{UNIF}_\eta^\dagger \otimes I} |0\rangle_{temp0} |0\rangle_{temp1} \sum_{i \in [\eta]} \sum_{j \neq i} \sum_{k \in [d]} \frac{\widehat{F_k^i(r_{ij})}}{\alpha_F} \frac{1}{\sqrt{d}\eta\eta} |i\rangle_{n_\eta} |0\rangle_{n_\eta} |k\rangle_{n_d} |0\rangle + |\perp''\rangle. \end{aligned}$$

The subnormalization factor, gate complexity, and number of ancilla qubits needed to perform this block encoding is characterized by the following theorem.

**Lemma 21** (Cost to block encoding potential gradient term). *Let  $V$  be a polynomial of degree  $2k$  containing no term of degree 1. Then, there exists a quantum circuit which constructs a block encoding of the potential gradient with subnormalization factor  $\alpha_F = \eta^{3/2}\sqrt{d}\lambda_V$ , with  $\alpha_V = \max_{\|r\| \leq \sqrt{d}L} \left| \frac{V'(r)}{r} \right|$ , using  $O(kdn^2(d+1) + \eta nd)$  Toffoli gates and Then, the operations outlined above construct a  $(\alpha_F, O(n_\eta + n))$ -block encoding of the potential gradient and uses  $O(2n + \lceil\log(d)\rceil)$  additional qubits.*

*Proof.* The construction of PREP requires two applications of the preparation of the uniform superposition over  $\eta$  labels, and one application of the uniform superposition of  $d$  labels. These operations have complexity  $O((2n_\eta + n_d) \log(\frac{1}{\epsilon}))$ . The controlled swap operations require  $2(\eta dn + n_\eta)$  Toffoli gates operations. To implement the  $nd$  qubit quantum Fourier transforms require  $O((nd)^2)$  Toffoli gates. The implementation of  $U_F$  is given by the polynomial degree times the cost reported Eq. (J4) and is  $O(kdn^2)$ . Finally, we uncompute these operations which entails another  $O((nd)^2)$  Toffolis for the QFT and  $O(2\eta dn)$  to uncompute the uniform superposition.  $\square$

## 2. Block encoding gradient operator

The block encoding of the  $\eta d$ -dimensional gradient operator is significantly simplified in the plane wave basis as the derivative operator takes the form of a scalar multiplication. Our goal now is to block encode the operation

$$\sum_{i \in [d\eta]} |i\rangle \otimes \nabla_i \quad (J6)$$

where  $k_m = \frac{2\pi m}{L}$ . This can be performed using the same block encoding strategy that we employed to construct the *position* operator  $|r\rangle \rightarrow r|r\rangle$ . Indeed, this operation can be constructed with just a single additional ancilla qubit that is prepared in the quantum state  $\frac{1}{\beta^{1/4}}|0\rangle + \beta^{1/4}|1\rangle$ , with normalization factor  $\frac{\beta+1}{\sqrt{\beta}} \in O(\max\{\sqrt{\beta}, \sqrt{\beta^{-1}}\})$ . On the  $|0\rangle$  state we perform controlled application of the inequality test COMP, and on the  $|1\rangle$  state we perform controlled application of the operator  $U_F$ , which in turn requires  $2k - 2$  controlled applications of  $U_r$ .

## 3. Proof of Theorem 5

**Theorem 5.** *Let  $N = 2^n$  be the number of plane wave modes per degree of freedom, for  $\eta$  particles occupying a  $d$ -dimensional reciprocal lattice  $\mathbf{G} = \mathbb{Z}_N^d$ , corresponding to a discretization of the real space  $[-L, L]^d$  for each particle. Let  $V$  be a potential function given by a polynomial of degree  $2k$  in the pair-wise distance between any distinct pairs particles  $i, j$ , with no term of degree 1, and let  $\alpha_V = \max_{\|r\| \leq \sqrt{d}L} \left| \frac{V'(r)}{r} \right|$ . Then there exists a quantum circuit that block encodes the plane wave representation of the operator*

$$\mathcal{A} = \sum_{j \in [\eta]} |0\rangle\langle j+1| \otimes A_j^\dagger + |j+1\rangle\langle 0| \otimes A_j \quad (46)$$

with subnormalization factor

$$\alpha_A \in O\left(\sqrt{\beta d} \eta^{3/2} L \alpha_V + \sqrt{\frac{\eta d}{\beta}} \frac{N}{L}\right), \quad (47)$$

using

$$\tilde{O}(\eta dn + 2kdn^2 + (nd)^2) \quad (48)$$

*Toffoli or simpler gates, with the logarithmic factors hidden by the  $\tilde{O}$  notation arising from small overheads to compile finite precision rotation gates and multi-controlled operations.*

*Proof.* The block encoding of each  $A_j$  term requires one usage of the quantum circuit which block encodes  $\nabla V$  and one usage of the circuit which block encodes  $\nabla$ . By Lemma 21 this is done with  $O(kdn^2(d+1) + \eta nd)$  Toffoli or simpler gates, and the gradient operator requires an additional  $O(n)$  Toffoli or simpler gates. Each of these block encodings are obtained with subnormalization factor  $\alpha_F$  and  $\alpha_V$  respectively. Then, we form the LCU of these block encodings using a straightforward variation of the quantum circuit from Fig. 9 and using an additional ancilla qubit which is prepared in the state

$$\frac{1}{\sqrt{\alpha_A}} \left( \sqrt{\alpha_F} \beta^{1/4} |0\rangle + \sqrt{\alpha_V} \beta^{-1/4} |1\rangle \right), \quad (J7)$$

where

$$\alpha_A = \alpha_F \sqrt{\beta} + \alpha_V \sqrt{\beta^{-1}}. \quad (J8)$$

Thus, with  $\alpha_F \in O\left(\eta^{3/2}\sqrt{d}L\alpha_V\right)$ , and  $\alpha_\nabla \in O\left(\sqrt{\eta d}\frac{N}{L}\right)$ , we have

$$\alpha_A \in O\left(\sqrt{\beta d}\eta^{3/2}L\alpha_V + \sqrt{\frac{\eta d}{\beta}}\frac{N}{L}\right). \quad (\text{J9})$$

□